Characterization of Fetal Alcohol Spectrum Disorders (FASD) Associated Dental defects - Insights from zebrafish (*Danio rerio*)

by

Parnia Azimian Zavareh

A Thesis submitted to the Faculty of Graduate
Studies of The University of Manitoba
In partial fulfillment of the requirements of the degree of

Master of Science

Department of Oral Biology
Faculty of Dentistry
University of Manitoba
Winnipeg, Manitoba, Canada

ABSTRACT

Exposure to alcohol in utero produces a wide spectrum of morphological and behavioral outcomes in the offspring, commonly referred to as fetal alcohol spectrum disorders (FASD). Limited studies are available on craniofacial malformations and tooth anomalies associated with FASD. One possible mechanism for the detrimental effects of alcohol is its interactions with signaling pathways such as Wnt which are important for proper tooth development. To study the harmful effects of alcohol, zebrafish (*Danio rerio*) has been identified as a well-established animal model.

The present study attempts to investigate the effect of alcohol on early zebrafish tooth development. The effects of prenatal alcohol exposure on tooth length, width, number, and shape were analyzed at 15, 20, 25, and 30 dpf. To examine the Wnt-alcohol interaction we analyzed the effect of Wnt agonist, lithium chloride (LiCl), and Wnt antagonist, WC59, and their combination with alcohol on the development of the dentition. Whole-mount cartilage and bone staining and imaging techniques were applied to determine the effects of alcohol on the above-mentioned parameters. The whole-mount In-situ hybridization was used to determine the expression of Wnt10a and Wnt10b which are specific ligands responsible for tooth development.

The tooth height and width of the alcohol-treated samples were significantly less than the control at 15 dpf {(height- 58.29 ± 0.90 µm vs. 69.81 ± 0.39 µm), (width- 14.29 ± 1.24 µm vs. 22.73 ± 0.87 µm), $P < 0.001$)} and 20 dpf, {(height- 63.96 ± 1.56 µm vs. 72.40 ± 0.72 µm), (width- 22.35 ± 1.15 µm vs. 24.65 ± 0.61 µm), $P < 0.001$)}, but at 25 and 30 dpf, there was no significant difference ($P > 0.05$). No significant change was seen in the number of teeth in alcohol-treated samples ($P > 0.05$). In the LiCl treatment group, we observed an increase in the tooth length and width ($P = 0.001$) and a decrease in these metrics in the WC59 treated samples compared to the control at all time points ($P < 0.001$). Interestingly, the combined treatments of alcohol and LiCl as well as alcohol and WC59 showed a noticeable decrease in tooth length and width compared to the control or alcohol-only treatment at 15, 20, 25, and 30 dpf ($P < 0.001$). Compared to controls, Alizarin red-stained whole-mount zebrafish samples showed hypo-mineralized enamel tissues at treated samples at all time points.

This study summarizes the effects of alcohol and its interaction with the Wnt signaling pathway on the development of dentition and highlights the importance of zebrafish in studying the phenotypic characteristics of fetal alcohol spectrum disorder.

ACKNOWLEDGEMENT

I express my heartfelt gratitude to my supervisor, Dr. Devi Atukorallaya for the opportunity and support throughout the last two years. I will fall short of words to express how thankful I am to her. I express my sincere gratitude for her advice and guidance and also for her valuable feedback throughout this project. Her great patience and kind guidance were very important to complete this project successfully.

Secondly, I would like to thank my committee members, Dr. Kangmin Duan and Dr. Barbara Triggs-Raine for their encouragement and guidance throughout my research project. Their in-depth analysis of my project further helped me to develop my project.

I could not have completed this work without the unwavering support of Dr. James Gilchrist. Dr. Gilchrist your patience and guidance made this work possible.

Next, I also thank our team of smart Summer/Co-op students Emma Cwiklinski, Natasha Hargreaves, and Justin Lane.

Special thanks go to Vivianne, Nisha, and Ankita for every little support they provided me, the assistance in laboratory work, and helping me with handling the equipment.

I must acknowledge the wonderful lab mate I have made in this journey. Special thanks go to Praneeth: My word will not do enough justice to express the gratitude that I have towards you. I treasure every bit of lab work we shared. Thanks for making this 2-year journey so memorable for me.

Finally, I am much grateful to the University of Manitoba and the Natural Sciences and Engineering Research Council, Canada (NSERC) for funding this study and supporting the Atukorale lab.

DEDICATION

Dedicated to my loving parents and my sister for their valuable support, sacrifice, and love throughout my academic journey.

&

To my husband, Faraz Moharrami, for inspiring me every day to be the best version of myself. Without his endless love and support, I wouldn't have had the courage to tackle my dreams.

TABLE OF CONTENTS

LIST OF FIGURES

LIST OF TABLES

LIST OF ABBREVIATIONS

FASD- fetal alcohol spectrum disorder

FAS- fetal alcohol syndrome

CNS- central nervous system

ARBDs- alcohol-related birth defects

CLP- cleft lip with or without cleft palate

CP- cleft palate

PAR- peer assessment rating

DNA- deoxyribonucleic acid

RNA- ribonucleic acid

Shh- the sonic hedgehog

CYP2E1- cytochrome P450 2E1

O_{2^-} superoxide anion radical

$H_2O_{2^-}$ hydrogen peroxide

OH- hydroxyl radical

Wnt- wingless Int-1

FZD- frizzled receptor

TGFβ-transforming growth factor β

BMPs- bone morphogenic proteins

FGF- fibroblast growth factor

SOD- superoxide dismutase

DMFT- decayed, missing and filled teeth

dpf- days post fertilization

MD- mediodorsal

D- dorsal

hpf- hours post fertilization

Int--1integration site 1

MMTV- mouse mammary tumor virus

OODD- odonto-onycho-dermal dysplasia

SPSS- schöpf—schulz—passarge syndrome

EtOH- ethanol

LiCl- lithium chloride

WC59- Wnt-c59

cb5- fifth ceratobranchial

V- ventral

CCAC- canadian council of animal care's requirements

MS222- tricaine methanesulphonate

PFA- paraformaldehyde

PBS- phosphate-buffered saline

KOH- potassium hydroxide

TP- tip of the tooth

UB- the uppermost point of the base of the tooth

LB- the lowermost point of the base of the tooth

DepC- diethyl pyrocarbonate

WMISH- whole-mount in-situ hybridization

SPSS- statistical product and service solutions

EKW- ekkwill

TU- Tubingen

CHAPTER 1: INTRODUCTION

1.1. Birth defects

Birth defects are complex, multifactorial conditions that refer to "any anomaly, functional or structural, that presents in infancy or later in life and is caused by events preceding birth, whether inherited or acquired (1, 2). In the United States, birth defects are estimated to impact 3% of newborns, accounting for 20% of all infant deaths (3). Birth defects develop from complex interactions between genetic and environmental factors (4) such as alcohol, folic acid deficiency, maternal diabetes, infection, and pharmaceutical agents. The overall number of these factors can be inconceivably large. Given that at least 80,000 synthetic chemicals are created annually, it is difficult to even grasp how environmental influences affect birth abnormalities with a greater magnitude more being produced naturally (5). The onset, duration, and dosage of alcohol exposure, as well as genetics, can vary the effects environmental factors have on the developing fetus, further complicating our knowledge of the genesis of birth abnormalities (6). Genetic influences might also be confounding. Numerous types of genetic variation exist, including major chromosomal rearrangements, splicing anomalies, insertion/deletions, and single nucleotide polymorphisms (1). The variance in phenotypes we observe in the human population is caused by these changes (7, 8). Additionally, many genetic modifications that cause phenotypes to manifest only do so in conjunction with other genetic and/or environmental factors (9-11). It can be challenging to determine how genetic and environmental variables contribute to birth abnormalities in clinical populations since sample numbers, reliance on self-reports, and ethical issues are significant barriers (11). Although infant death rates have declined over the past 40 years (12, 13), birth abnormalities continue to create permanent physiological and psychological problems that necessitate substantial, costly medical care that can reach $1 billion in annual costs (CDC 2007). As a result, birth abnormalities remain a serious public health concern. Unfortunately, we lack methods to prevent and/or treat the causes of birth abnormalities because the underlying etiologies are still poorly understood (9-11).

1.2. Fetal Alcohol Spectrum Disorder (FASD)

Alcohol which has the chemical name of ethanol / ethyl alcohol is a well-established teratogen and the most popular psychoactive drug (14, 15). Alcohol addictions are due to several factors such as ease of preparation, traditional usages, social and cultural acceptance of alcohol as a beverage (16). Consuming alcohol during pregnancy is a serious health problem that can have adverse impact on

a developing fetus (2). In 1968, Lemoine and colleagues first described a set of birth defects identified in 127 children exposed prenatally to ethanol (17). Shortly after, in 1973, Jones and Smith coined the term Fetal Alcohol Syndrome (FAS) to described the constellation of birth defects that results from prenatal ethanol exposure, which included growth impairments, developmental delay, craniofacial malformations, central nervous system (CNS) abnormalities and heart, limb, and kidney anomalies (18, 19). Since 1973, a larger range of morphological and organ deformities as well as cognitive deficits have been added to the list of birth defects linked to prenatal ethanol exposure. These deficits are now generally referred to as FASD (20-24). They may also involve functional comorbidities like attention deficit and hyperactivity disorder, learning challenges, speech delays, intellectual disabilities, coordination and fine motor impairments, and other long-term health problems. This umbrella term identifies the "range of outcomes from prenatal alcohol exposure" from alcohol-related birth defects (ARBDs), which are hard to diagnose, to FAS, the most apparent and severe form of FASD (25, 26). The prevalence of FASD incidence in general population is approximately 0.77% (21, 27), ranging from 2-5% in United States to 30% in some parts of the world with higher incidences of binge drinking (24, 28, 29). In Canada, where the prevalence of FASD has been estimated at 1 in 100 people, which corresponds to more than 330,000 affected individuals in Canada, prenatal alcohol exposure is the primary cause of neurodevelopmental impairments (19, 30). However, these numbers are typically thought to be an underestimate, and the percentage of kids with suspected FASD may actually be much higher (31). Children exposed to prenatal alcohol are underdiagnosed, and adult diagnoses of FASD are uncommon due to social stigma, a lack of knowledge about the illness's prevalence, as well as poor screening and diagnostic capabilities (32). To improve FASD research and clinical care, a globally recognised diagnostic method is required (33). It is anticipated that in the near future there will be greater awareness of the risks of prenatal alcohol exposure, and new public health initiatives will evolve to reduce exposed pregnancies, more effective and accessible diagnostic tools, and develop treatments that focus on the effects of prenatal alcohol exposure at multiple levels of functioning (24).

1.3. Craniofacial malformations

Over one third of all congenital birth defects are craniofacial malformations, which are a variety of developmental defects affecting the differentiation and growth of the skull (craniosynostosis), facial bones (hemifacial microsomia, deformational plagiocephaly), jaw (micrognathia, cleft lip with or without cleft palate, and cleft palate only), and teeth (tooth agenesis) (2, 4). The most

typical manifestations of craniofacial dysmorphology in FASD are short palpebral fissures, a smooth philtrum, and a thin upper lip vermilion (34). One of the most prevalent craniofacial deformities in children with FASD is cleft lip with or without cleft palate (CLP) or cleft palate only (CP), which results from a failure of neural crest-derived processes to fuse during face development (35, 36). The development of the CLP and CP in response to alcohol exposure has been established by numerous investigations using rodent, avian, fish, and Xenopus models (37-39). Alcohol has been shown to slow the growth of the ethmoid bone in zebrafish models by altering the number, shape, and stacking of chondrocytes as they develop into cartilage (40-42). Other craniofacial traits associated with FASD include maxillary hypoplasia, malformed noses (small, upturned, cleft, and flat nasal bridge), and deformed ears (narrow canals, prominent/deformed pinnae, and otosclerosis). The philtral region of the upper lip, the alveolar ridge containing the upper incisors, and the anterior portion of the hard palate all fail to develop properly in alcohol-treated mouse embryos, according to analysis (43, 44). Early chick embryos exposed to ethanol show a marked increase in the prevalence of parietal bone deformities and premaxilla shortening, which can result in malformations of the midface (45).

Alcohol-related birth defect is a rare diagnosis that is made when there is a prenatal alcohol exposure history and a malformation that is known to be associated with prenatal alcohol exposure (eg, affecting the cardiovascular or skeletal system) (29, 46).

Malocclusions can give additional hints for diagnosing FASD in later life when some facial characteristics may have become less obvious (47). The peer assessment rating (PAR) index is a widely accepted and commonly used method with a high reliability to evaluate the severity of malocclusions and to compare treatment results and success (48). These malocclusions could be due to anomalies in the upper anterior jaw segment and the transversal plane. Notably, crossbites or edge-to-edge bites are significantly more prevalent in this group. (49). It is advised that children with FASD have early and ongoing orthodontic care in order to identify and correct malocclusions that could cause facial asymmetry (47).

1.4. Mechanisms of alcohol teratogenicity

There are numerous theories as to how alcohol causes birth defects (2, 16, 50). Studies have shown that alcohol diffuses through the placenta and distributes rapidly into the fetal compartment (51-53) where alcohol also has a slower elimination rate (54)—accumulating in the amniotic fluid (52). Alcohol can affect at three main stages (1) gametogenesis, 2) preimplantation and 3) gastrulation

of embryogenesis and could cause epigenetic modifications to the manifestations of FASD (55, 56). Animal models have provided the first strong evidence that alcohol was indeed teratogenic (24). For example, murine and zebrafish studies on FASD, suggested that DNA methylation, posttranslational histone modification, and noncoding RNAs disruptions are the frequent epigenetic mechanisms affected by the alcohol exposure (57, 58). Further, the suppression of Hox gene activity due to upregulation or downregulation of miRNA in developing mouse brain can impair cell cycle induction and stem cell maturation, which may result in malformations in the central nervous system. These findings highlight the importance of proper regulation of miRNA expression during brain development to ensure proper neural development and function. (59). Further, alcohol competitively affects retinoic acid biosynthesis pathways and its metabolism in embryos of zebrafish, frog, and mouse. This directly leads to the developmental malformations in craniofacial region and skeleton in vertebrates (40, 60, 61). Studies conducted on zebrafish, chicken and mouse embryos have shown that alcohol inhibits the mevalonate pathway and cholesterol biosynthesis, which adversely affects the sonic hedgehog (shh) signal transduction pathway which leads to characteristics midline phenotypes of cyclopia, holoprosencephaly, craniofacial hypoplasia, loss of midline craniofacial structures, neural tube defects, and neural crest-specific cell death (62-64). Embryonic alcohol exposure also interferes with insulin signaling leading to neurodevelopmental abnormalities such as impaired viability, metabolism, synapse formation, and acetylcholine production (65). Alcohol exposure inhibits some enzymes which are produced in the Golgi apparatus which leads to cytoplasmic retention of multiple polysial neural cell adhesion molecules and impairs cellular interactions and causes cellular migration-related errors, heterotopias, morphological brain defects (64, 65). This causes defects in the neuron–glia interaction, synaptogenesis, neuronal migration, growth, and morphogenesis (64). Furthermore, alcohol can compromise endogenous antioxidant capacity, for example, by decreasing glutathione peroxidase levels or generating free radicals as by-products of its Cytochrome P450 2E1 (CYP2E1) metabolism (15, 66). The above explained cellular defects are initiated with the formation of reactive superoxide free radicals such as superoxide anion radical (O_2), hydrogen peroxide (H_2O_2) and highly reactive hydroxyl radical (OH) within the cell during the metabolism of the alcohol molecules (67). During neurogenesis these highly reactive agents target polyunsaturated fatty acids side chains in brain tissue membranes which can then lead to inhibition of cell differentiation, disturbance of cell–cell interactions, and changes in cellular metabolism which leads to uncontrolled apoptosis (68). Numerous studies showed that alcohol can affect Wingless Int-1 (Wnt) signaling pathway (69, 70). Inhibition of Wnt signaling can occur after chronic alcohol consumption through oxidative stress and result in inhibition of bone formation

accompanied by increased bone marrow adiposity (71). It has been shown that fourteen transcripts associated with Wnt signaling were altered by alcohol treatment (72). One of the most highly downregulated Wnt factors was the Frizzled receptor (FZD5), which was lowered to nearly undetectable levels in alcohol-treated cells (72).

1.5. Tooth development in human

Teeth develop from the underlying mesenchyme that comes from the neural crest, the surface ectoderm of the first branchial arch, and the frontonasal prominence (73). At the locations of the future dental arches of the maxilla and the mandible, a thicker epithelial stripe called the dental lamina forms before the creation of individual teeth. Long ago, detailed descriptions of the developmental anatomy and histology of tooth morphogenesis were published (73). The creation of the epithelial placode, epithelial budding, mesenchyme condensation surrounding the bud, and folding and growth of the epithelium, which produces the shape of the tooth crown, are the key aspects of tooth morphogenesis (73). Dentin and enamel, two mineralized components that are distinctive to teeth, are created by specialised cells called odontoblasts and ameloblasts, which separate from mesenchyme and epithelium, respectively. The primary regulatory mechanism directing the development of teeth is communication between the two tissues, the epithelium and the mesenchyme (73). The initiation and morphogenesis of the tooth, as well as the differentiation of the odontoblasts and ameloblasts at the interface of the two tissues, are regulated by a series of reciprocal epithelial-mesenchymal interactions. In the past 15 years, researchers have discovered the "language" used by epithelial and mesenchymal cells to communicate (74, 75). Cells communicate in the same language throughout the embryo and during all developmental processes, and this language has endured throughout evolution (76). It is composed of mainly secreted signal molecules and growth factors. Members of the four preserved families Transforming Growth Factor β (TGFβ) (which includes Bone Morphogenic Proteins (BMPs) and activins), Fibroblast Growth Factor (FGF), hedgehog (which only contains Shh), and Wnt are the most researched and widely used signals. There are several molecules involved in the signal pathways in addition to the actual signals, most notably cell surface receptors, transcription factors that mediate the signal to the nucleus, and molecules that control gene expression (76).

1.6. Effect of prenatal alcohol exposure on tooth development

Tooth development shares several common features with organs as morphologically diverse as

hair, and mammary glands as the origin of all these organs are neural crest cells (77). It is a transient population of cells that arises during the early stages of embryogenesis at the junction between the neuroectoderm of the closing neural tube and the surface ectoderm through a series of interactions between these two tissues (78, 79). Numerous studies have shown that alcohol adversely affects multiple events in neural crest cell development (80-82). Moreover, alcohol exposure causes abnormal neural crest cell migration patterns such as loss of left–right symmetry and increased apoptosis (83). The lower endogenous superoxide dismutase (SOD) activity in neural crest cells may enhance their sensitivity to the stress of reactive oxygen intermediates (84, 85). Oxidative stress and free radicals together contribute to the apoptosis of alcohol-exposed neural crest cells (16, 67). The development of cranial neural crest populations is most commonly affected by alcohol, with reductions in their derived facial bone and cartilage, cranial nerves, and tooth structure (5, 80). There are many animal studies that focused on the effect of alcohol on developing dentition (86, 87). The eruption of teeth were delayed in offspring of macaque monkeys whose mothers were exposed to ethanol (88). In rat, retardation of the molar tooth eruption was seen on postnatal day 14.5 (89). Another study demonstrated a delay in eruption and post eruptive growth of the incisors in offspring whose mothers had been given ethanol intraperitoneally on the seventh day of pregnancy (gastrulation period) (90). Alcohol exposure in pregnant mini-pigs produces ultrastructural changes in secretory ameloblasts, retardation of cell differentiation within the tooth germ and calcification of the dentin matrix (91). Furthermore, it has been shown that alcohol exposure during pregnancy influences the secretory function in the ameloblasts, which in turn influences enamel formation (91). Another animal study has shown that alcohol exposure results in reduced development of the tooth germ and has the most severe effect on enamel matrix formation (44).

The article by Streissguth et al. was the first to describe dental position alterations and malocclusions in patients with prenatal alcohol exposure (92, 93). Agenesis, twisted teeth, and diastemas were all noted by Church et al. who were the first to clearly detail the quantity and shape of dental defects in serial cases of 22 people (94). The presence of dental abnormalities and alterations was amply demonstrated in Andrade's work, along with a correlation between these findings and systemic renal changes that result from the same genetic flaw as numerous tooth abnormalities (95). Naidoo et al. study which compared 90 people with FAS to a control group, found no instances of an enamel structural anomaly (96). The DMFT index (caries severity score indicating caries incidence: Decayed, Missing and Filled Teeth) was higher in children with FASD compared to the control score, although statistically not significantly different, and the missing teeth accounted for the majority of this index in both groups, according to a recent study by Blanck-

Lubarasch et al (36). Similar to this, Da Silva et al. found that the prevalence of caries was much greater in the 68 children with FASD when compared to the control group (97% vs 64.7%) (19).

1.7. Animals model to study FASD

Due to the difficulty in accurately quantifying some variables, such as maternal diet or health, or the amount and timing of ethanol exposure during pregnancy, FASD studies in humans have common limitations (97). Numerous experimental model systems are being made by scientists to investigate how ethanol affects the growing embryo. For many years, a number of animals have been employed to research the consequences of fetal alcohol exposure (98). Animal models offer a genetically tractable platform that enables reliably reproducible investigations and allows for a level of genetic and environmental control that is not attainable in human studies (99). Animal models for the study of FASD that have been exposed to alcohol range across the animal kingdom, from fruit flies to higher vertebrates. Zebrafish, xenopus, chicken, rat, and mouse are popular vertebrate models (26). Each animal model has strengths that make them suitable for figuring out the aetiology of ethanol-induced birth abnormalities, despite the fact that no single animal model completely recapitulates all symptoms of FASD in humans (1). The effectiveness of an animal model heavily depends on how the alcohol therapy was handled and the outcome. The research of FASD benefits greatly from the use of mammals (100). Although primates might represent the gold standard, there are several drawbacks, namely the lengthy study times and ethical limitations (100). Rodents are the most commonly used mammals in FASD research because they are simple to handle, have a short gestation period, have a large number of offspring, and can be used to evaluate how prenatal alcohol exposure-related impairments affect metabolic pathways, molecular biology, cell signaling, synaptic plasticity, and cognition during foetal development. This facilitates the investigation of factors influenced by alcohol exposure at the neuroanatomical, neurochemical, and behavioral levels (101). Additionally, by accurately defining the alcohol use pattern (timing and dose), it is possible to identify time-sensitive windows and thresholds for dangerous doses during pregnancy (101). Compared to mice, rats have the advantages of being bigger and having more complex behavior. Mice, especially those of the C57BL/6 strain, are the most often used mammal due to their simplicity of care, accessibility to transgenic and disease models, short lifespan, and fundamentally similar genetics and physiology to humans. Alcohol intake has been linked to teratogenic effects in mice, including skeletal and soft-tissue defects, altered neurogenesis processes, and craniofacial deformities (102, 103). The biggest drawback of

utilizing rodent for FASD research is that, unlike humans, they spend their third trimester after birth; Therefore, without the impact of the placental barrier, the mechanisms of absorption, distribution, metabolism, and elimination in rodents differ from those in the human uterus (104). Among the fish models, zebrafish has been emerged as an excellent model for FASD (105). Zebrafish are easy to keep, have external fertilization (106) so eggs are not affected by any placental influence or parental care (107), have rapid development, and ethanol metabolizing genes (108) have evolutionarily conserved between zebrafish and humans. Thus, zebrafish can model human development and be used to study effects of teratogenic factors, like ethanol (109).

1.8. Zebrafish (*Danio rerio*)

1.8.1. Zebrafish as a model organism

Zebrafish (*Danio rerio*) is an important model organism in biological research in recent times (42, 110, 111). It is a bony fish (teleost) that belongs to the family Cyprinidae under the class Actinopterygii (ray-finned fishes) (112). Zebrafish is a tropical freshwater fish, inhabitant of rivers of Himalayan region of South Asia particularly India, Nepal, Bhutan, Pakistan, Bangladesh, and Myanmar (113, 114). They live in shallow ponds, canals, and streams, preferably in still or slowly moving waters that range in temperature from 6°C to 38°C (115); hence, they can be well maintained in aquaria made of high-quality plastic and glass (116). The capacity of the tank is determined as per the number of fish housed. A maximum of 10-12 zebrafish can be accommodated in 10 gal. of water. Soft water is ideal (117) for the housing of zebrafish, particularly when a pH of 7 is maintained (118). Being omnivorous, zebrafish eat both plant and animal material, including zooplankton, insects, algae, fish scales, sand, dirt, and invertebrate eggs (119). George Streisinger (University of Oregon) employed Zebrafish as a biological model for the first time in the 1970s because it was less complex than mice and easier to genetically alter (120). The idea of employing zebrafish embryos to examine the cell differentiation and organization of the nervous system greatly intrigued Streisinger's colleagues, especially Chuck Kimmel at his university (121, 122). Zebrafish have been employed for in vivo chemical toxicity testing more and more, despite the fact that mammals are still thought of as the gold standard for developmental toxicity evaluation (123, 124). Zebrafish models have been successfully used to study the developmental, reproductive, cardiovascular, neurodevelopmental, and ocular developmental toxicity of hazardous substances (125). Considering this, in 2021, a quick search in the PUBMED/ NCBI database with “zebrafish” as a keyword resulted in about 42,700 articles

(110). Due to the continual development and accessibility of a wide range of materials and methodologies, zebrafish stands out among the teleost as a popular fish model used worldwide to comprehend human diseases. Currently, thousands of transgenic and mutant zebrafish types are housed in three international centers, including centers in North America, Europe, and China (https://zebrafish.org/home/guide.php https://www.ezrc.kit.edu/; http://en.zfish.cb/SocietyEN.html). These facilities offer unrestricted access to hundreds of phenotypes that imitate the symptoms of human diseases (42). Zebrafish have many physiological and genetic similarities with humans, including the innate immune system, musculature, and digestive tract (126-128). In addition, 70% of human disease genes share functional similarities with zebrafish genes (129) allowing for a more direct extrapolation of results than studies utilising invertebrates. This justifies the large investment in this species in a number of translational scientific research fields (130). Scientists use zebrafish because of the wide range of characteristics that make it a great model organism. Despite having different morphology and histology from mammals, including the absence of certain organs like the lungs, prostate, and mammary glands, it retains the basic features of the vertebrate body plan and its structural, molecular, and physiological components (131, 132). The embryo develops quickly outside of the mother and is optically clear, making it simple to experiment with and observe. The blastula stage of the embryo only lasts for three hours, and gastrulation is finished in five. At roughly 18 hours, the embryo is transparent and has exceptionally well-developed ears, eyes, segmenting muscles, and a brain (133). By 24 hours, segmentation is finished, and the majority of the principal organ systems have developed. The embryo emerges from the egg shell at 72 hours and begins searching for food two days later. The embryo transforms quickly over the course of just 4 days into a little version of an adult (133). With a generation time of only around 10 weeks, adult zebrafish reach sexual maturity relatively quickly. This little fish also has a high fertility rate (134). The zebrafish can lay about 200 eggs per week when kept under optimal conditions (135). This fish model can spawn all year round in lab settings, ensuring a steady supply of offspring from selected partners. This transparent fish is therefore an ideal candidate for large-scale genetic techniques to identify novel genes and to learn more about their specialised functions in vertebrates (136, 137). Since transgenes can be injected into the cytoplasm of zebrafish rather than the pronuclei of mouse embryos, the equipment required for this type of operation is less expensive, and the method itself is simpler (138). The zebrafish is a very hardy fish and is very easy to raise. In addition to the previously listed characteristics, zebrafish also have very low space and maintenance requirements. This fish is a desirable model organism for developmental, toxicological, and transgenic studies because of these characteristics (139).

Figure 1.1: The zebrafish (Danio rerio). (A) Zebrafish embryo in the egg. (B) Adult zebrafish.

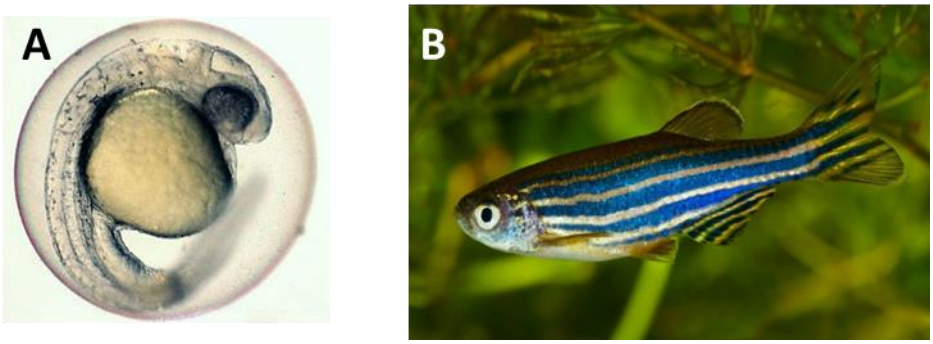

1.8.2. Zebrafish as a model organism to study craniofacial and tooth development

Zebrafish has long been regarded as a viable model for research on craniofacial morphogenesis and the connections between genetic and environmental factors that lead to craniofacial abnormalities. Several studies summarize the application of zebrafish models in understanding craniofacial development (140, 141) and anomalies (142-145), as a model for orofacial clefts (42, 145, 146), and to study the effect of hormones on craniofacial malformations (147). Moreover, zebrafish have also been employed in dentistry research for purposes such as determining the toxicity and safety of dental products (148-150), studying oral infectious diseases (151-155) and the risk of systemic diseases as a result of periodontitis (152, 156-159). The zebrafish is a popular model for illustrating how the cranial sutures and skull vault grow. The zebrafish neurocranium anterior end is similar to the mammalian hard palate (140). The polyphyodonty homodont dentition of teleosts gave rise to the specialised diphyodont and heterodont dentition of humans (160). A robust vasculature processes tooth formation and replacement in the zebrafish dentition (161). Zebrafish have been employed by researchers to examine the phenotypic variety of human birth abnormalities because of these similarities (112).

Since zebrafish are polyphyodonts, they undergo numerous tooth replacement cycles over the course of their lifetime (162). Zebrafish have no teeth in their mouths; instead, they have teeth on their fifth ceratobranchial (cb5) arches, also referred to as their pharyngeal jaws (163). This bone carries three rows of teeth, the ventral (V), mediodorsal (MD) and dorsal (D) rows, which present five ventral teeth (1 V–5 V), four mediodorsal teeth (1 MD–4 MD) and two dorsal teeth (1 D–2 D) in adult fish (164), respectively. Around 48 hours after fertilisation (hpf) the epithelium lining

the cb5 bone begins to thicken (165, 166). An asymmetrical bell-shaped enamel organ is created as the thicker epithelium gradually invaginates into the underlying mesenchyme (165). The cytodifferentiation of the cells in the enamel organ results in the formation of enamelloid and dentin. When fully developed, the teeth emerge into the pharynx cavity and attach to the pharyngeal bone. In zebrafish, the first tooth to erupt is 4V1 at 4 days post fertilisation (dpf). There are a few differences between zebrafish and mammalian tooth development. For instance, it is impossible to distinguish the crown from the root of a zebrafish tooth, the underlying dentin lacks dentinal tubules, and the teeth are covered in a layer of hyper-mineralized enameloid rather than enamel (166, 167). Other than these differences, zebrafish tooth is a fine model for studying tooth development.

Figure 1.2: lower pharyngeal jaw containing the pharyngeal teeth in adult zebrafish (168). Lower pharyngeal jaw bears three rows of teeth, the ventral (V), mediodorsal (MD) and dorsal (D) rows, which present five ventral teeth (1 V–5 V), four mediodorsal teeth (1 MD–4 MD) and two dorsal teeth (1 D–2 D).

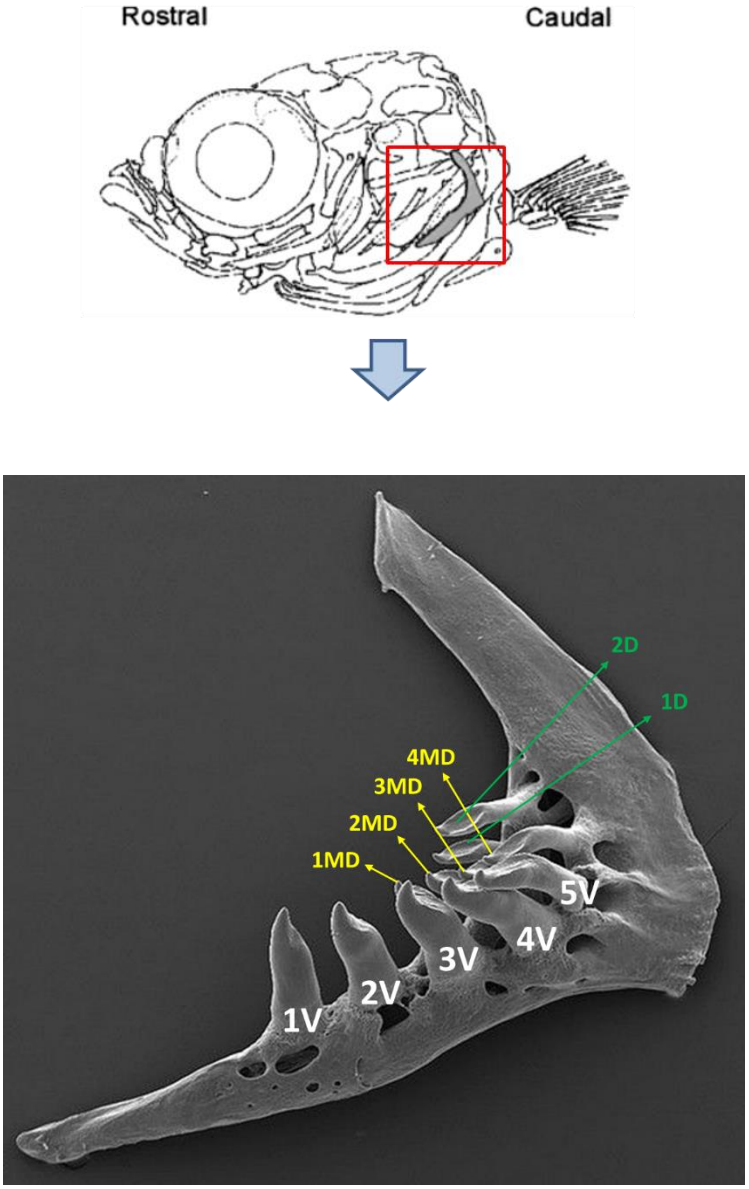

1.8.3. Zebrafish as a FASD model

The zebrafish is a well-known model that has a variety of experimental, biological, and behavioural traits that make it an excellent choice for researching how embryonic ethanol affects development (169). Early gastrulation and neurulation alcohol exposure in zebrafish resulted in a variety of craniofacial abnormalities, which are indications of FASD (112). Mammalian models, such as mice, are more similar to human development, but in utero development is difficult to study, particularly early developmental stages (169). Zebrafish can produce hundreds of fertilized eggs per mating, allowing many embryos to be studied (98). These embryos are externally fertilised, therefore the same breeding couples can be used repeatedly for various research without sacrificing the mothers (1). This prevents variance caused by maternal physiology and rearing, making high-throughput investigations possible that are not possible with mammalian models.
In addition, zebrafish embryos allow for control of the onset, duration and dosage of the alcohol exposure (98). In contrast to the majority of alcohol administration techniques used with mammals, zebrafish eggs can be submerged in an alcohol solution, and the developing embryo inside the egg can absorb alcohol (98). The embryos are simply taken out of the ethanol solution and put in untreated embryo medium to cease the exposure to ethanol. Zebrafish can therefore be used to research acute, discreet, and/or chronic ethanol exposures in a variety of dosages in hundreds of embryos at once. Zebrafish embryos are also translucent, making them an effective tool for in vivo imaging assessments. Researchers are now able to link the effects of early developmental stages to later structural and behavioral results. The most significant factor is that zebrafish have a wide range of tools for genetic modification, from transgenesis to the most recent developments in CRISPR/Cas mutagenesis. As was already mentioned, the entire zebrafish genome has been sequenced, allowing researchers to use reverse genetics to introduce mutations and observe the results (170). Zebrafish are not the only animals that have high fertility and external fertilisation. For ethanol-treatment paradigms and live imaging investigations, Xenopus and other fish species both produce a lot of external embryos. Even though there are fewer experiments with chickens, live imaging and explant analysis are still possible. The genetic capabilities of zebrafish are not shared by Xenopus, chickens, or other fish species. Mice offer a potent genetic model, though direct manipulation of embryos and subsequent imaging can be challenging and frequently result in the sacrifice of the mother and embryo, restricting longitudinal embryonic investigations. In addition, the onset, duration, and dosage of the ethanol exposure in producing the FASD abnormalities in zebrafish are straightforward and accurate in comparison to rodent models. The zebrafish has quickly demonstrated strong conservation of the impact ethanol has on development,

which is comparable to other model systems, despite the fact that no particular research attribute is unique to zebrafish and that it was not the first to start characterising the complex etiology of FASD. In the end, the combination of the tools in zebrafish that make it a potent model to explore the etiology of FASD constitutes the special contribution of zebrafish to FASD research (1, 171, 172).

1.9. Wnt signaling pathway

In 1982, Nusse and Varmus discovered the first Wnt gene, also known as integration site 1 (int-1), as a gene that was triggered by the integration of the mouse mammary tumor virus (MMTV) in virally produced breast cancers (173). The secreted, cysteine-rich protein encoded by Int-1 is challenging to purify into a biologically active form. Genetic systems were used to initially identify the signalling pathway linked to this protein. In 1987, the fly Wingless gene, which controls segment polarity during larval development in Drosophila melanogaster (174), was shown to be a homolog of int-1(175). Because of the homology between int-1 and Wingless, the gene was renamed Wnt1 (Wingless plus int1) (176) and was eventually recognized as the founding member of a large Wnt gene family. The cysteine-rich, glycosylated, lipid-modified secreted Wnt proteins, which have a molecular weight of about 40,000, regulate embryonic development, cell proliferation, differentiation, and migration. At least 19 Wnt proteins have been identified in mammals (173). The canonical signalling pathway and the noncanonical signalling pathway are two separate Wnt signalling pathways that have been identified. The -catenin-dependent canonical Wnts, including as Wnt1, Wnt2, Wnt3, Wnt3a, and Wnt7a, make up one class of Wnt proteins. The noncanonical Wnts, which act independently of or inhibit the canonical Wnt signalling pathway, include Wnt4, Wnt5a, Wnt5b, Wnt6, and Wnt11 (173).

1.9.1. Role of Wnt signaling pathway in tooth development

The Wnt signalling pathway was first directly linked to tooth development in the late 1990s. In both humans and mice, the dental epithelium and mesenchyme express a number of Wnt signalling molecules, including as Wnt ligands, receptors, transducers, transcription factors, and antagonists, throughout the development of the tooth (177, 178). Wnt 3, Wnt4, Wnt6, Wnt7b, and Wnt10b are expressed in the epithelium. Wnt5a shows localized expression in the mesenchyme and dental papilla. Similar expression patterns of Wnt3, Wnt5a, LRP5, Fz6, -catenin, Lef1, and Dkk1 are seen in mouse and human tooth development (178). Targeting the canonical Wnt pathway has an

impact on tooth development. Nuclear catenin is found in the dental epithelium and the underlying mesenchyme during tooth development, and the canonical Wnt signalling pathway is engaged at various stages of tooth morphogenesis. The formation of teeth with abnormal shapes is caused by the inhibition of canonical Wnt signalling, demonstrating the importance of canonical Wnt signalling in the early development of teeth (173).

1.9.2. Wnt10a and Wnt10b function in tooth development

Wnt10a is a ligand in the Wnt/β-catenin pathway that is expressed in the dental epithelium and mesenchyme at the bud stage and cap stage (173). Recent evidence has shown that Wnt10a mutations play a major pathogenic role in human tooth agenesis (179, 180). Wnt10a mutations have been reported in various ectodermal dysplasia syndromes, rare autosomal-recessive odonto-onycho-dermal dysplasia (OODD) (181, 182), and severe autosomal recessively inherited Schöpf—Schulz—Passarge syndrome (SPSS) (183-185). OODD and SSPS share a common ectodermal dysplasia involving hair, teeth, nails, and skin, characterized by dry hair, hypodontia (tooth agenesis), smooth tongue, nail dysplasia, hyperkeratosis of the skin, and palmoplantar keratoderma. Currently, OODS and SSPS are considered a part of the same disorder within the Wnt10a mutations (186, 187). Additionally, Wnt10a mutations have been described to be the most common causes of non-syndromic severe hypodontia with minor signs of ectodermal dysplasia (188) and autosomal dominant inherited isolated hypodontia. Other research revealed that the condition taurodontism, which is defined by problems in the tooth root furcation of deciduous molars, was present in dysplasia and biallelic Wnt10a mutations (189). Moreover, Wnt10a-/- mice show taurodontism (190, 191), indicating that there must be a significant role of Wnt10a in tooth root morphogenesis (192).

Wnt10b was first implicated in isolated tooth agenesis in one family where oligodontia was discovered to be inherited as an autosomal dominant condition, as well as in three other unrelated people (193). The mouse dental epithelium was found to co-express Wnt10b and Wnt10a during the earliest stages of tooth development. Wnt10b was initially restricted to the incisor epithelium, but as tooth development progressed, it began to express itself distally in the molar primordia (194). Although, there are limited studies about the role of Wnt10b in tooth development, it has been proved that the inhibition of Wnt10b can have adverse effects in the development of the dentition.

Figure 1.3: Canonical Wnt-β-catenin pathway. In the presence of a Wnt signal, as the dishevelled protein (Dvl) recruits the Axin2 and inhibits GSK-3, β-catenin is not phosphorylated and therefore not destroyed. It can translocate to the nucleus and activate transcriptions genes. Through inhibition of GSK-3 beta, lithium chloride (LiCl) activates canonical signaling pathway. Extracellular exportation of WNT ligand is prohibited due to a lack of a necessary lipid attachment to WNT by WC59.

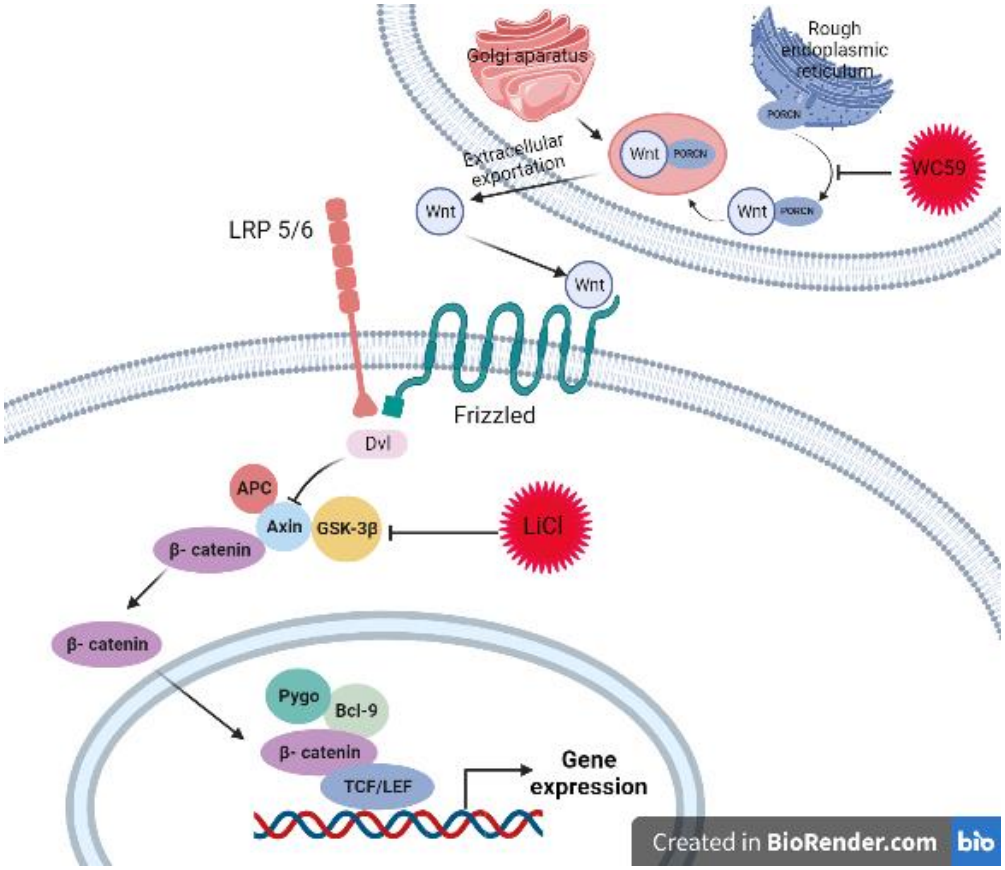

CHAPTER 2: HYPOTHESIS, OBJECTIVES, AND RATIONALE

2.1. Hypothesis

Exposure to alcohol during embryonic development and Wnt–alcohol interactions can cause defects in the tooth development.

2.2. Objectives and Rationales

Objective 1: To characterize the dental phenotype induced by alcohol in zebrafish

2.2.1. Rational for objective 1:

Numerous clinical and experimental animal studies show that embryonic alcohol exposure can affect the early tooth development. Zebrafish is an excellent model system to investigate the mechanisms of alcohol teratogenicity due to rapid, transparent early development and large brood sizes. The zebrafish embryos can be easily exposed to alcohol and the effect of timing and dosage of alcohol on development can be conveniently studied in zebrafish models. Studying zebrafish will provide many advantages toward understanding the effect of alcohol exposure on morphogenetic mechanisms of tooth development.

2.2.2. Sub-objectives:

1. To analyze the shape of the tooth in zebrafish
2. To analyze the mineralization of zebrafish dentition
3. To analyze the tooth length and width in zebrafish
4. To analyze the cusp length in zebrafish teeth

Objective 2: To identify the alcohol and Wnt signaling pathway interaction on zebrafish tooth development

2.2.3. Rationale for objective 2:

Alcohol exerts a variety of diverse effects on craniofacial and tooth development. Based on numerous studies, it has been found that alcohol exposure leads to ultrastructural alterations in secretory ameloblasts, which in turn affects the formation of enamel. Furthermore, the importance

of genetic determinants in regulating the effects of alcohol has been shown in various studies. Wnt signaling is vital for proper development of the head and face and plays important roles in various aspects of craniofacial development ranging from axis formation to survival of cranial neural crest cells to development of the dentition. Alcohol could interact with the Wnt cell signaling pathway and could cause tooth anomalies by causing defects in enamel matrix formation.

2.2.4. Sub-objectives:

1. To analyze the dental phenotype in zebrafish samples treated with the Wnt signaling pathway activator (LiCl) and inhibitor (WC59) and in combination with alcohol

2. To analyze the early expression of Wnt10a and Wnt10b genes which are specific for tooth development

CHAPTER 3: MATERIALS AND METHODS

3.1. Zebrafish Strains and Maintenance

These experiments conducted on male and female wild-type AB zebrafish (Danio rerio), purchased from zebrafish Genetics and Disease Models Core Facility, Hospital for Sick Children (Toronto, Ontario, Canada). The fish were housed in the Tecniplast rack system colonies according to Institutional Animal Care and Use Committee protocols at the central animal care facility at the Bannatyne campus, University of Manitoba. Water in the system circulates through the UV filters. The system's pH was 7.4, the water's conductivity was 764 µS, and the water's temperature was held constant at 27°C. The fish were given commercially prepared zebrafish food twice daily (Gamma micro 300 ZF, SKRETTING). For feeding fish of various ages, the following feeding schedule was used. Breeders were fed live Artemia fransicana (brine shrimps) and Gamma 300 diet. Gamma 150 food (Gamma micro 150 ZF, SKRETTING) and live Artemia fransicana were fed to 1-3 month-old fish. Gamma 75, Rotifera, and Artemia fransicana were used to feed fish that were under a month old (Gamma micro 75 ZF, SKRETTING). Larval fish of 5 dpf to 14 dpf were fed with Rotifera and gamma 75. Approximately three months old adult fish were primed two weeks prior to breeding. A second feeding of brine shrimp in the afternoon improved the frequency of feeding as well. Two males and two females were chosen for breeding based on their external appearance. Females with bloated stomachs that appeared to be carrying more eggs were chosen as good females. Two males and two females fish were placed in breeding tanks that were only partially filled with system water in the evening to prepare for breeding. Males and females were separated by a divider. A 27 °C water bath was used to set up the breeding tank for the night. The next morning, the partitions were taken down, and the breeding tanks were tilted slightly to create the typical beach breeding, where the female fish prefer to lay their eggs. The bottom of the tanks were checked for eggs three hours after the divider had been taken out, and breeders were taken out of the tanks. A disposable pipette was used to collect the embryos, which were then put in a clean Petri dish with water that had been prepared with 0.01% methylene blue. Using the aforementioned media, eggs were washed three times. The eggs that were dead or damaged were then removed after they had been examined under a microscope to establish their age. The eggs were put into sterile Petri dishes with 25 eggs each, embryo media (0.01% methylene blue in system water), and were then incubated at a temperature of 27°C. The animal care protocol numbers for the fish samples utilised in this experiment are 17-041 (AC11315) and 18- 021 (AC 11360). Adult zebrafish were kept on a 14/10 day/night cycle and fed a diet of live shrimp supplemented with Gemma 300. We obtained embryos through spontaneous spawning. The eggs were washed and raised under typical circumstances. Fish were grown in accordance with the

Canadian Council of Animal Care's requirements (CCAC).

3.2. Alcohol, Wnt signalling pathway activator (LiCl) and inhibitor (WC59) Treatment and Embryo Fixation

The samples were subjected to five different chemical treatments after 10 hpf. Namely, 1% of ethanol (EtOH) solution (Cat. No. HC13001GL, Fisher Scientific, Hampton, NH, USA), 2 mM LiCl (Cat. No. 866405-64-3, TCI, USA), 10nM WC59 (Cat. No. 500496, Sigma Aldrich, USA) and a combined treatment of 1% EtOH + 2 mM LiCl and 1% EtOH + 10nM WC59. These concentrations have been used previously and calculated as the effective concentrations in fish research (195). Approximately 50 embryos, were placed in the petri dish containing each of the above solutions. Treatments were terminated after 12 hours. Embryos were washed three times with 0.01 % methylene blue solution (embryo medium) to remove any residual solutions. The embryos were separated into two batches and grown separately at 28.5 °C, changing the embryo medium once every day. They were euthanised at 15, 20, 25 and 30 dpf by 1% tricaine methanesulphonate (MS222) (Cat. No. 118000500; Acros Organics, Hampton, NH, USA) and fixed overnight in 4% paraformaldehyde (PFA), then stored in phosphate-buffered saline (PBS). We examined a total of 370 embryos: 16 embryos from 4 biological replicates (clutches) were used for each treatment and each age group.

3.3. Whole-Mount Double Staining

For the tooth analysis, acid-free double cartilage and bone staining was performed. Standard protocol for Alcian blue and Alizarin red staining was used for the experiment (Appendix 1) (196). Briefly, the fish were transferred to 50% EtOH and agitated for 10 minutes at room temperature. The samples were stained overnight in 0.02% Alcian blue (Cat. No. AC400460250 Acros Organics, Hampton, NH, USA) and 0.5% Alizarin red (Cat. No. LC105908, LabChem, Zelienople, PA, USA). Alizarin red is a calcium chelating agent that binds to calcium ions in mineralized bone and cartilage, resulting in a red-colored precipitate (196). When zebrafish embryos are immersed in a solution of alizarin red, the stain penetrates the mineralized tissues and binds to the calcium ions in the bone, allowing the skeletal structures to be visualized under a microscope (196). Alcian blue, on the other hand, binds to the negatively charged glycosaminoglycans in cartilage. When

zebrafish embryos are immersed in a solution of alcian blue, the stain penetrates the cartilaginous tissues and binds to the glycosaminoglycans, resulting in a blue-colored staining of the cartilage (196).The next day they were rinsed in distilled water by inverting the tube containing the samples and water two times. For removing the excess blue color from the fish more than 20 dpf they were transferred to 1% potassium hydroxide (KOH) (Cat. No. 134060010; Fisher Chemicals, Hampton, NH, USA) and agitated for 1 hour in room temperature. After removing the 1% KOH the samples were bleached in 3% hydrogen peroxide in 1% KOH for 20 min. This step should be done with open leads of the tubes and without any agitation. All specimens were processed through an ascending series of glycerol in 1% KOH and then transferred to the storage solution (100% glycerol) (197).

3.4. Tooth Measurements

For tooth analysis, embryos were examined at 15, 20, 25 and 30 dpf. The lower pharyngeal jaw was removed from each sample using fine dissection needles under a Nikon-SMZ 10A dissecting microscope. The pharyngeal jaws were positioned with the dorsal side facing up and the rostral side facing west. They were mounted in 100% glycerol with coverslip. The sample was examined under a Zeiss discovery V8 stereomicroscope (Zeiss, Germany), mounted on a binocular stereo microscope (Stemi 2000-C, Zeiss) with 8× magnification used to observe the tooth height and width, cusp shape and patterning. ZEN 2011 software (blue edition, Zeiss) was used to calculate the above-mentioned measurements. To measure the length and width of the pharyngeal tooth, the most rostral tooth in each age group was considered as a reference. In addition, three landmarks identified in all teeth were examined: the tip of the tooth (TP) and the uppermost (UB) and lowermost (LB) point of the base of the tooth relative to the downward curvature of the tooth towards the tip. Tooth length was the distance from TP to UB and tooth width was the distance from UB to LB.

Figure 3.1: Ventral view of a unicuspid pharyngeal tooth in zebrafish. Tooth length is considered from TP to UB and tooth width is considered from UB to LB. The double line arrow shows the cusp length. TP: tip of the tooth. UB: uppermost point of the tooth base. LB: lowermost point of the tooth base.

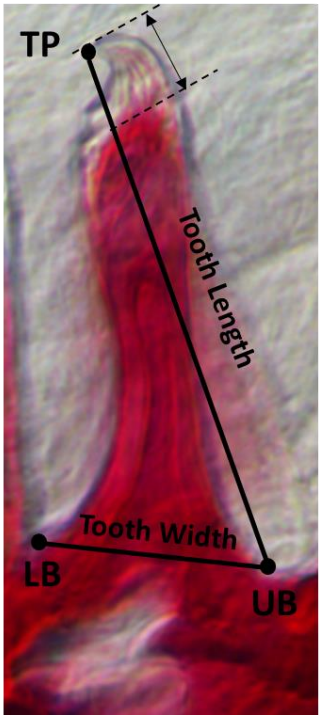

3.5. Protein probe preparation

3.5.1. Wnt10a and Wnt10b probe preparation

Probes were prepared according to the manufacturer's instructions (DIG RNA Labeling kit, SP6/T7, Cat. No. 11175025910; Roche). Briefly, 1 µg of zebrafish template DNA was mixed with 2 µl of 10X NTP labeling mixture, 2 µl of 10x Transcription buffer, 1 µl of protector RNAase inhibitor, and 2 µl of RNA polymerase. The mixture was mixed gently and centrifuged at 12,000x g for 1 minute. Samples were incubated for 2 hours in a 37˚C water bath. 2 µl DNAase was added, and incubation was continued for another 15 minutes and then the reaction was stopped by adding 2µl of 0.2M EDTA (Cat. No. 37560; VWR).

3.5.2. Detecting Wnt10a and Wnt10b

The probe strength was detected using the dot blot techniques according to the standard procedure (Appendix 2). Briefly, 1 µl of diluted Wnt10a and Wnt10b probes was added to the positively

charged nitrocellulose membrane (Cat. No.11209299001; Roche). The membrane was placed in a glass container and incubated for 40 minutes in the 100˚C hybridization oven. Next, the membrane was soaked in 20 ml of maleic acid buffer and incubated at room temperature for 2 minutes with shaking. Maleic acid buffer was made using 1.1607 g of 1 M maleic acid, 0.8766 g of 0.15 M sodium chloride, 0.3 ml of tween-20 (Cat. No. BP337-100; Fisher Scientific), and the solution was topped up to 100 ml using diethyl pyrocarbonate (DepC water). Membrane was incubated in the blocking buffer for 20 minutes with shaking. The 100 ml of blocking buffer was made by adding 2 ml of 2% sheep serum (Cat. No. BP2425; MP Biomedicals) 3 g of milk powder (Skimmed milk powder, commercially available) and topped up the solution with 10 x TBST in DepC. TBST buffer was made by adding 6.05 g of tris (Cat. No. BP152-500; Fisher Chemicals) and 8.76 g of sodium chloride in 800 ml of DepC water. The pH was adjusted to 7.5 with 1 M hydrochloric acid (Cat. No. SA48-1; Fisher Chemicals) and volume was made up to 1 L with DepC water. Finally, 10 ml of tween-20 was added to 1L of TBS buffer. Paper was washed with TBST for 5 minutes with shaking. Membrane was incubated in 10 ml of the antibody solution (Cat. No. 11093274910; Roche) for 30 minutes followed by two washes in washing buffer for 15 minutes for each wash. The antibody solution was made by adding 2 µl of Anti-Digoxigenin antibody into 10 ml of TBST buffer. The washing buffer was made by adding 1.1607 g of 1M maleic acid, 0.8766 g of 0.15 M NaCl, 0.3 ml tween-20. The final solution was made by adding DepC water to 100 ml. Membrane was incubated in the detection buffer for 5 minutes.

Detection buffer was made by adding 10 ml of 0.1 M Tris-HCl, 0.5844 g of 0.1 M NaCl, and the final volume was top up to 100 ml with DepC water. The 1 ml of BCIP/NBT Liquid substrate solution (Cat. No.ICN980771; MP Biomedicals) was added on top of the paper, kept in dark, and checked for a color reaction every five minutes. The first dot was detected at the highest concentration within 5 - 10 minutes. The reaction was stopped by adding TE buffer. TE buffer was made by adding 1 ml of 10 mM Tris-HCl, 0.2 ml of 1 mM EDTA (Cat. No. 37560; VWR) and the solution was top up with DepC water to 100 ml.

3.6. Whole-Mount in-situ Hybridization (WMISH)

3.6.1. Embryo fixation

WMISH was performed on the 48 hours wild-type zebrafish embryos. All the solution for this procedure were made in DepC water. The 48 hpf zebrafish were euthanized using 0.01% MS222 solution and fixed in 4% PFA overnight. Samples were bleached using 0.5% Potassium hydroxide, 3% hydrogen peroxide solution made in DepC water. Next, samples were dehydrated gradually through methanol (Cat. No. BP1105SS-28; Fisher chemicals) series in PBS (25%, 50%, 75%), and samples were stored in 100% methanol for more than three months before used for the experiment.

3.6.2. Whole-Mount in-situ Hybridization (WMISH)

WMISH was conducted according to the established protocol in the lab (Appendix 3) (198). Briefly, samples were rehydrated to PBS gradually through the methanol (Cat. No. BP1105SS-28; Fisher Chemicals) series (75%, 50%, 25%). Then samples were permeabilized using the proteinase K (1 µl proteinase K / 1000 µl of DepC, Cat. No.BP1700-100; Fisher Chemicals). Then the samples were incubated in the Hyb (-) solution. Hyb (-) solution was prepared by adding 50 ml of Deionized Formamide 100% (Cat. No.327235000; Acros), 25 ml of Saline- sodium citrate 20X (SSC) (Cat. No. BP1325-1; Fisher Chemicals), 0.1 ml Tween-20 final solution was top-up to 100 ml by adding 24.9 ml of DepC water. After that, samples were incubated with Wnt10a and Wnt10b probe in Hyb (+) solution at 70˚C, overnight. Hyb (+) solution was prepared by adding 3.56 ml of Hyb (-), 0.4 ml of Yeast tRNA (5mg/ml) (Cat. No. 10109509001; Roche) 0.04 ml of Heparin (50 µg/ml, Cat. No. BP2425; Fisher Chemicals) 0.0368 ml Citric acid and the final volume was adjusted to 6 ml with DepC water. After that, high stringency washes were performed to remove the non-specific binding of the probe. Next samples were incubated in the blocking buffer. Blocking buffer was made by adding 3920 ml of 1x PBST solution, 80 µl of 2% Heat inactivated sheep serum (Cat. No. BP2425; MPBiomedicals), 0.008g Bovine serum albumin (2 mg/ml) (Cat. No. SH30574.01; GE Life Sciences, HyClone Labs). The final volume was adjusted to 6 ml by adding DepC water. 1 µl of Antibody solution (Cat. No.11093274910; Roche) was added to 9 µl of blocking solution. From that 1 µl was added to each tube. Substrate solution of NBT/BCIP staining was used as a colorimetric detection of RNA. The reaction was conducted in the dark until proper color expression was detected. The color reaction stopped after 40 minutes. The samples were fixed in 4% PFA and dehydrated through methanol series. Whole-mount images were captured using a stereomicroscope in a solution prepared with 50% ethanol and 50% glycerol (Zeiss discovery V8).

3.7. Statistical analysis

Data obtained were subjected to the independent T-test using Statistical Product and Service Solutions (SPSS), version 21. The P-value of $P < 0.05$ was considered statistically significant. One-way ANOVA test were performed using SPSS 21 for analyzing the interaction of the treatments. Tukey's Pair-wise comparison for each treatment was conducted using SPSS, 21. For Tukey's test also p-value of $P < 0.05$ was considered statistically significant. Furthermore, Chi-square analysis was used to analyze the nominal data such as tooth shape and statistically significant outcomes reported as $P < 0.05$.

CHAPTER 4: RESULTS

4.1. Differences of the tooth mineralization between control and chemical treatment samples in 15, 20, 25 and 30 dpf

The acid-free double-stained tooth-bearing pharyngeal jaws of zebrafish and stereomicroscope observation of color intensity was performed to study the effect of different chemicals on tooth mineralization (Figure 4.1). The EtOH-treated samples showed a reduction in the intensity of alizarin red staining at 15 and 20 dpf compared to control (Figure 4.1 E & F) while it was the same at 25 and 30 dpf (Figure 4.1 G & H). The color intensity reduction means teeth were not fully mineralized until 25dpf. More intensity reduction was observed in LiCl-treated (Figure 4.1 I & J) and LiCl combined with EtOH-treated samples (Figure 4.1 M & N) compared to control at 15 and 20 dpf. These results showed that mineralization of the teeth was not complete until 25 dpf in these two treatment groups. The tooth mineralization in WC59-treated samples was started to complete at 30 dpf (Figure 4.1 T) and the color intensity reduction was observed at 15, 20, and 25 dpf compared to control (Figure Q, R & S). In EtOH and WC59 combined treatment, alizarin red color was barely identified in the teeth and limited to the tip of the teeth at 15 and 20 dpf (Figure U & V). At 25 dpf tooth mineralization was observed in most of the teeth but was not completed at 30 dpf (Figure W & X).

Figure 4.1: Acid-free double-stained tooth-bearing pharyngeal bones of zebrafish at 15,20,25 and 30 dpf. (A-D) Control samples that show tooth-bearing lower pharyngeal bones with six teeth in each bone. These teeth are unicuspid and directly attached to the underlying bone. At this stage the teeth are fully mineralized. **(E–H)** Samples exposed to 1% EtOH, **(I-L)** 2mM LiCl, **(M-P)** 2mMLiCl combined with 1%EtOH, **(Q-t)** 10nM WC59 and **(U-X)** 10nM WC59 combined with 1%EtOH at 10 h post-fertilisation shows malformed and hypo-mineralised teeth. Scale bar shows 20 µm.

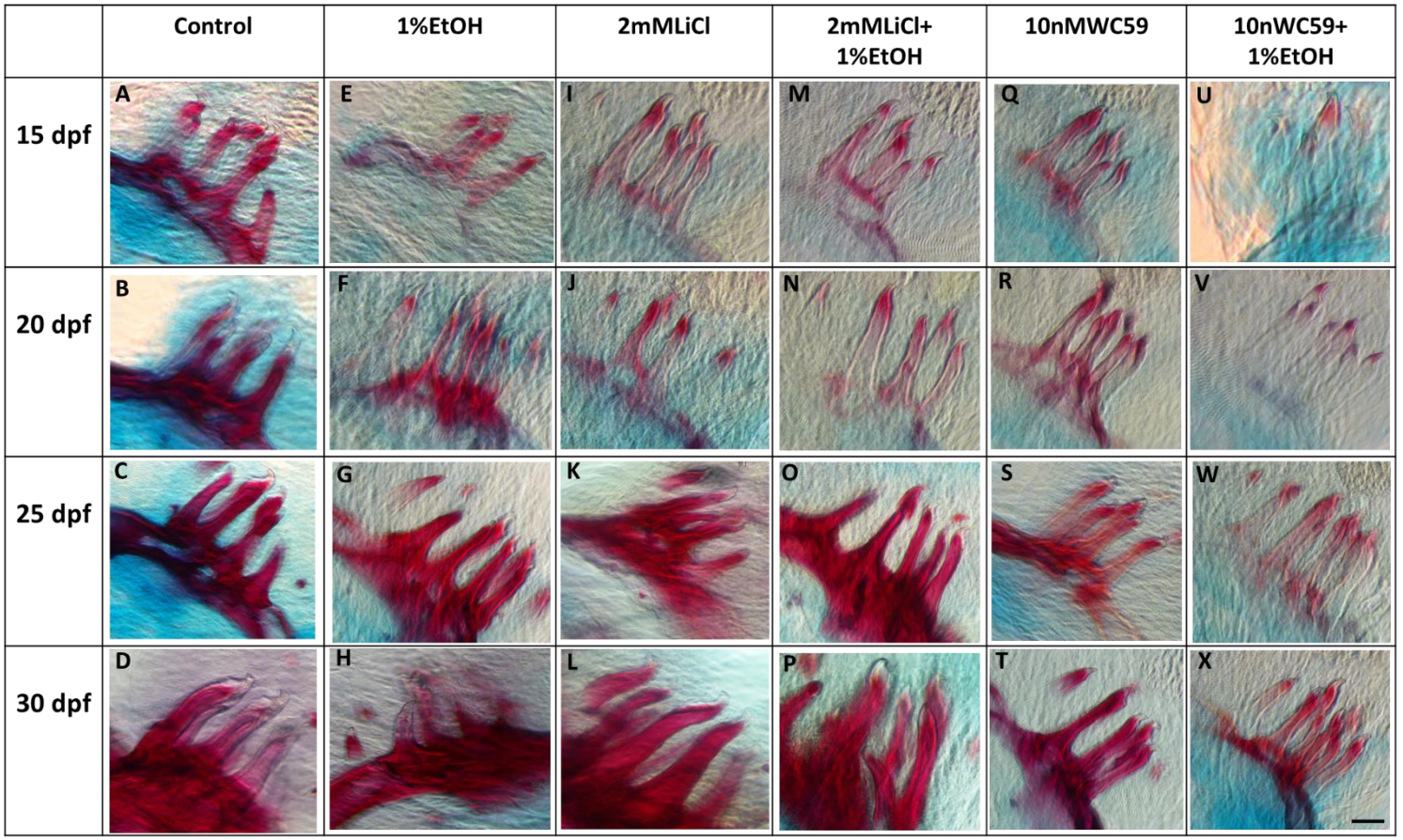

4.2. Differences in the tooth size between control and differential chemical treatment samples

Acid-free double cartilage and bone staining and microscopic tooth height and width analysis of 370 samples were collected and microscopic measuring of the tooth length and width were carried out to understand the effect of different chemicals on tooth development in the zebrafish populations (Table 4.1). According to the statistical analysis, the tooth height and width of the EtOH-treated 15 dpf and 20 dpf samples were significantly less than the control ($P < 0.05$) (Figure 4.2 & 4.3). However, there was no significant difference in height and width of the teeth between the control and EtOH-treated of 25 dpf and 30 dpf samples ($P > 0.05$) (Figure 4.4 & 4.5).

The tooth height and width of the LiCl-treated samples in 15, 20, and 25 dpf were significantly more than the control ($P < 0.05$) (Figure 4.2, 4.3 & 4.4). However, there was no significant difference in width of the teeth between the control and LiCl-treated samples at 30 dpf ($P > 0.05$) (Figure 4.5 B) while the tooth height was significantly more than the control samples in this time point ($P < 0.05$) (Figure 4.5 A).

We investigated that the combination of LiCl and EtOH treated samples showed a less tooth height and width than the control group in 15, 20, 25, and 30 dpf ($P < 0.05$) (Figure 4.2, 4.3, 4.4 & 4.5). This interesting result determined that the inhibitory role of EtOH might be stronger that the activation of Wnt signaling pathway through LiCl treatment. Moreover, the EtOH might has its inhibitory effects by blocking the Wnt signaling pathway as an important key for tooth development.

It was shown that the tooth height and width in WC59 treated samples were significantly less than in controls ($P < 0.05$) (Figure 4.2, 4.3, 4.4 & 4.5). Furthermore, these metrics in WC59 treated embryos were less than in EtOH treatment group (Figure 4.2, 4.3, 4.4 & 4.5). This is an interesting result that could be because of the stronger inhibitory role of WC59 compared to the EtOH adverse effects.

The WC59 and EtOH combine treatment group illustrated that the tooth development was noticeably suppressed in terms of its length and width. Our results showed that the tooth length and width in this combination treatment group were significantly less than control samples ($P < 0.05$) (Figure 4.2, 4.3, 4.4 & 4.5).

Table 4.1: Sample size, mean tooth length and width measured with ZEN 2011 software in control and treated samples at 15, 20, 25, and 30 dpf. The samples were collected from 4 different clutches. Mean height of the tooth was measured by the maximum length from the tip of the tooth to the upper base of the tooth. Tooth width was measured from upper base to the lower base of the tooth.

15 dpf Samples	Sample Size	Tooth Length(µm) Mean (SD)	Tooth Width (µm) Mean (SD)
Control	12	69.81 (0.39)	22.73 (0.87)
1% EtOH	16	58.29 (0.90)	14.29 (1.24)
2mMLiCl	16	71.89 (1.46)	25.49 (0.94)
1%EtOH + 2mMLiCl	16	54.35 (1.16)	17.48 (0.73)
10nMWC59	15	52.65 (1.09)	14.32 (0.53)
1%EtOH + 10nMWC59	16	40.09 (0.90)	13.54 (0.84)

20 dpf Samples	Sample Size	Tooth Length (µm) Mean (SD)	Tooth Width (µm) Mean (SD)
Control	13	72.40 (0.72)	24.65 (0.61)
1% EtOH	16	63.96 (1.56)	22.35 (1.15)
2mMLiCl	17	78.50 (0.82)	28.17 (0.93)
1%EtOH + 2mMLiCl	17	61.42 (0.75)	19.12 (0.98)
10nMWC59	15	59.90 (0.75)	18.13 (0.41)
1%EtOH + 10nMWC59	15	55.25 (0.90)	19.27 (0.94)

25 dpf Samples	Sample Size	Tooth Length (µm) Mean (SD)	Tooth Width (µm) Mean (SD)
Control	12	90.85 (1.14)	29.18 (0.78)
1% EtOH	17	91.43 (1.32)	30.17 (1.13)
2mMLiCl	17	100.57 (0.98)	39.86 (0.52)
1%EtOH + 2mMLiCl	16	67.57 (0.37)	23.87 (0.47)
10nMWC59	15	65.02 (0.93)	24.43 (0.89)
1%EtOH + 10nMWC59	15	63.02 (1.21)	22.86 (1.33)

30 dpf Samples	Sample Size	Tooth Length (µm) Mean (SD)	Tooth Width (µm) Mean (SD)
Control	13	98.76 (0.40)	48.74 (0.47)
1% EtOH	16	98.05 (1.03)	48.19 (0.98)
2mMLiCl	17	122.63 (0.75)	48.22 (0.49)
1%EtOH + 2mMLiCl	17	77.94 (1.98)	32.69 (5.55)
10nMWC59	15	71.88 (0.59)	28.06 (0.72)
1%EtOH + 10nMWC59	16	69.90 (0.97)	27.17 (0.94)

Figure 4.2: Comparing the tooth length (A) and width (B) in control and treated samples at 15 dpf. There is a significant difference between the treated groups with the control in both tooth length and width ($P < 0.05$).

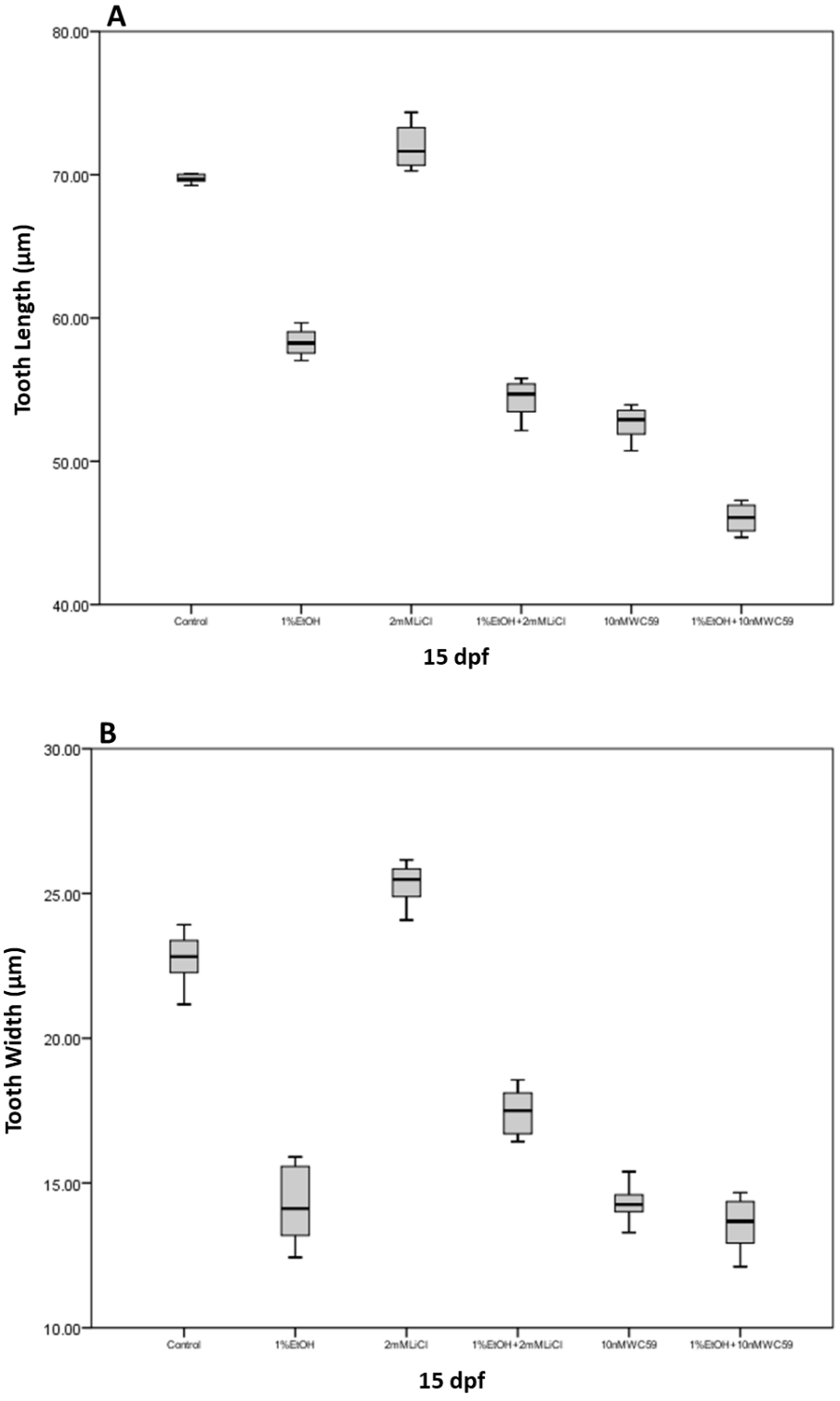

Figure 4.3: Comparing the tooth length (A) and width (B) in control and treated samples at 20 dpf. There is a significant difference between the treated groups with the control in both tooth length and width ($P < 0.05$).

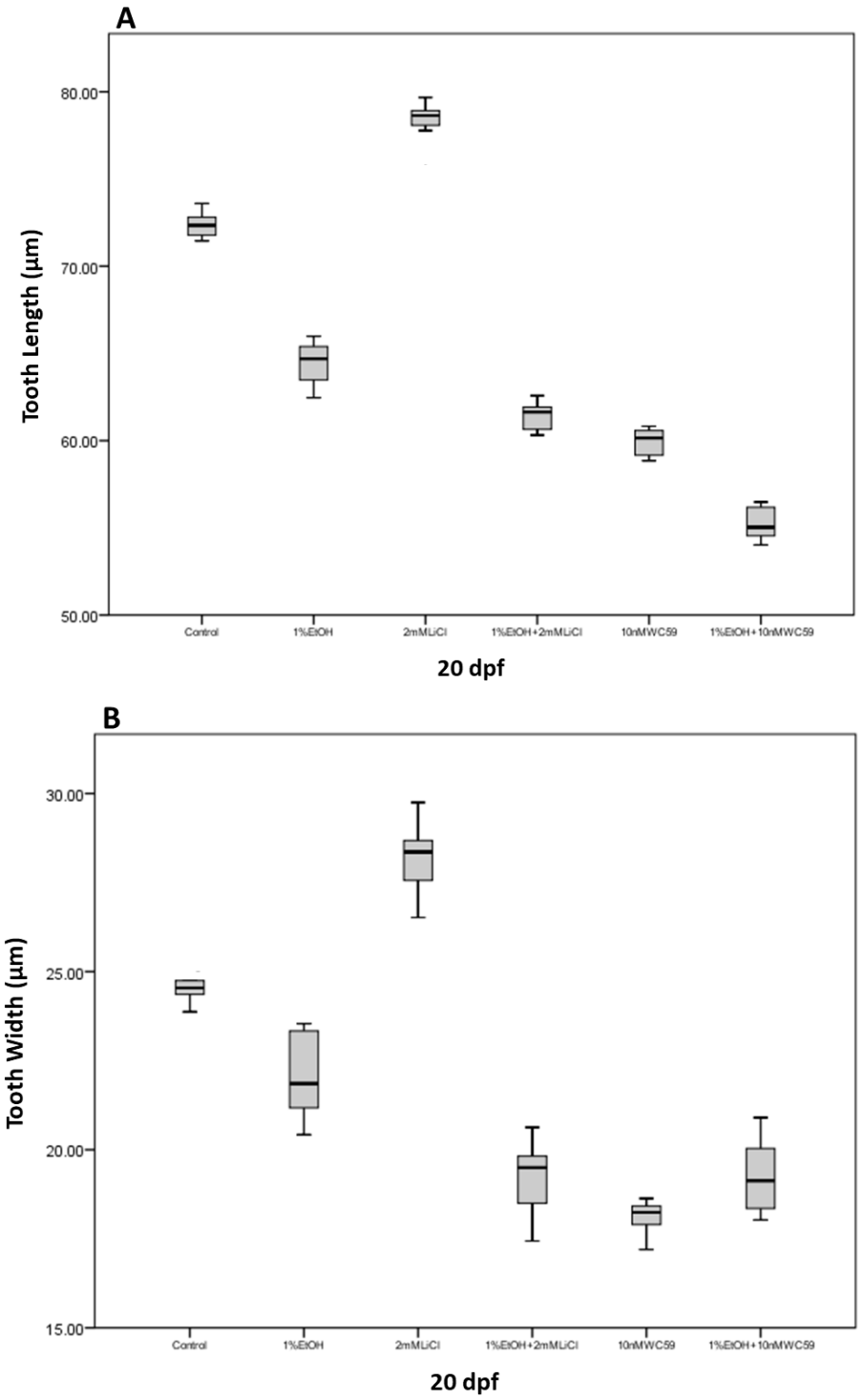

Figure 4.4: Comparing the tooth length (A) and width (B) in control and treated samples at 25 dpf. There is a significant difference in tooth length and width between the 2mMLiCl, 1%EtOH+2mMLiCl, 10nMWC59, and 1%EtOH+10nMWC59 treatment groups with the control ($P < 0.05$), while there was no significant difference between 1%EtOH-treated samples with the control ($P > 0.05$).

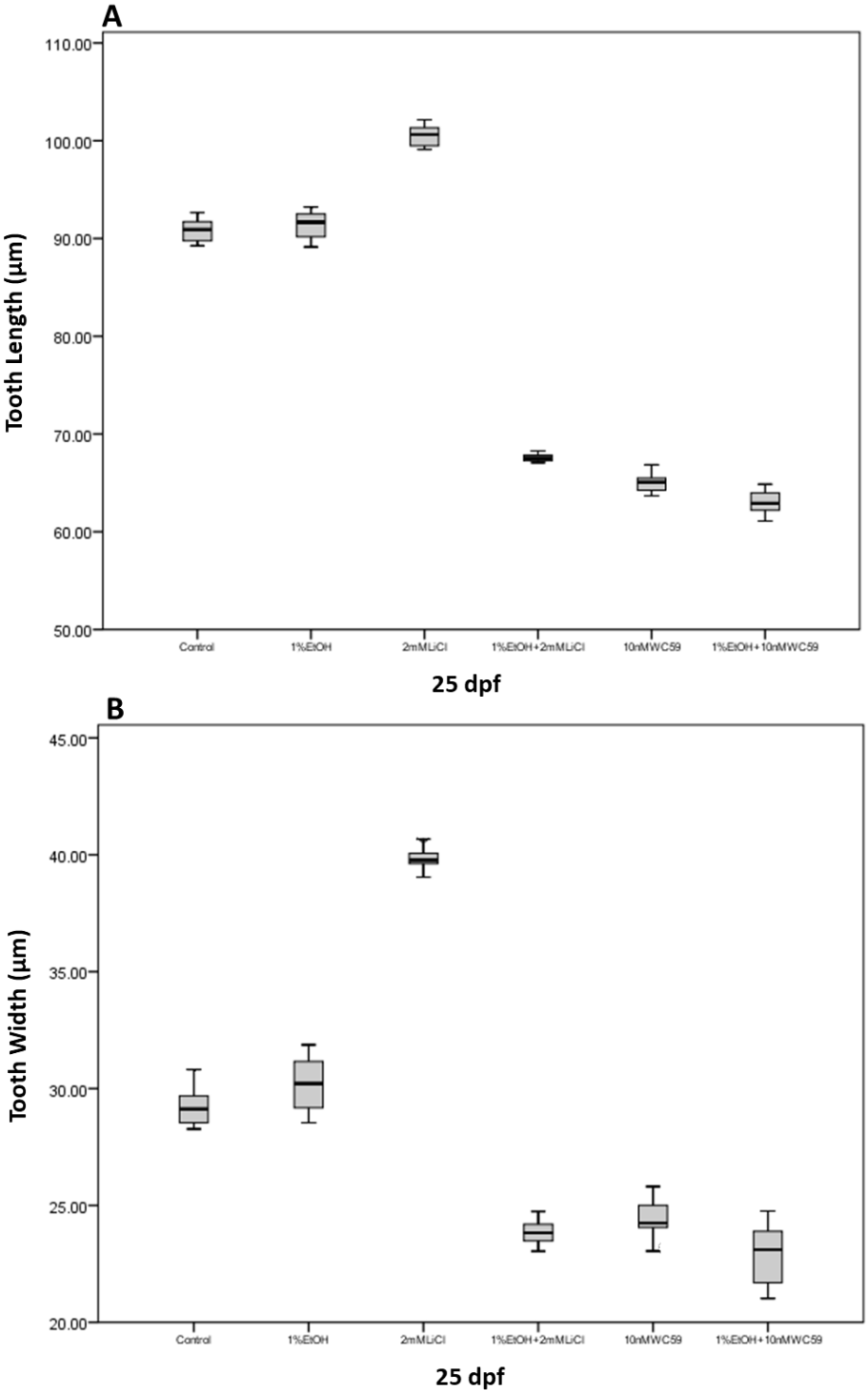

Figure 4.5: Comparing the tooth length (A) and width (B) in control and treated samples at 30 dpf. There is a significant difference in tooth length between the 2mMLiCl, 1%EtOH+2mMLiCl, 10nMWC59, and 1%EtOH+10nMWC59 treatment groups with the control ($P < 0.05$), while there was no significant difference between 1%EtOH-treated samples with the control ($P > 0.05$). There is a significant difference in tooth width between the 1%EtOH+2mMLiCl, 10nMWC59, and 1%EtOH+10nMWC59 treatment groups with the control ($P < 0.05$), while there was no significant difference between 1%EtOH- and 2mMLiCl-treated samples with the control ($P > 0.05$).

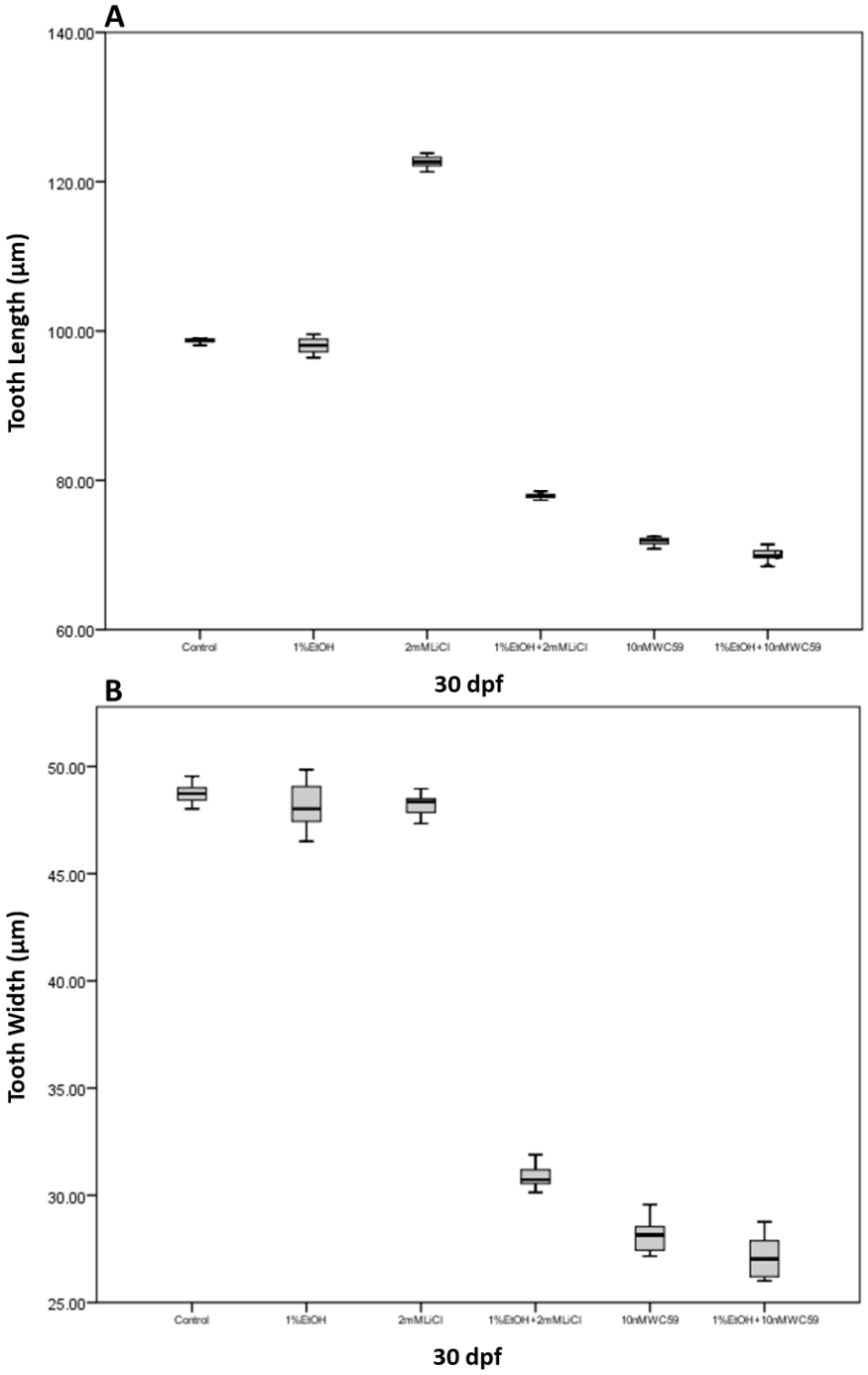

4.3. Comparing the fluctuation of tooth size in different time points between control and chemical-treated samples

We also investigated the changes of the tooth length and width of chemical-treated samples in the 30 days lifetime of the larvae. Tooth length and width differences between EtOH-treated samples and the control were decreasing from 15 dpf to 20 dpf. More decreasing was seen in the difference from 20 dpf time point to the 25 dpf and these metrics became higher than in EtOH-treated samples at 25 dpf but not significantly. At 30 dpf the EtOH-treated tooth length and width were similar to the control (Figure 4.6).

In the LiCl-treated samples, the tooth length difference with the control increased constantly until it reached more than 20 µm (Figure 4.7). However, the tooth width followed a different path. Tooth width difference between treated samples and control remained the same from 15 dpf until 20 dpf while a significant increase was observed at 25 dpf. Interestingly, the tooth width of LiCl-treated samples tended to decrease from 25 dpf to 30dpf until this metric became the same as control in 30 dpf (Figure 4.7). This result revealed that the LiCl has the activating effect on tooth development through increasing the length of the tooth and probably by activating the ameloblasts and result in the overproduction of the enameloid.

In the LiCl and EtOH combined treatment group the differences of tooth length and width between treated samples and control tended to increase with the time. The tooth length and width of treated samples were significantly less than the control at all the time points due to the fact that EtOH showed a strong inhibitory effect on tooth development (Figure 4.8).

The differences of tooth length and width between WC59-treated samples and control were increasing over the time which means the inhibitory role of WC59 on tooth development became stronger through further subsequent tooth replacement cycles (Figure 4.9).

The fluctuation of tooth length and width in the EtOH combined with WC59 treatment group was similar to the WC59 treatment group from 15 to 30 dpf although these metrics in this combined treatment were less than WC59-treated samples (Figure 4.10).

Figure 4.6: Comparing the fluctuation of tooth length and width between control and 1% EtOH-treated samples at 15, 20, 25, and 30 dpf. The height and width of the EtOH-treated 15 dpf (height 58.29 vs 69.81 µm, width 14.29 vs 22.73 µm) and 20 dpf samples (height 63.96 vs 72.40 µm, width 22.35 vs 24.65 µm) were significantly less than the control ($P < 0.05$). However, there was no significant difference in height and width of the teeth between the 25 dpf and 30 dpf control and EtOH-treated samples ($P > 0.05$).

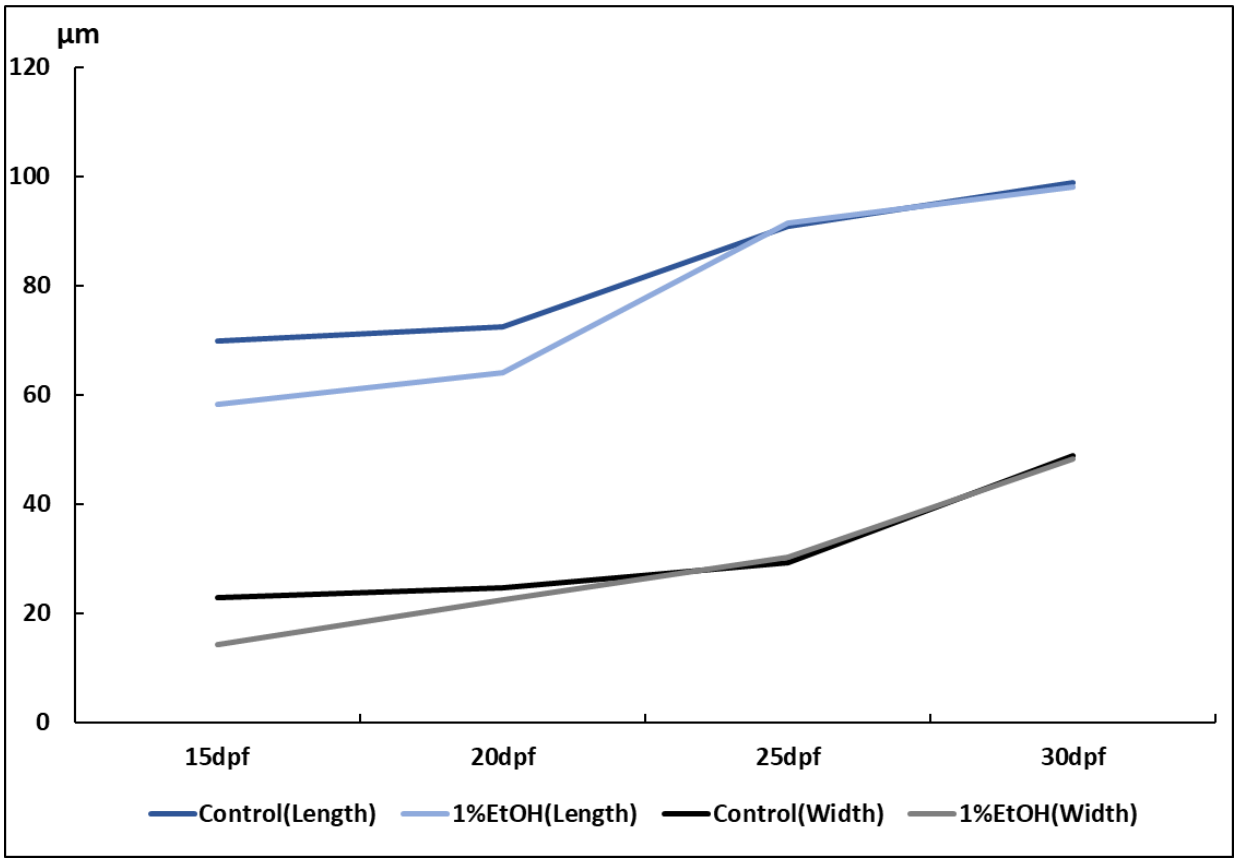

Figure 4.7: Comparing the fluctuation of tooth length and width between the control and 2mM LiCl-treated samples at 15, 20, 25, and 30 dpf. The tooth height of the LiCl-treated samples was significantly more than the control at all the time points ($P < 0.05$). The tooth width of the LiCl-treated 15, 20 and 25 dpf samples were significantly more than the control ($P < 0.05$) while there was no significant difference in tooth width between LiCl-treated 30 dpf samples and the control ($P > 0.05$).

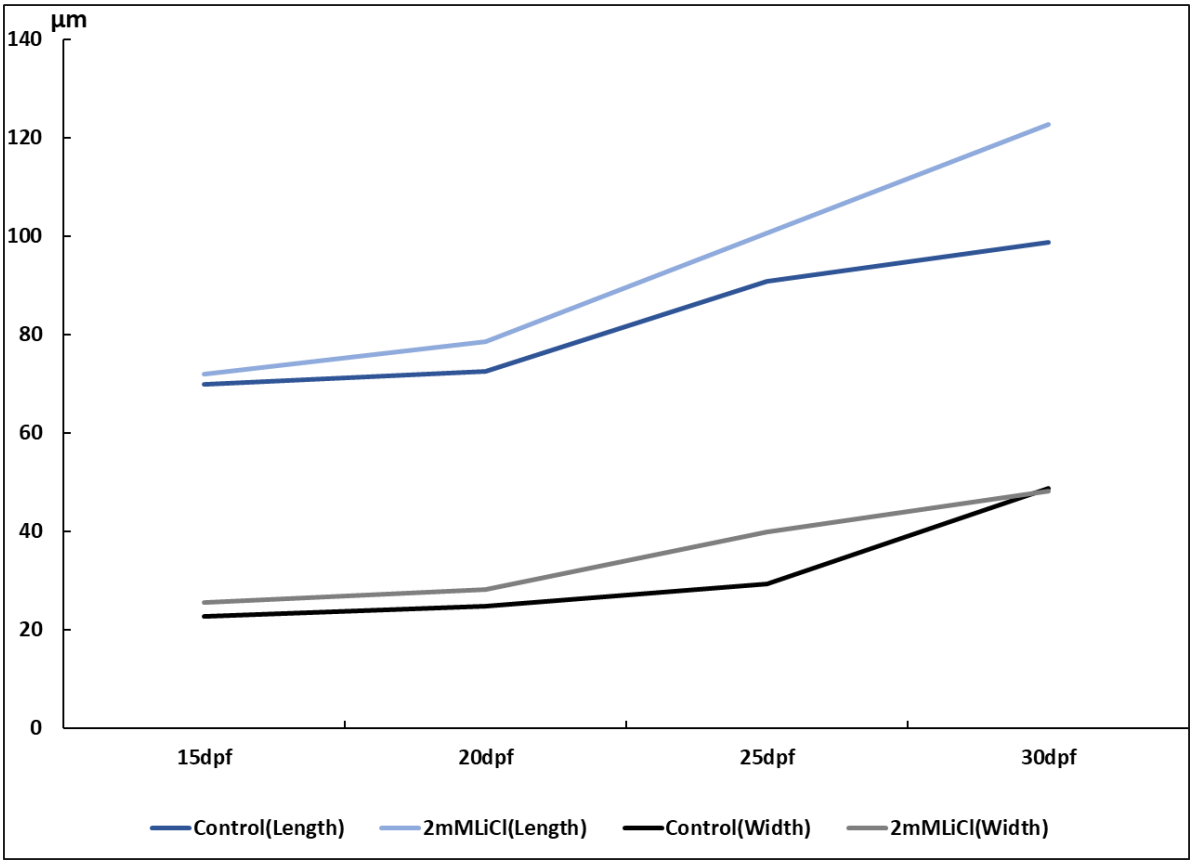

Figure 4.8: Comparing the fluctuation of tooth length and width between the control and 1% EtOH + 2mM LiCl-treated samples at 15, 20, 25, and 30 dpf. The tooth height and width of the EtOH and LiCl combined-treated samples were significantly less than the control ($P < 0.05$)

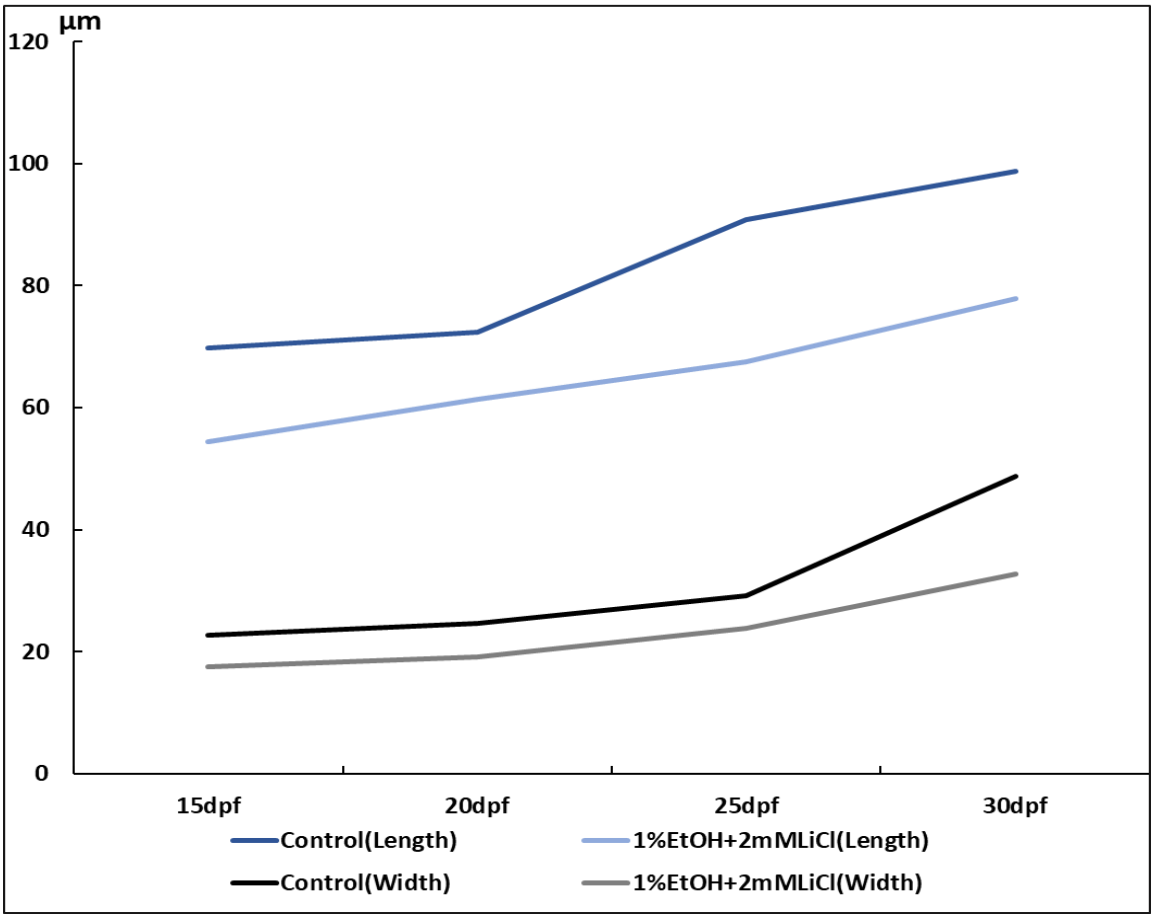

Figure 4.9: Comparing the fluctuation of tooth length and width between the control and 10nM WC59-treated samples at 15, 20, 25, and 30 dpf. The tooth height and width of the WC59-treated samples were significantly less than the control ($P < 0.05$).

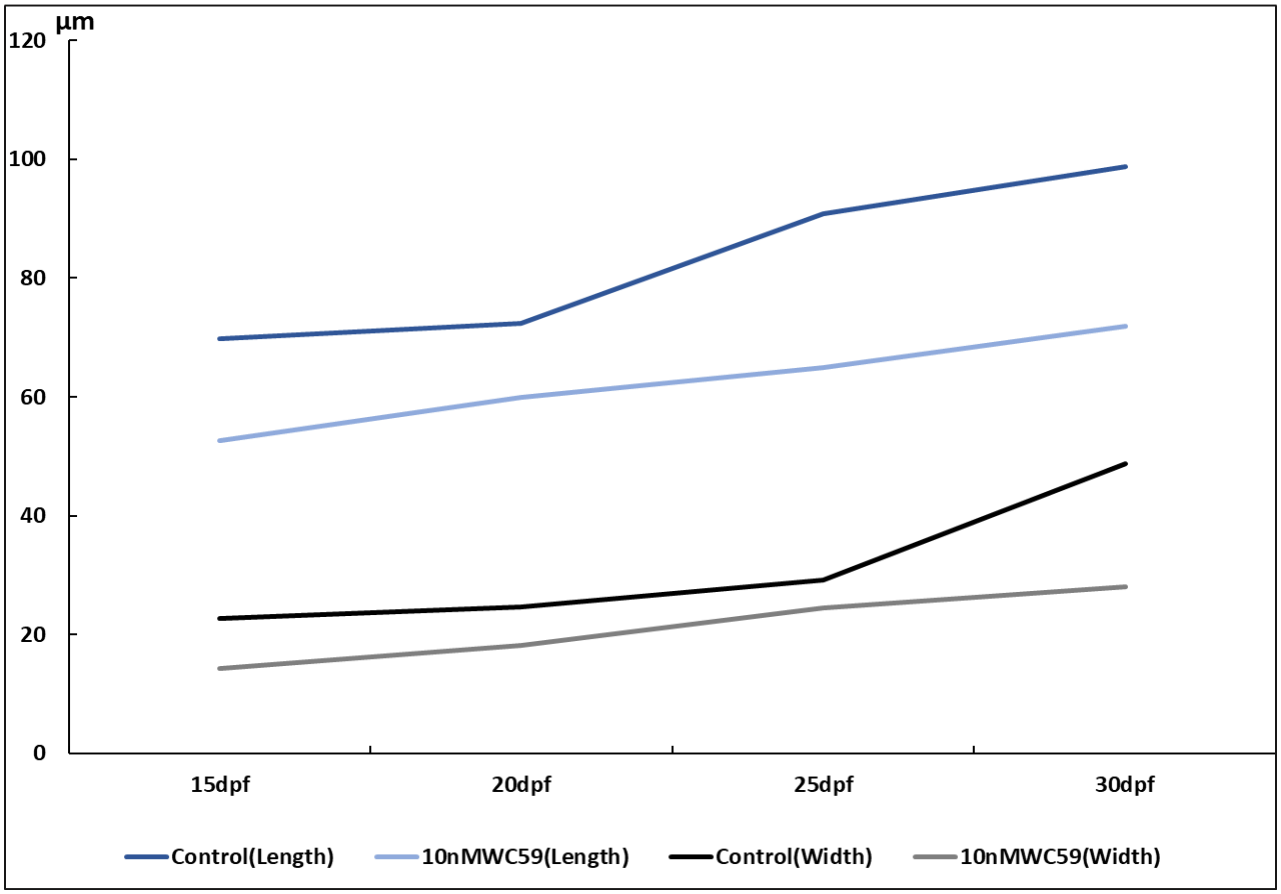

Figure 4.10: Comparing the fluctuation of tooth length and width between the control and 1% EtOH + 10nM WC59-treated samples at 15, 20, 25, and 30 dpf. The tooth height and width of the EtOH and WC59 combined-treated samples were significantly less than the control ($P < 0.05$).

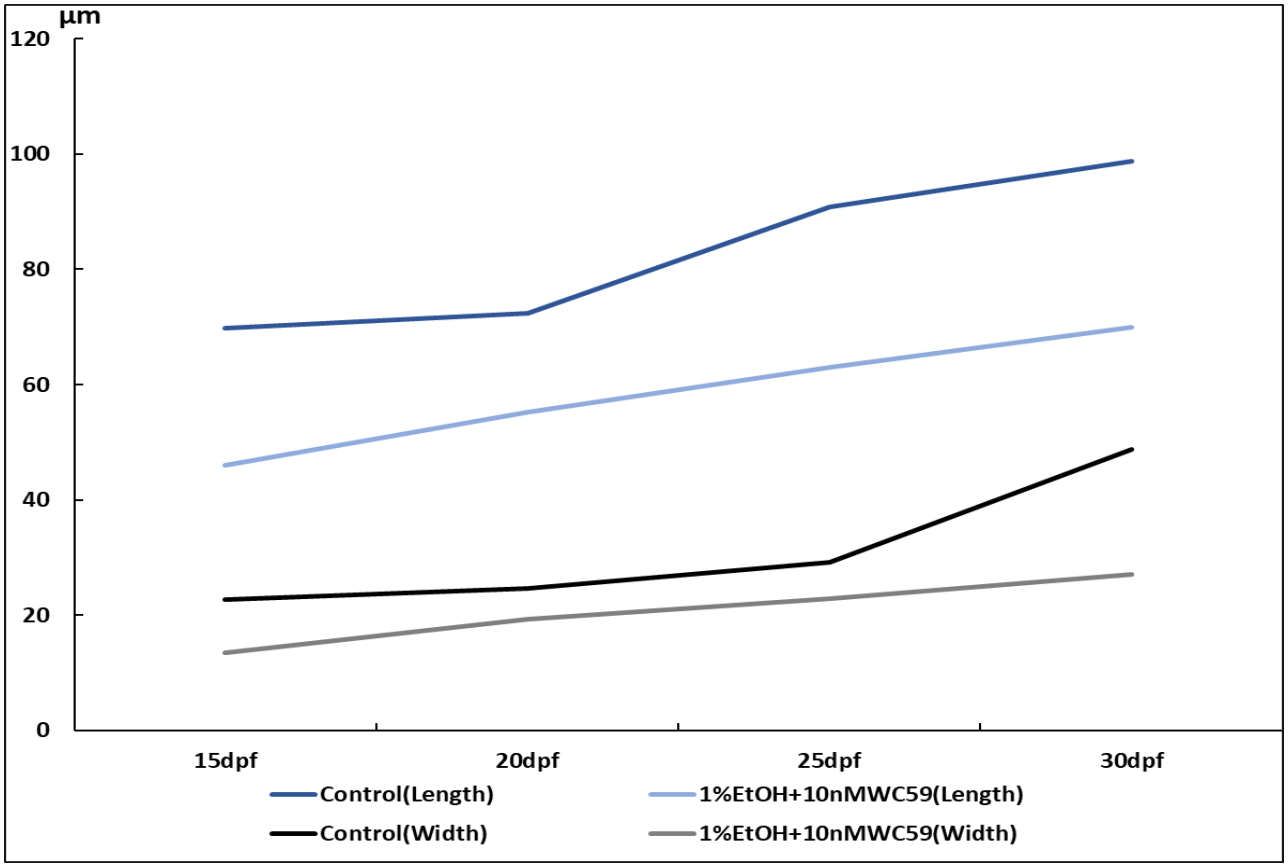

4.4. Comparing the tooth size between 1%EtOH and combined-treated samples

To better understand the interaction of EtOH and Wnt signaling pathway in tooth development, statistical analysis of mean tooth length and width of EtOH treatment group with either combined treatment of EtOH + LiCl and EtOH + WC59 was performed. One-way ANOVA was used to determine if the obtained mean length and width significantly differed. The results showed a significant difference between the recorded mean length and widths at 15, 20, 25, and 30 dpf (P = 0.1x10-4). Tukey's pairwise comparison was used to compare the differences in mean length and width between each pair (Table 4.3). According to obtained P-values (shown as sig. in the table), both combined treatments mean length and width were significantly different from the EtOH mean as shown in Table 4.3. When compared to the EtOH treatment, the length and width reduction observed in the combined treated samples was significant at all the time points except the tooth width of EtOH and WC59 combined treatment at 15 dpf.

Table 4.3: Tukey's pairwise comparison for control and combined treatment groups for mean length and width of the zebrafish tooth at 15, 20, 25, and 30 dpf.

Dependent Variable: Tooth Length (15dpf)

Tukey HSD

(I) Group	(J) Group	Mean Difference (I-J)	Std. Error	Sig.
1%EtOH	control	-11.51396*	.34889	.000
	2mMLiCl+1%EtOH	3.94438*	.32301	.000
	10nMWC59+1%EtOH	12.20625*	.28239	.000

Dependent Variable: Tooth Width (15dpf)

Tukey HSD

(I) Group	(J) Group	Mean Difference (I-J)	Std. Error	Sig.
1%EtOH	control	-8.44542*	.37734	.000
	2mMLiCl+1%EtOH	-3.19563*	.34935	.000
	10nMWC59+1%EtOH	.74563	.36036	.109

Dependent Variable: Tooth Length (20dpf)

Tukey HSD

(I) Group	(J) Group	Mean Difference (I-J)	Std. Error	Sig.
1%EtOH	control	-8.44692*	.41094	.000
	2mMLiCL+1%EtOH	2.54000*	.38334	.000
	10nMWC59+1%EtOH	8.70400*	.41391	.000

Dependent Variable: Tooth Width (20dpf)

Tukey HSD

(I) Group	(J) Group	Mean Difference (I-J)	Std. Error	Sig.
1%EtOH	control	-2.29712*	.36143	.000
	2mMLiCL+1%EtOH	3.23221*	.33716	.000
	10nMWC59+1%EtOH	3.08217*	.34230	.000

Dependent Variable: Tooth length (25dpf)

Tukey HSD

(I) Group	(J) Group	Mean Difference (I-J)	Std. Error	Sig.
1%EtOH	control	.57936	.38896	.306
	2mMLiCL+1%EtOH	23.86353*	.35933	.000
	10nMWC59+1%EtOH	28.40686*	.43989	.000

Dependent Variable: Tooth width (25dpf)

Tukey HSD

(I) Group	(J) Group	Mean Difference (I-J)	Std. Error	Sig.
1%EtOH	control	.98931*	.32386	.011
	2mMLiCL+1%EtOH	6.30765*	.29919	.000
	10nMWC59+1%EtOH	7.31631*	.40106	.000

Dependent Variable: Tooth Length (30dpf)

Tukey HSD

(I) Group	(J) Group	Mean Difference (I-J)	Std. Error	Sig.
1%EtOH	control	-.71736*	.25989	.023
	2mMLiCL+1%EtOH	20.10246*	.24244	.000
	10nMWC59+1%EtOH	28.40686*	.43989	.000

Dependent Variable: Tooth Width (30dpf)

Tukey HSD

(I) Group	(J) Group	Mean Difference (I-J)	Std. Error	Sig.
1%EtOH	control	-.54063	.25982	.106
	2mMLiCL+1%EtOH	17.35408*	.24236	.000
	10nMWC59+1%EtOH	21.02604*	.30671	.000

4.5. Differences in tooth number between the control and chemical treatment groups at 15, 20, 25, and 30 dpf

We counted the attached teeth in the acid-free double-stained slides of the pharyngeal jaw at each time point (The black arrow heads in Figure 4.11) . The results of EtOH-treated samples showed that the tooth number was significantly less than the control at 15 dpf (Figure 4.12). Thus, hypodontia was observed at 15 dpf EtOH-treated samples while the number of the tooth in treatment group was similar to the control at 20, 25, and 30 dpf (Figure 4.12). A significant increase in tooth number was seen in LiCl treatment group at 25 dpf while this parameter was significantly less than the control at 15 and 20 dpf (Figure 4.12).This result revealed that LiCl can cause tooth agenesis whether by increasing or decreasing the number of the teeth. The tooth number of the LiCl and EtOH combined treatment group showed a significant decrease compared to the control at 30 dpf but not 15, 20 and 25 dpf (Figure 4.12). The Wnt inhibitor in WC59 treatment group decreased the tooth number significantly in 25 and 30 dpf (Figure 4.12). Interestingly, tooth number decreased significantly in EtOH combined with WC59-treated samples at all the time points compared to the control (Figure 4.12).

Figure 4.11: Acid-free double-stained tooth-bearing pharyngeal bones of zebrafish at 25 dpf. The lower pharyngeal bones which are fifth ceratobranchial arch bears nine attached teeth (black arrowhead). At this stage the teeth are fully mineralised. White arrowheads show exfoliated teeth.

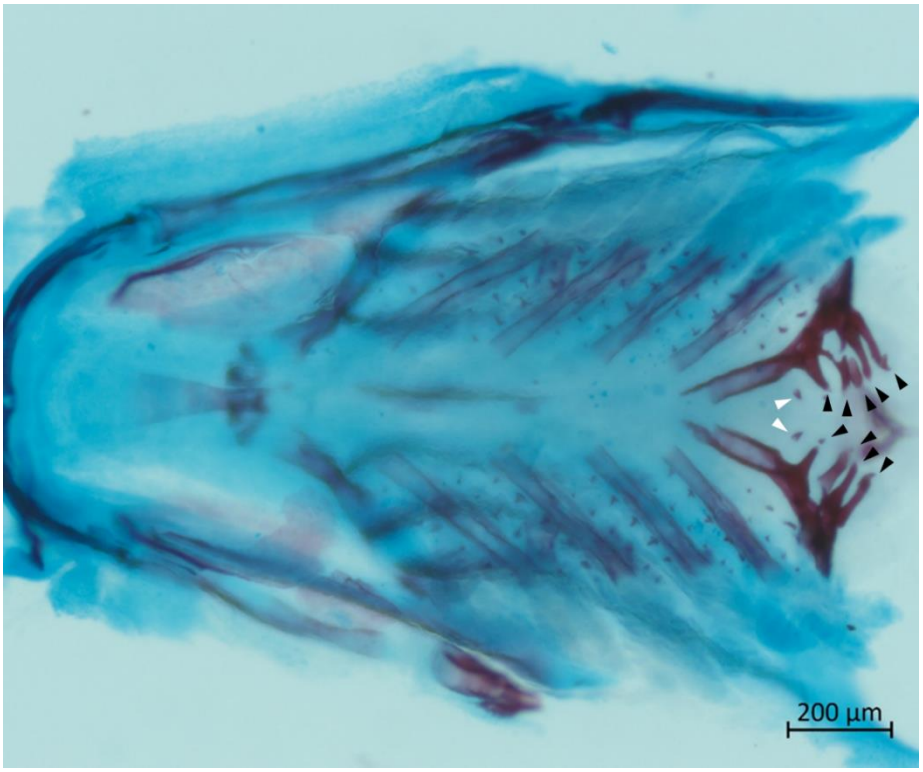

Figure 4.12: Comparing tooth number between the control and different chemical-treated samples at 15, 20, 25, and 30 dpf. Asterisks show P<0.05.

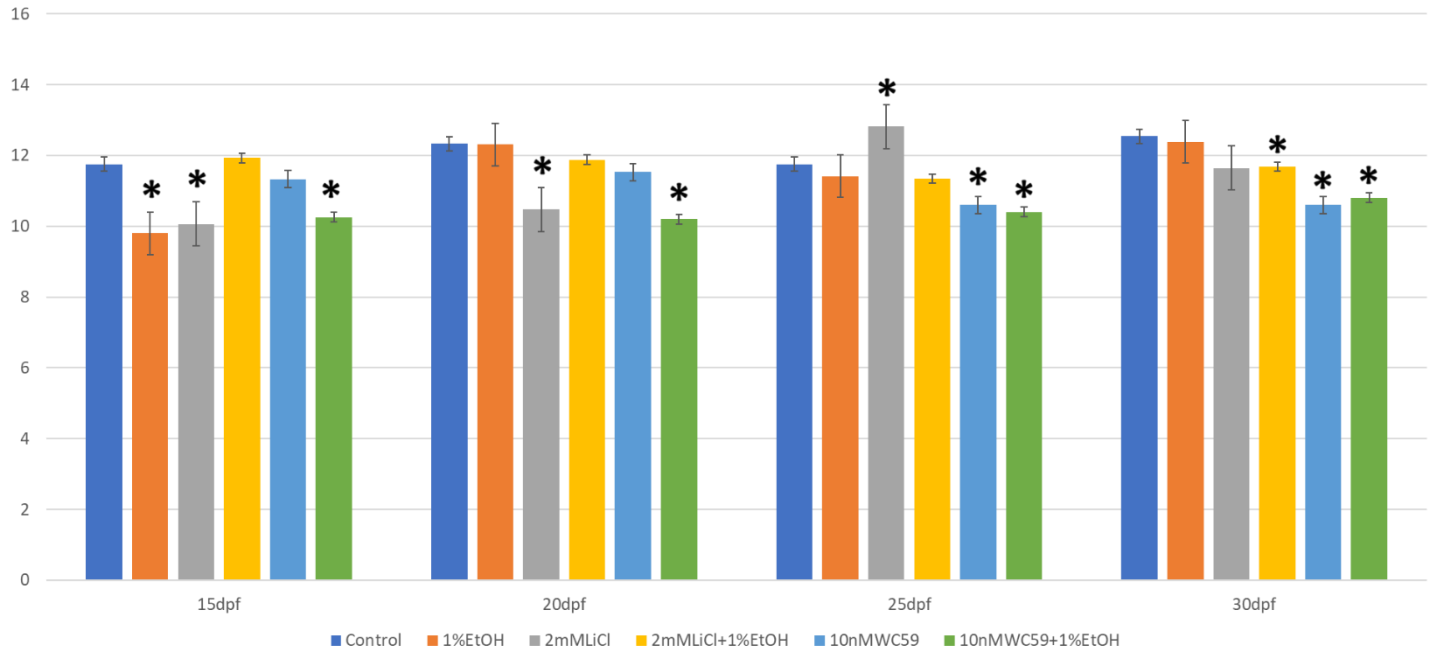

4.6. Differences in shape of the tooth cusp between the control and chemical treatment groups at 15, 20, 25, and 30 dpf

The alizarin red-stained samples revealed that the cusp of the zebrafish tooth has a shape of a hook (Figure 4.13 A). This shape can be affected by different chemicals and become straight (Figure 4.13 B). 100% of the EtOH-treated samples at 15dpf showed a straight cusp while 18.75% of the samples at 20dpf, 76.48% of the samples at 25dpf and 87.5% of the samples at 30dpf had hook-like shape tooth (Figure 4.14). As mentioned before this result can show that the adverse effects of EtOH are significant in first-generation teeth and then decrease through subsequent tooth replacement cycles.

The tooth shape in all LiCl-treated samples at 15 and 20 dpf were hook-like. Whereas 64.7 % of the samples at 25 dpf and 82.23% of the samples at 30 dpf were straight (Figure 4.15).

Interestingly, in EtOH and LiCl combined treatment group the cusp shape tended to change from 20 dpf. It means that the tooth cusps of all samples were hook-like shape at 15dpf then it became straight in 52.94% of the samples and ended up straight shape in all the samples at 25 and 30 dpf (Figure 4.16).

The cusp shape changes in WC59 treatment group showed an unreasonable flow. The 20% of the samples had hook-like cusp shape at 15dpf while the tooth cusp in all the samples at 20 dpf were straight. It was observed that the tooth cusp of 53.33% of the samples at 25dpf and 80% of the samples at 30 dpf had a straight shape (Figure 4.17).

EtOH and WC59 combined treatment had a strong adverse effect on the cusp shape and result in a straight cusp shape in all the samples at all the time points (Figure 4.18).

Figure 4.13: Alizarin red-stained pharyngeal tooth of zebrafish at 30 dpf. (A) shows a tooth with hook-like shape cusp in control sample. **(B)** shows a tooth with straight cusp in WC59-treated sample.

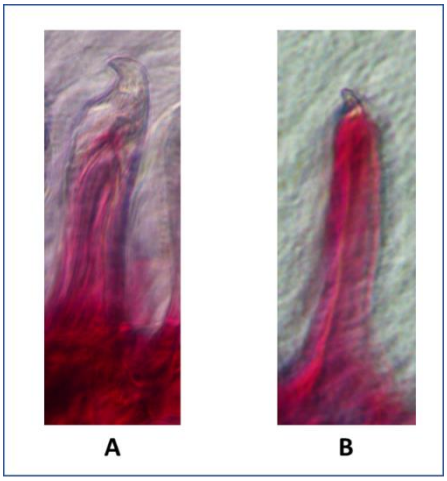

Figure 4.14: Comparing tooth cusp morphology between the control and 1% EtOH–treated samples at 15, 20, 25, and 30 dpf

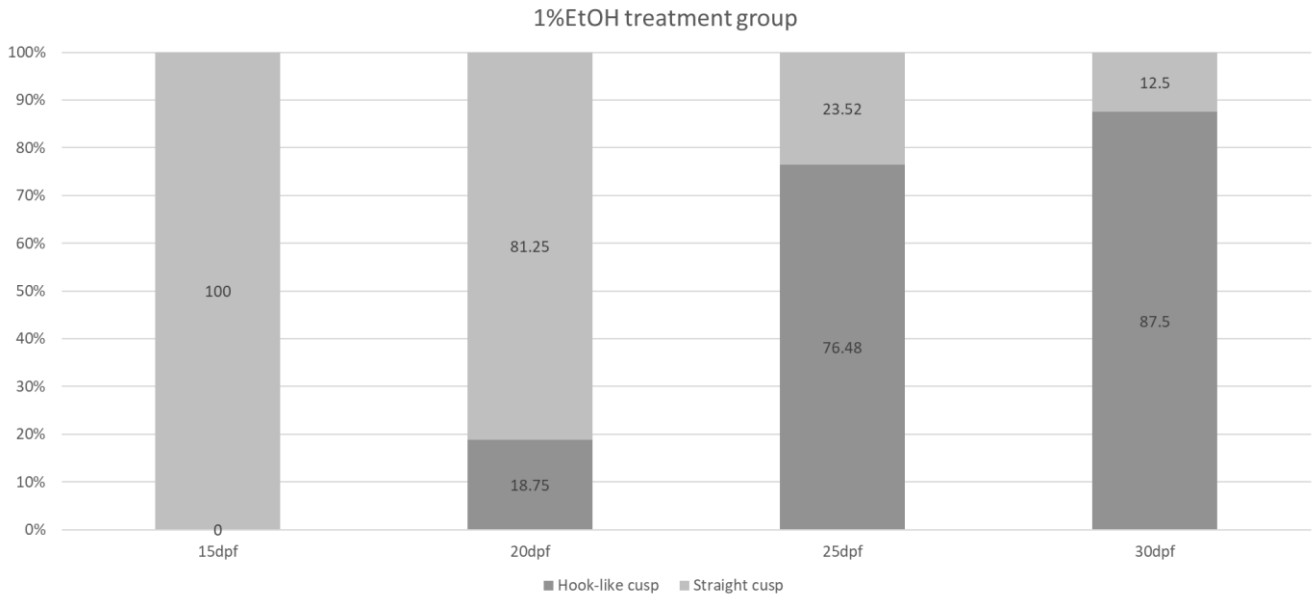

Figure 4.15: Comparing tooth cusp morphology between the control and 2mM LiCl–treated samples at 15, 20, 25, and 30 dpf

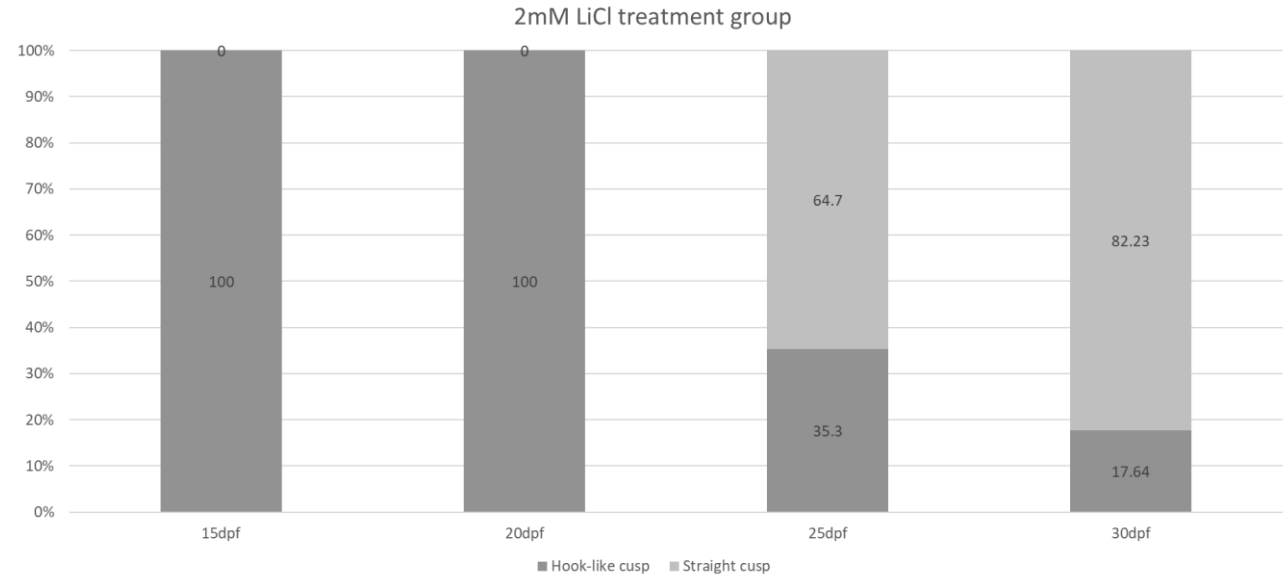

Figure 4.16: Comparing tooth cusp morphology between the control and 1%EtOH + 2mM LiCl–treated samples at 15, 20, 25, and 30 dpf

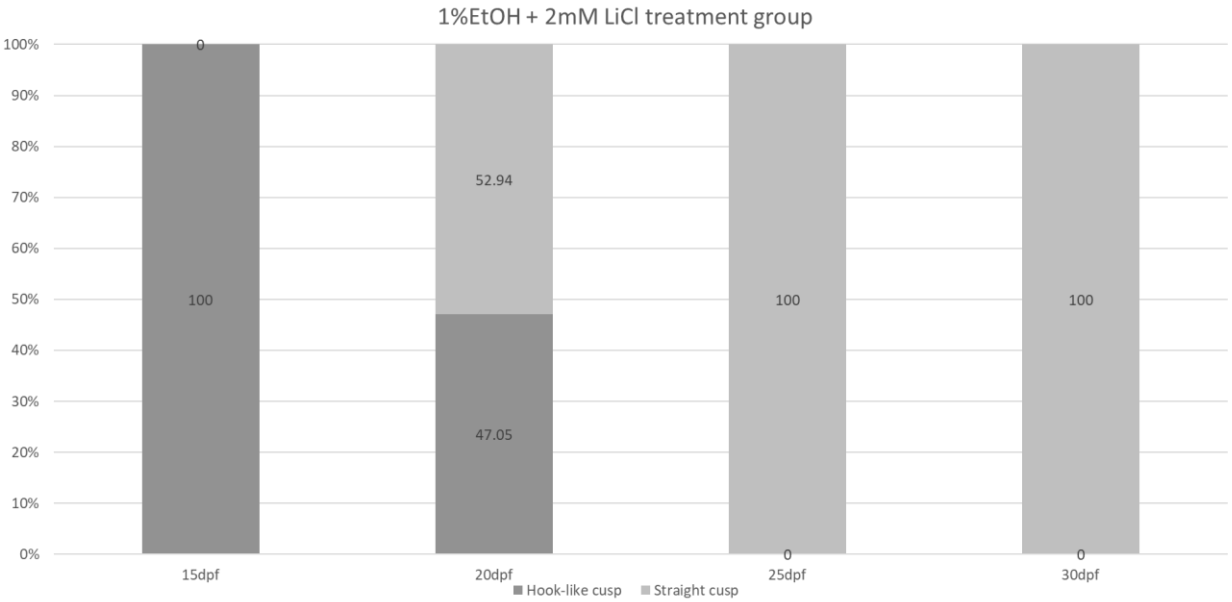

Figure 4.17: Comparing tooth cusp morphology between the control and 10nM WC59–treated samples at 15, 20, 25, and 30 dpf

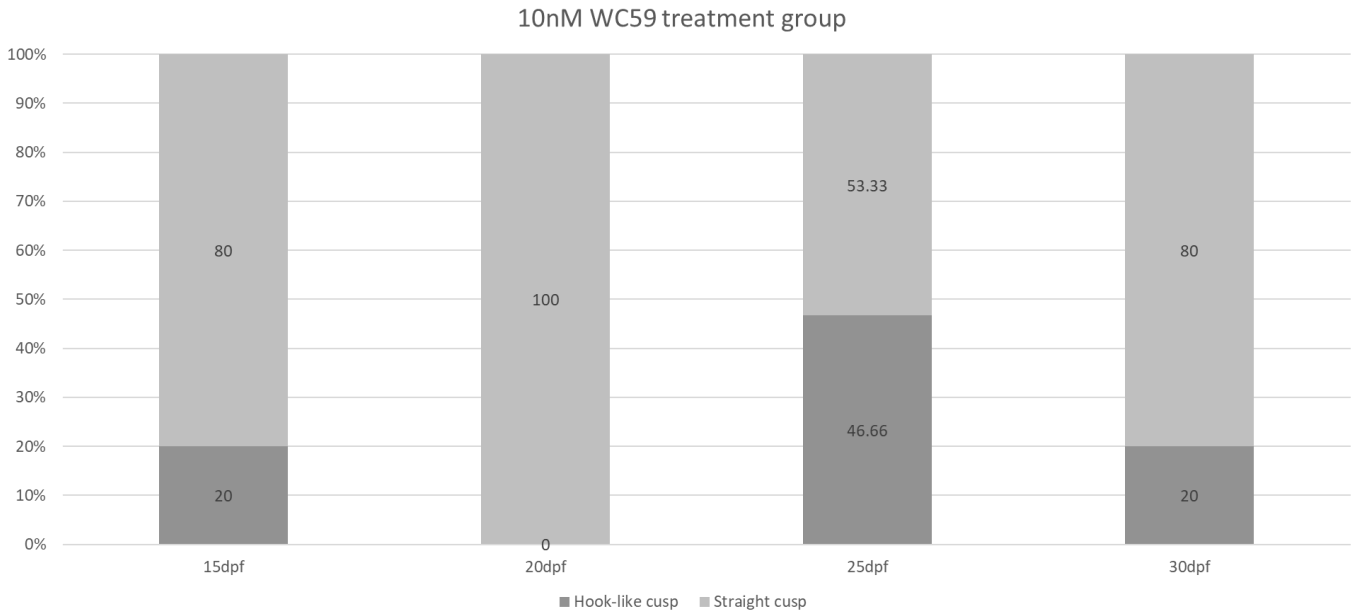

Figure 4.18: Comparing tooth cusp morphology between the control and 1% EtOH + 10nMWC59–treated samples at 15, 20, 25, and 30 dpf

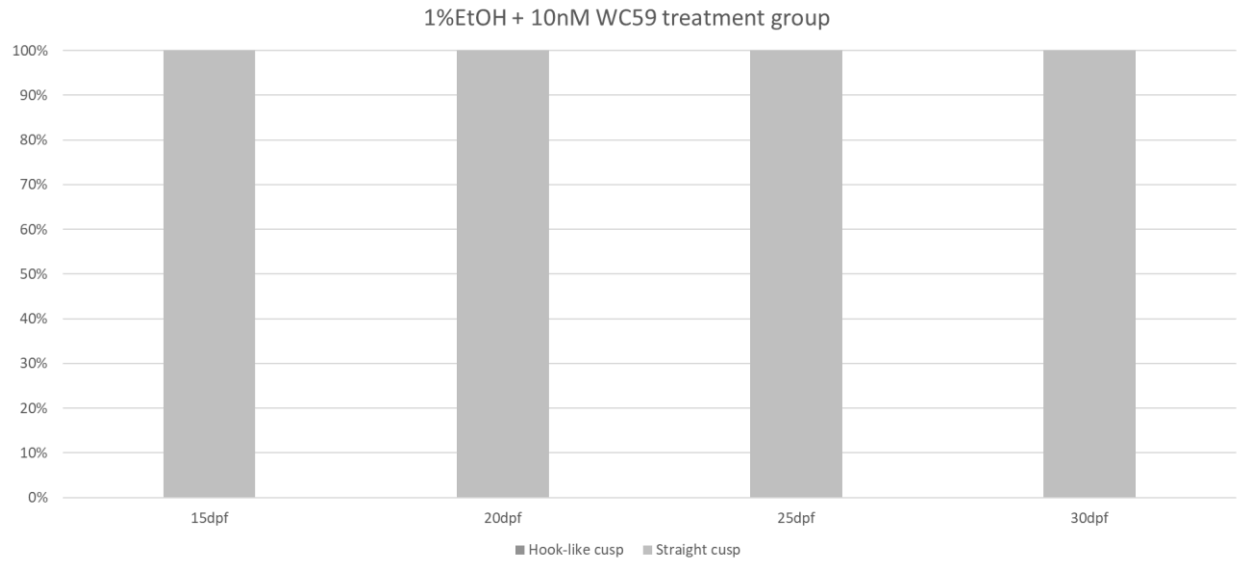

4.7. Differences in cusp size between the control and chemical treatment groups at 15, 20, 25, and 30 dpf

The microscopic analysis of the length of the zebrafish tooth cusp reveals that the chemical treatments can have effects on the enameloid part of the tooth. At 15 and 20 dpf, the cusp length in the 1%EtOH, 1%EtOH + 2mM LiCl, 10nM WC59 and 1%EtOH + 10nMWC59 treatment groups was significantly less than the control while in the 2mM LiCl-treated samples it was significantly more than the control (Figure 4.19 & 4.20). At 25 and 30 dpf the cusp length in the 1%EtOH + 2mM LiCl, 10nM WC59 and 1%EtOH + 10nMWC59 treatment groups was significantly less than the control while in the 2mM LiCl-treated samples it was significantly more than the control (Figure 4.21 & 4.22). Furthermore, there was no significant difference in cusp length between the 1%EtOH-treated samples and the control at 25 and 30 dpf (Figure 4.21 & 4.22).

Figure 4.19: Comparing the cusp length between the control and chemical-treated samples at 15 dpf. There was a significant difference in cusp length between the 1%EtOH, 2mMLiCl, 1%EtOH+2mMLiCl, 10nMWC59, and 1%EtOH+10nMWC59 treatment groups with the control ($P < 0.05$).

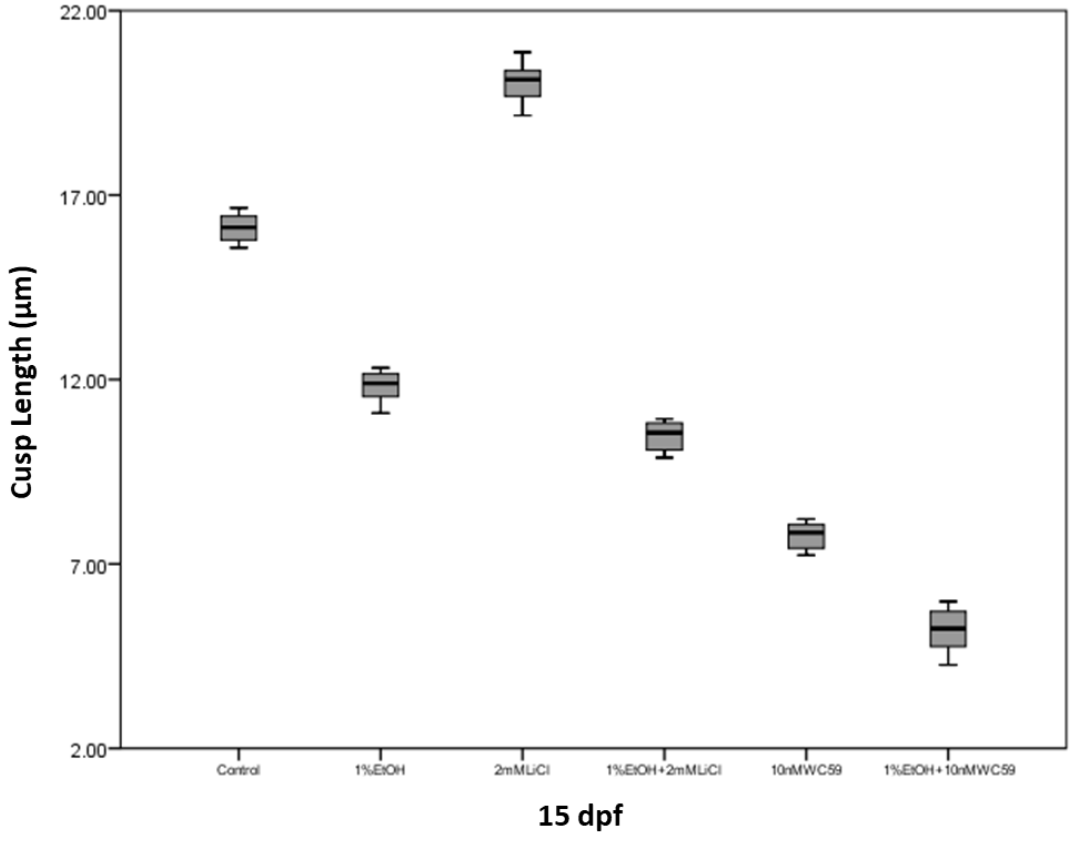

Figure 4.20: Comparing the cusp length between the control and chemical-treated samples at 20 dpf. There was a significant difference in cusp length between the 1%EtOH, 2mMLiCl, 1%EtOH+2mMLiCl, 10nMWC59, and 1%EtOH+10nMWC59 treatment groups with the control ($P < 0.05$).

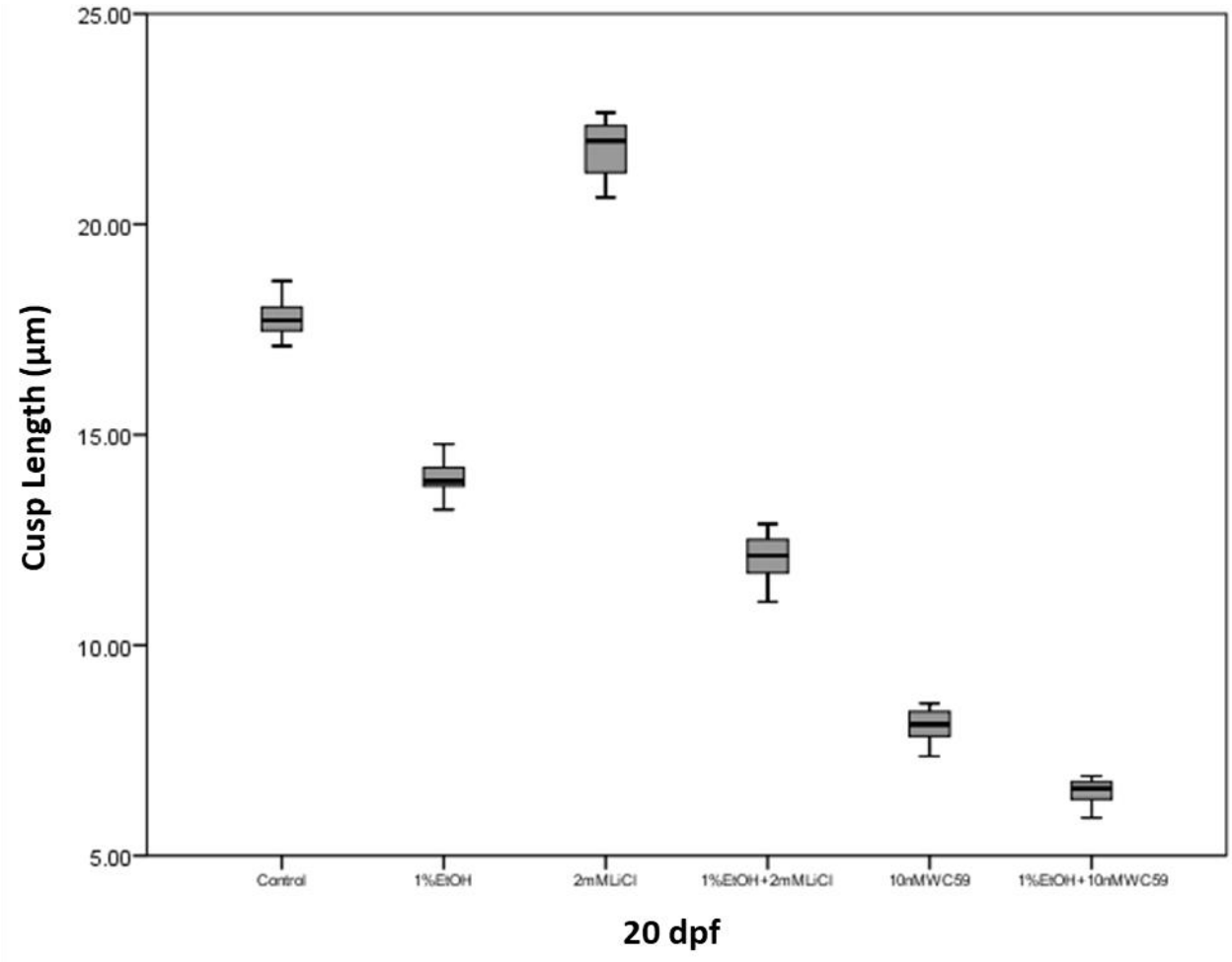

Figure 4.21: Comparing the cusp length between the control and chemical-treated samples at 25 dpf. There was a significant difference in cusp length between the 2mMLiCl, 1%EtOH+2mMLiCl, 10nMWC59, and 1%EtOH+10nMWC59 treatment groups with the control ($P < 0.05$), while there was no significant difference between 1%EtOH-treated samples with the control ($P > 0.05$).

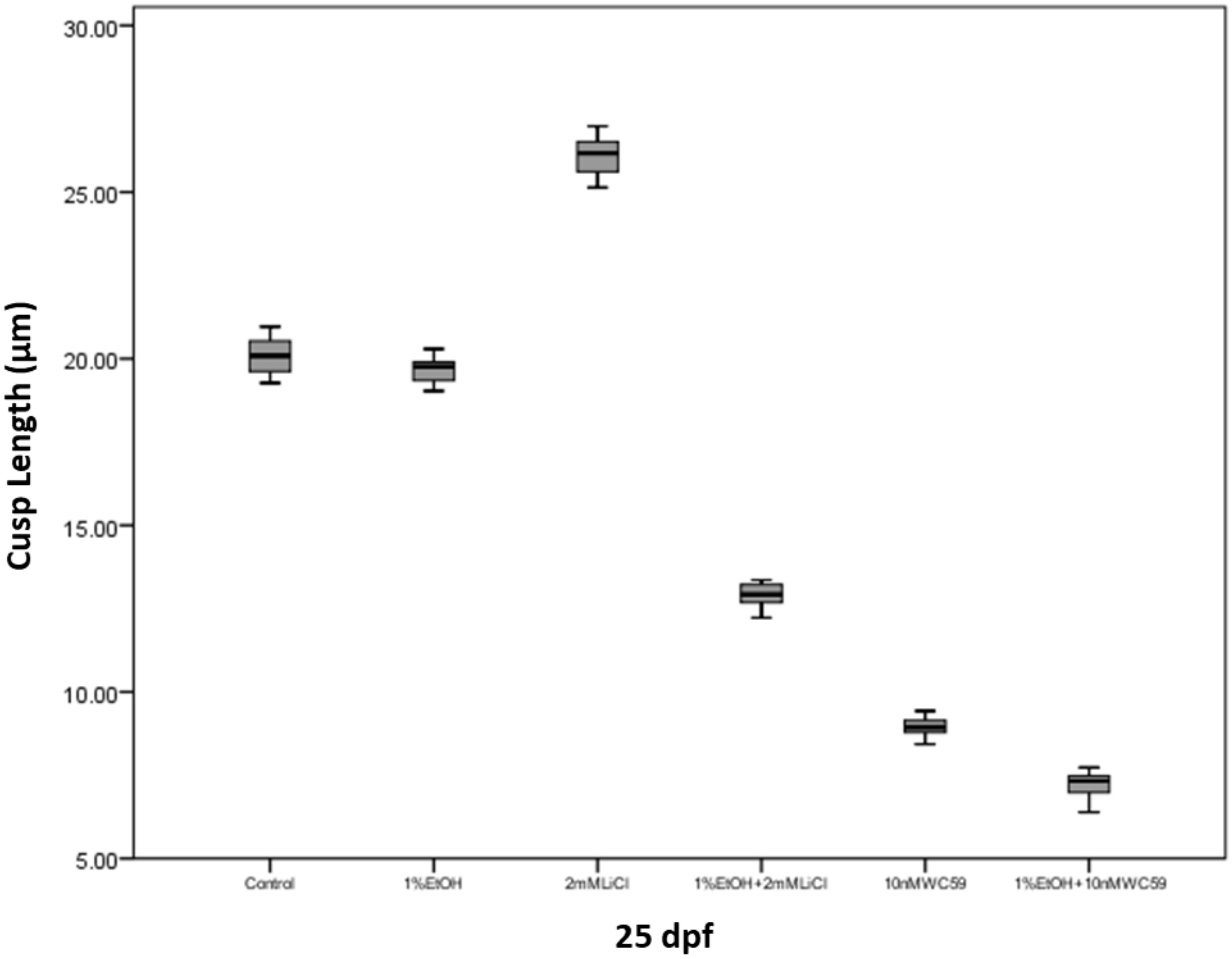

Figure 4.22: Comparing the cusp length between the control and chemical-treated samples at 30 dpf. There was a significant difference in cusp length between the 2mMLiCl, 1%EtOH+2mMLiCl, 10nMWC59, and 1%EtOH+10nMWC59 treatment groups with the control ($P < 0.05$), while there was no significant difference between 1%EtOH-treated samples with the control ($P > 0.05$).

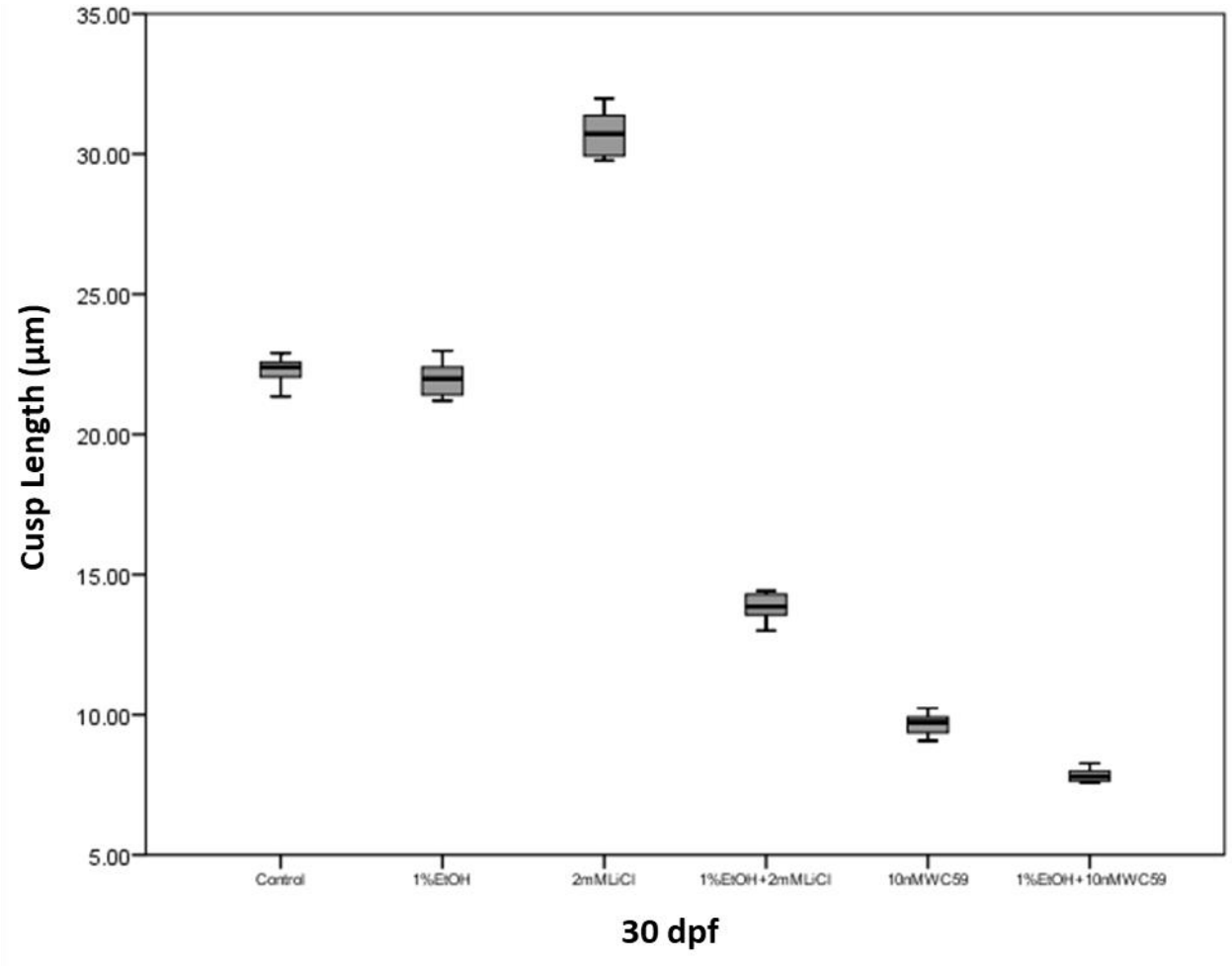

4.8. Comparing the cusp length proportion with the tooth length between different chemical treatment groups and control at 15, 20, 25, and 30 dpf

We also measured the proportion of the cusp length to the tooth length to investigate whether they play their inhibitory or activating role through affecting the enameloid secretion and/or dentine secretion. The statistical analysis of the proportion of cusp length to tooth length of the zebrafish tooth revealed that the chemical treatments had noticeable effects on the enameloid part of the tooth. At 15 and 20 dpf, the proportion of cusp length to tooth length in the 1%EtOH-treated samples was significantly less than the control while there was no significant difference in the proportion of cusp length to tooth length between the 1%EtOH-treated samples and control at 25 and 30 dpf (Figure 4.23). In 2mM LiCl-treated samples there was a significant increase in the proportion of cusp length to tooth length compared to the control at all the time points (Figure 4.24). However, this metric was significantly less than the control in the 1%EtOH + 2mM LiCl, 10nM WC59 and 1%EtOH + 10nMWC59 treatment groups at 15, 20, 25, and 30 dpf (Figure 4.25, 4.26 & 4.27).

Figure 4.23: Comparing the cusp length proportion with the tooth length between 1%EtOH treatment group and control at 15, 20, 25, and 30 dpf. The cusp length proportion significantly decreased in EtOH-treated samples at 15 and 20 dpf while there was no significant difference between EtOH treatment group and control at 25 and 30 dpf.

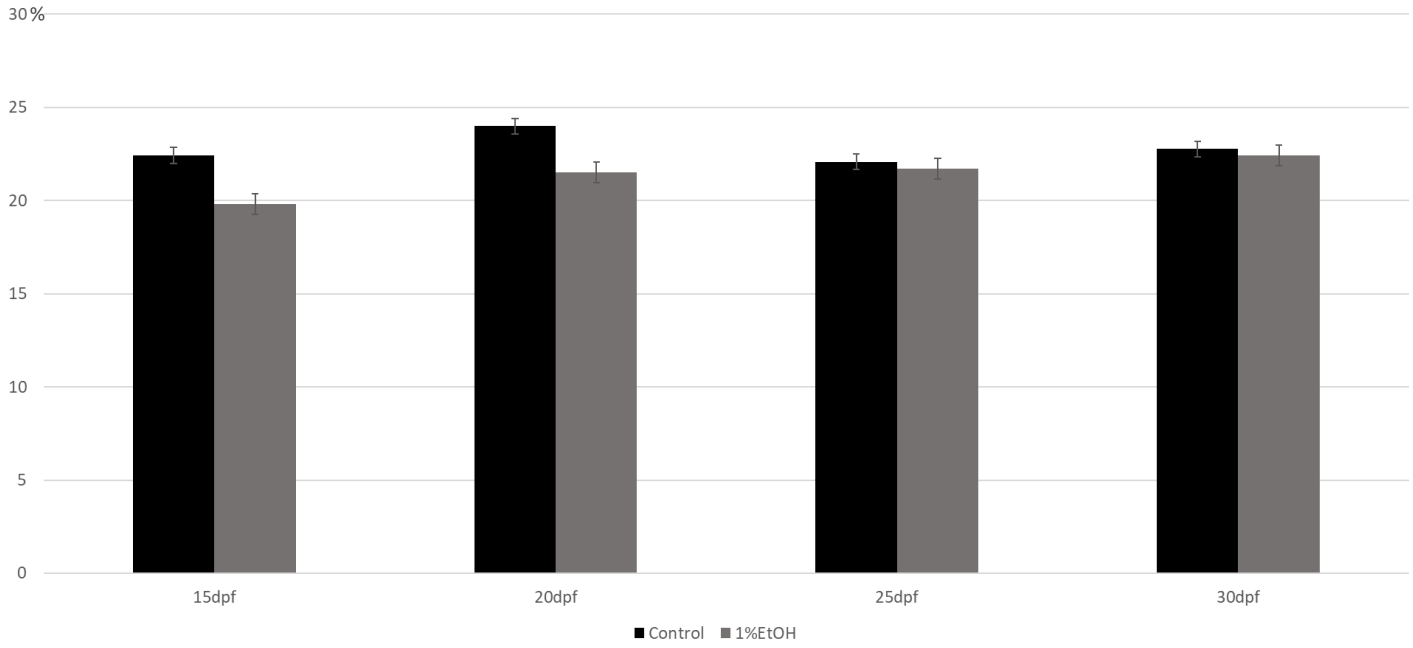

Figure 4.24: Comparing the cusp length proportion with the tooth length between 2mM LiCl treatment group and control at 15, 20, 25, and 30 dpf. The cusp length proportion significantly increased in LiCl-treated samples compared to the control at all the time points.

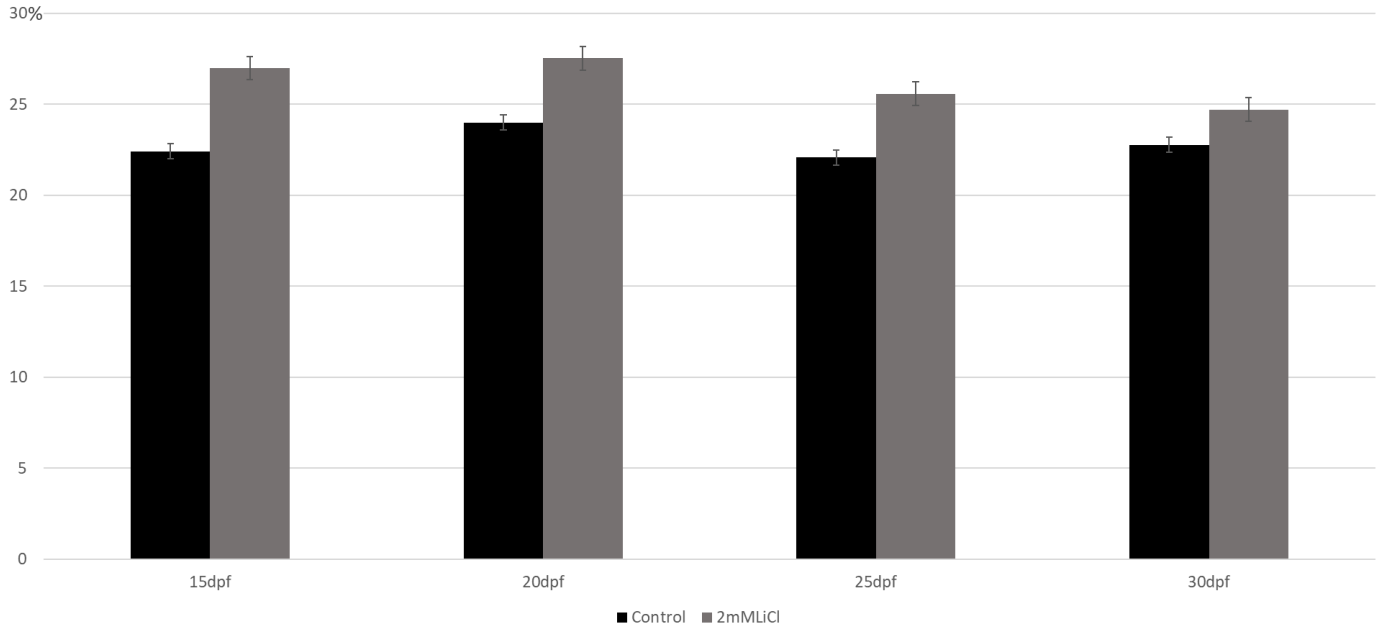

Figure 4.25: Comparing the cusp length proportion with the tooth length between 1%EtOH + 2mM LiCl treatment group and control at 15, 20, 25, and 30 dpf. The cusp length proportion significantly decreased in EtOH + LiCl-treated samples compared to the control at all the time points.

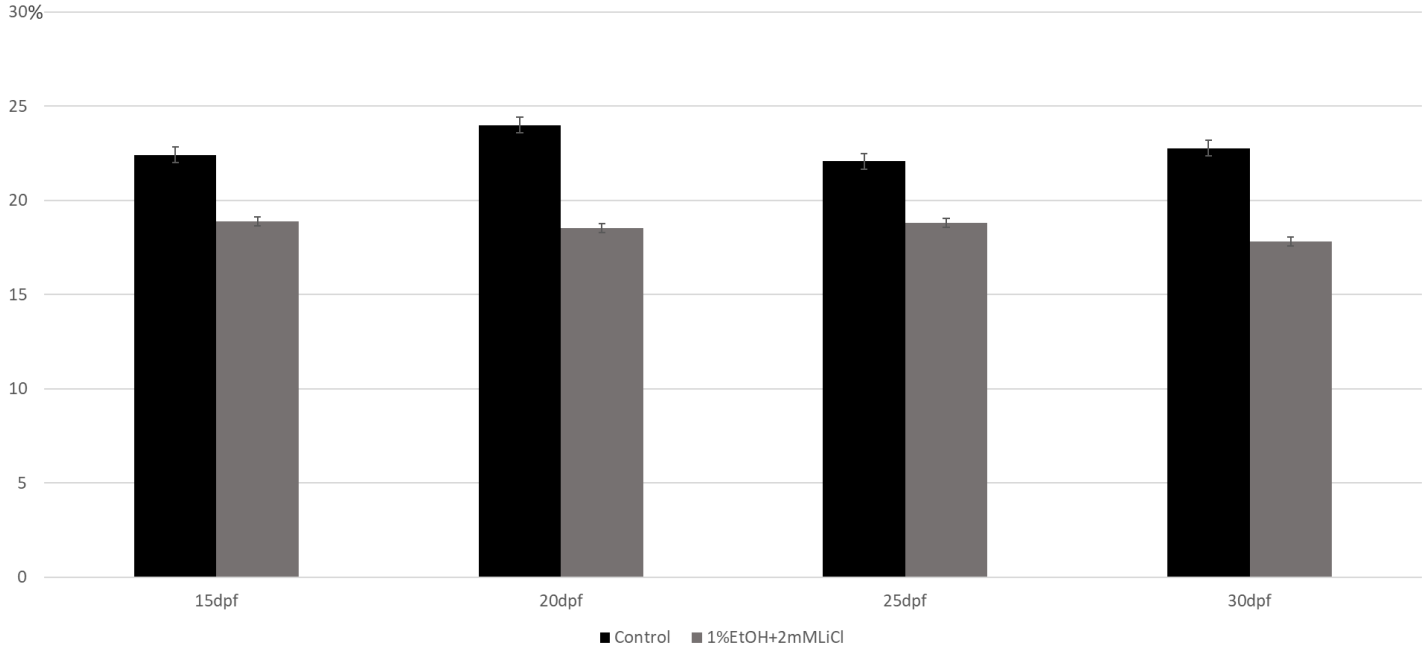

Figure 4.26: Comparing the cusp length proportion with the tooth length between 10nM WC59 treatment group and control at 15, 20, 25, and 30 dpf. The cusp length proportion significantly decreased in WC59-treated samples at all the time points.

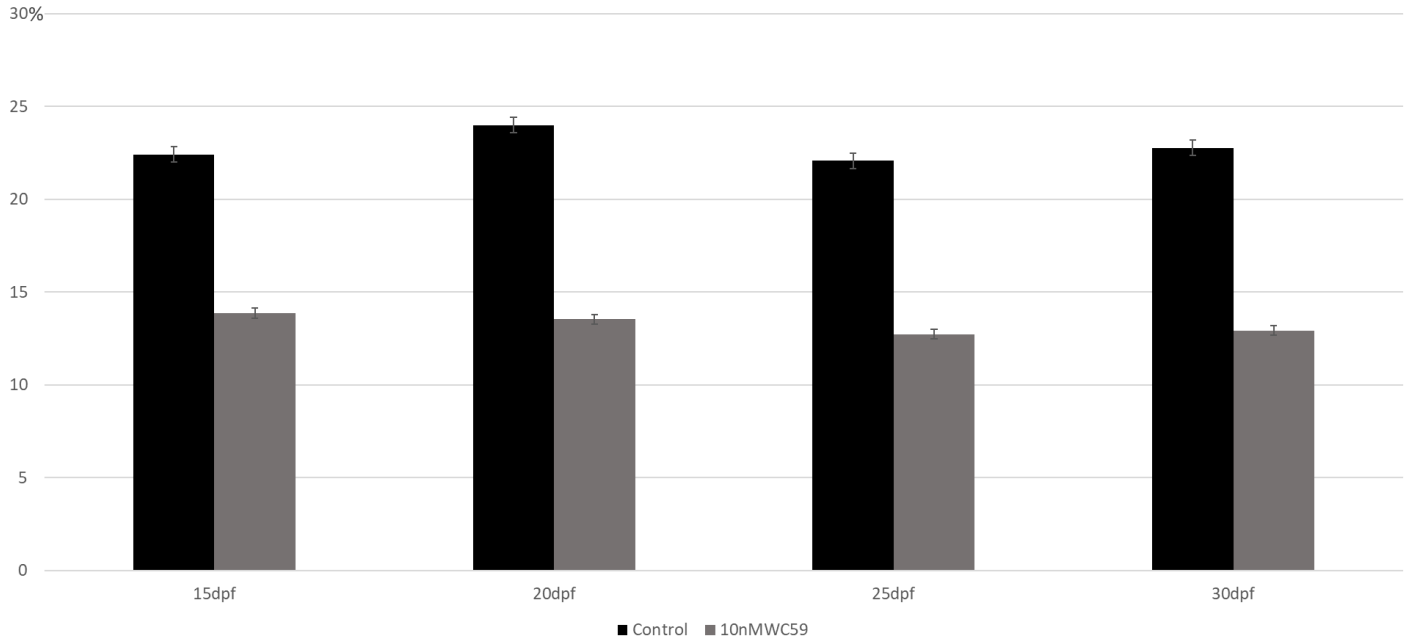

Figure 4.27: Comparing the cusp length proportion with the tooth length between 1%EtOH + 10nM WC59 treatment group and control at 15, 20, 25, and 30 dpf. The cusp length proportion significantly decreased in EtOH + WC59-treated samples at all the time points.

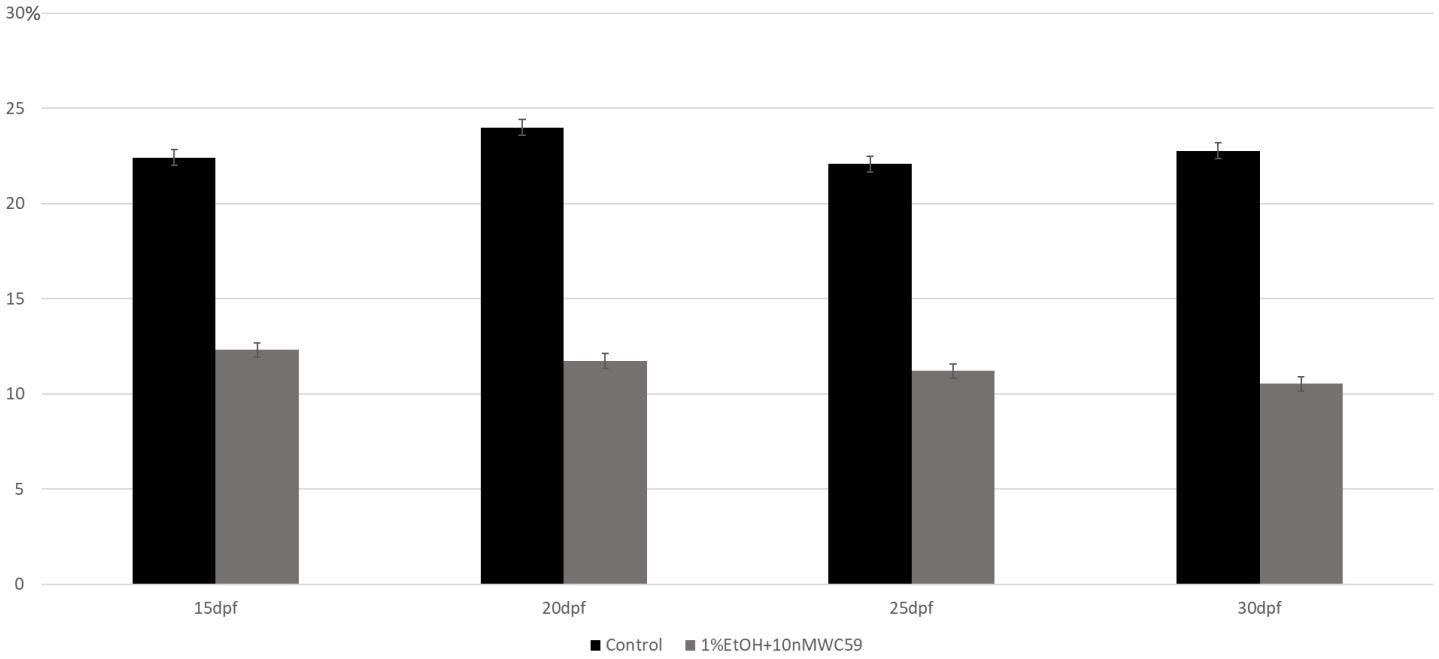

4.9. Results of WMISH

WMISH was performed for the 48 hours post fertilization (hpf) zebrafish using Wnt10a and Wnt10b probes to identify the Wnt10a and Wnt10b expression in an area of tooth development. The expression of the Wnt10a and Wnt10b after treatments was detected using the colorimetric method. Treatments include 1% EtOH, 2mM LiCl, 10nM WC59 and combined treatment of EtOH + LiCl and EtOH + WC59. Each treatment was conducted from 10 hpf to 12 hpf. Wnt10a and Wnt10b expression was detected as purple color. The negative control was not treated with the Wnt10a and Wnt10b probes (Figure 4.28 A). Expression of Wnt10a and Wnt10b was detected in the developing craniofacial region and around the pharyngeal cavity in 48 hpf in the control sample (Figure 4.28 B & C). In a 1% EtOH-treated sample, overall Wnt10a and Wnt10b expression was reduced compared to the control sample which was observed from the decreased intensity of purple color (Figure 4.28 D & E). In the 2mM LiCl treated sample, the overall expression of Wnt10a and Wnt10b noticeably increased around the developing craniofacial region and pharyngeal cavity (Figure 4.28 F & G). With the treatment of 10nM WC59 and 1% EtOH combined with 2mM LiCl, the overall Wnt10a and Wnt10b expression was reduced but the expression was still detectable around the pharyngeal cavity and craniofacial region (Figure 4.28 H, I, J & K). The overall expression of Wnt10a and Wnt10b reduced noticeably in the 1% EtOH combined with 10nM WC59 treated sample compared to the control sample (Figure 4.28 L & M). Collectively, the Wnt10a and Wnt10b expression in 1% EtOH, 1% EtOH combined with 2mM LiCl, 10nM WC59 and 1% EtOH combined with 10nM WC59 treated samples was reduced while the Wnt10a and Wnt10b expression increased in 2mM LiCl treated sample compared to the control sample.

Figure 4.28: Whole-Mount in situ Hybridization of 48 hpf zebrafish for Wnt10a and Wnt10b probes. B, D, F, H, J, L: Samples of Wnt10a probe. C, E, G, I, K, M: Samples of Wnt10b probe. A: Negative control for the experiment, B & C: Control, D & E: 1% EtOH, F & G: 2mM LiCl, H & I: 10nM WC59, J & K: 1%EtOH + 2mM LiCl combined treatment, L & M: 1%EtOH + 10nM WC59 combined treatment. Expression of Wnt10a and Wnt10b was prominent in the control sample. The expression was detected around the pharyngeal cavity and developing craniofacial region. In all the treatment groups the overall expression of Wnt10a and Wnt10b had reduced except the LiCl treatment group. Expression of Wnt10a and Wnt10b was significantly enhanced in the LiCl-treated samples around the pharyngeal cavity and developing craniofacial region. e: eye, pr: pharyngeal region, fm: future mouth, y: yolk sac. Scale bars indicate 50 µm.

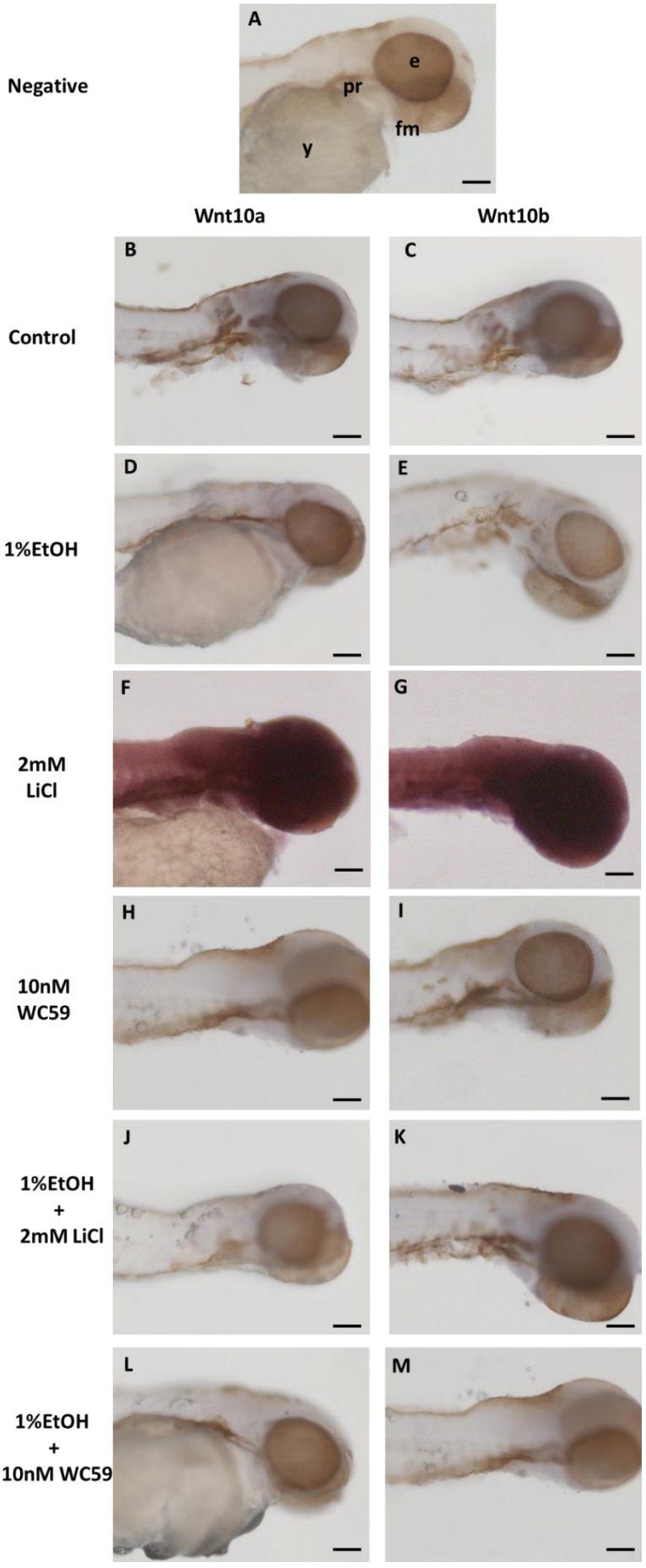
Negative
A
e
pr
fm
y
Wnt10a
Wnt10b
Control
B
C
1%EtOH
D
E
2mM
LiCl
F
G
10nM
WC59
H
I
1%EtOH
+
2mM LiCl
J
K
1%EtOH
+
10nM WC59
L
M

CHAPTER 5: DISCUSSION

5.Discussion

In this study, I tried to mimic the FASD dental phenotype by exposing the zebrafish model animal to 1% ethanol (171 mM) and investigated its effects on tooth development. Ethanol is known to have a strong effect on the craniofacial structures of the developing fetus, particularly on tooth development (36, 44). FASD is an umbrella term that can result from prenatal alcohol exposure and comprises a range of symptoms, including minor craniofacial anomalies, growth retardation, neurological abnormalities, cognitive and behavioral impairment, and birth defects (199-201). I used zebrafish as an excellent model in which to investigate the craniofacial effects of FASD, especially the tooth development (2, 105, 166). Zebrafish are easy to keep, eggs develop ex-situ, so are not affected by any placental influence or parental care (107, 202), and ethanol metabolizing genes (108, 132) as well as craniofacial structure are evolutionarily conserved between zebrafish and humans. In order to analyze tooth defects, we performed the alcian blue and alizarin red double staining. We chose the period of 10 hpf to 24 hpf for the study because this is the time when neural crest cell migration, development of the neural tube, and organogenesis begin in the developing zebrafish embryo (41, 203). Zebrafish has several wild-type fish strains. For example, AB, EKW (Ekkwill), TU (Tubingen) etc. According to previous studies, zebrafish exhibit a strain-dependent sensitivity to ethanol (204). AB strain and EKW (Ekkwill) strains have higher survivability upon ethanol exposure. TU strain in zebrafish was found to be more vulnerable to ethanol with a remarkably high mortality rate. However, AB larvae exhibit more skeletal defects compared to the EKW strain (204). Therefore, we chose wild-type AB zebrafish strain to examine tooth defects in our study. Exposure of zebrafish to ethanol can induce various defects in the fish body. Further, zebrafish exhibit a dose-dependent sensitivity to ethanol (204). Exposure to the 1% or 1.5% ethanol reduces the overall body size by reducing the body length and width (106, 109). Reduced body width reduces the distance between the eyes in zebrafish (106). In this study, zebrafish pharyngeal teeth showed acute sensitivity to 1 % ethanol at different ages. Ethanol decreased the tooth length and width and cusp length, as well as altered mineralization and cusp shape. Furthermore, I attempted to show an interaction of ethanol and the Wnt signaling pathway on tooth development. Wnt signaling pathway has been shown a crucial role in the early development of teeth (173). Inhibition of Wnt signaling can cause the formation of teeth with abnormal shapes (205). I found that the Wnt signaling activator (LiCl) in combination with ethanol caused a significant decrease in tooth length and width with shape anomalies while the treatment of LiCl alone resulted in a significant increase in these metrics. Moreover, Wnt signaling inhibitor (WC59) combined with ethanol treatment showed a noticeable decrease in tooth length and width with the

distorted shape of the teeth. This study also discovered a reduced expression of Wnt10a and Wnt10b in the developing craniofacial region and around the pharyngeal cavity with all the treatments except the LiCl.

5.1 Prenatal alcohol exposure can cause adverse effects on tooth development

FASD, which is a completely avoidable developmental disorder with resulting negative lifetime consequences receives far too little attention and is underestimated even by specialists across the world (206, 207). The most important problem with FASD is the complexity of diagnosis. According to the four-digit code by Astley and Clarren four diagnostic criteria are crucial for the verification of FASD: (1) Growth deficiency, (2) damage or dysfunction of the central nervous system (CNS), (3) facial phenotype, and (4) gestational exposure to alcohol (208). CNS anomalies and growth deficiency commonly observed in FASD have been documented to manifest a diverse spectrum of symptoms that deviate from their typical presentations (24). For number three, facial phenotype, the fading of abnormal facial features with age can complicate diagnosis (209, 210). For the fourth point (gestational alcohol exposure), it is obvious that not every mother would respond truthfully to this question and for children in foster care this question might be impossible to answer (209). Previous studies have been trying to identify the specific craniofacial malformations of FASD as a tool for early diagnosis, especially oral abnormalities and dental defects (24, 36, 44). In the study of 68 children with FASD, it is observed that the prevalence of caries is significantly higher than the control (211). In some studies, the DMFT index (caries severity score indicating caries incidence: Decayed, Missing and Filled Teeth) was higher than the control (36, 211). A higher rate of DDE (Developmental Defects of Enamel) compared to the control group was observed in one study (36) while in other research no cases of an enamel structural abnormality were reported (212, 213). Enamel hypoplasia (214), Enamel hypo maturated (95, 96), absent teeth, displaced or rotated teeth, diastema (94), delay eruption (215), malocclusion (93, 216), dental crowding (217), overjet, and open bite (44) are other dental anomalies that has been studied in children with FASD. Focusing on the early diagnosis of the orofacial anomalies of FASD can lead to better management of adverse effects of FASD on children's social life.

Numerous animal studies focused on the effect of prenatal alcohol exposure on the developing dentition (86, 87). Retardation of tooth eruption in offspring of macaque monkeys (88) and rat models (89, 90), delaying of cell differentiation within the tooth germ and reduced dentin and

enamel matrix formation in pregnant mini-pigs (91) are examples of FASD-like tooth anomalies in animal models.

Zebrafish is a useful model in studying craniofacial development, yet the effect of alcohol on its tooth development has not been well studied. The zebrafish like all Cyprinids, lost both oral and anterior pharyngeal teeth 65 million years ago and retain 11 teeth on each half of the fifth ceratobranchial arch (218). The teeth of adult zebrafish, like human dentition, consist of dentine surrounding a pulp cavity and covered by a hypermineralized cap (168, 219, 220). There are a few differences between the zebrafish and human teeth. Zebrafish dentition does not have distinguishable crown and roots and the teeth are directly attached to the supporting bone. The hypermineralized layer, known as enameloid, is a dentine-like structure containing collagenous components (221). The underneath dentine lacks of dentinal tubules, and the dentin collagen fibers are arranged along the long axis of the teeth (167). Despite these differences, zebrafish tooth can be a promising model to understand tooth anomalies in humans.

Microscopic analysis of the alizarin red-stained pharyngeal tooth of zebrafish has shown that ethanol can cause a reduction in tooth mineralization at 15 and 20 dpf compared to the control (Figure 4.1 E & F). It means teeth started to be fully mineralized at late stages (25 dpf) (Figure 4.1 G & H) compared to the control samples in which the first pair of teeth has begun mineralization at 82 hours post fertilization (222) and become fully mineralized at 4-6 dpf (164, 223). As mentioned before, many studies have shown that ethanol administered in vivo during pregnancy influences the secretory function of the ameloblast and hence enamel formation (36, 91). Furthermore, exposure to ethanol during pregnancy caused a reduction in the development of tooth germ and secretion of the dentine matrices (44). Another finding in my study is that the tooth height and width of the EtOH-treated samples were less than the control at 15 dpf and 20 dpf (Figure 4.2 & 4.3). However, these metrics were the same between the control and EtOH-treated samples at 25 dpf and 30 dpf (Figure 4.4 & 4.5). Also, we found that tooth length and width differences between the EtOH-treated group and control were decreasing with the age (Figure 4.6). These findings showed that the adverse effects of EtOH are significant in first-generation teeth and then decrease through subsequent tooth replacement cycles. Among the features of FAS, micrognathia and small teeth associated with a highly arched palate have been reported in many studies (43, 224). By counting the attached teeth at each time point we demonstrated that tooth number decreased in EtOH-treated samples at 15 dpf while it was similar to the control at 20,25 and 30 dpf (Figure 4.12). It can be concluded that ethanol is not associated with developing hypodontia. Unfortunately, no study to date has investigated alcohol as a risk factor for hypodontia

and there is no report of hypodontia in children with FASD (225). In our study, all the EtOH-treated samples in 15dpf showed a straight cusp while the hook-like shape tooth increased until 30 dpf at which 87.5% of the samples had hook-like shape tooth (Figure 4.14). As mentioned before, these results can show that the adverse effects of EtOH are significant in first-generation teeth and then decrease through subsequent tooth replacement cycles. Misshapen teeth have been observed as one of the adverse effects of prenatal alcohol exposure (226).

In our study, the microscopic analysis of the length of the zebrafish tooth cusp and statistical analysis of the proportion of cusp length revealed that the EtOH can have effects on the enameloid part of the tooth. At 15 and 20 dpf, the cusp length in the 1%EtOH treatment group was significantly less than the control (Figure 4.19 & 4.20) but not at 25 and 30 dpf (Figure 4.21 & 4.22). These interesting results can reveal that ethanol has a significant inhibitory effect on ameloblasts and suppress the enameloid formation which can reduce the size of the tooth. Many researchers have reported that ethanol can cause cellular alterations in the inner enamel epithelium of the tooth germ during the bud stage and can influence the secretion of ameloblasts, which in turn can influence enamel formation (36, 44).

According to the available literature, ethanol treatment is not only found to have an effect on tooth development but also can cause other craniofacial abnormalities. Among the most ethanol, sensitive structures are the eye, otic capsule, and ethmoid plate. This ethanol-induced craniofacial dysmorphogenesis was found to be mainly the result of increased cell apoptosis, regenerative capacity, and compensated facial primordial growth (227). Further, in zebrafish after ethanol exposure, malformed body cavities and fin displacement were found (227). According to previous studies, exposure to different chemicals such as fluoride, zirconium oxide nanoparticles , metal alloys and the chemicals in toothpaste were found to increase tooth and craniofacial anomalies in zebrafish. In detail, fluoride-treated teeth were discovered to have pits and roughness as well as an increase in organic components by using scanning electron microscopy and compositional analysis (228). In another study it was shown how different types of toothpaste for children affected molecular mechanisms of odontogenesis in zebrafish embryos (229).
We identified ethanol has an adverse effect on tooth development. However, gene–ethanol interactions associated with craniofacial is needed to be investigated for specific cell-signaling pathway genes. Studies pertaining to the molecular mechanisms of gene–ethanol interactions will provide important information on identifying the etiology of the visible phenotypic characters of FASD.

5.2 Alcohol can cause dental anomalies through interactions with Wnt signaling pathway

Numerous studies have implicated the major role of Wnt signaling pathway in tooth development in humans (173, 205, 230, 231). The Wnt gene family consists of a large family of secreted glycoproteins that specify various cell lineage during embryogenesis. Several Wnt genes, such as Wnt4, Wnt5a, Wnt6, Wnt10a and Wnt10b are broadly expressed in dental epithelium and mesenchyme (231). During tooth development, nuclear beta-catenin is observed in both the dental epithelium and the underlying mesenchyme, and the canonical Wnt signaling pathway is activated at multiple stages of tooth morphogenesis (230, 232, 233). Consistent with an essential role of Wnt/beta-catenin signaling in early tooth development, mutation, or inhibition of Wnt pathway result in different tooth anomalies such as oligodontia (234, 235), tooth agenesis (236) taurodontism and misshaped crowns (190). The crucial role of Wnt pathway in tooth development has been also shown in many animal studies (237-239). Some previous works on mouse models showed that activation of Wnt signaling causes dramatic changes in tooth number (230, 232, 240). Gregory R. Handrigan et al observed that canonical Wnt signaling enables ordered tooth replacement in snakes by promoting dental epithelial cell proliferation (237). L.Sarkar et al suggest that Wnt signaling is required early in tooth germ formation of Xenopus animal model (241). A specific study on the Malawi cichlid model demonstrated that manipulation of Wnt/β-catenin in vivo with small molecules resulted in dose-dependent effects on both tooth replacement and tooth shape (242). After treating the cichlid embryos with the Wnt/β-catenin pathway agonist, LiCl (0.5 mM), teeth in multiple positions are delayed in eruption (242). The active role of Wnt signaling in a time window between late cytodifferentiation of a tooth and early morphogenesis of its successor has been shown in zebrafish studies (243). Moreover, Yuan et al provided evidence that Wnt10a is critical for tooth development and mutations in this gene lead to arrest of normal tooth development in zebrafish (234).

In this study, we showed the role of Wnt signaling pathway in tooth size, tooth number, and cusp shape of zebrafish dentition by treating the embryos with the Wnt pathway agonist, 2mM LiCl, and antagonist, 10nM WC59. The 2mM LiCl treated Malawi cichlids embryos developed locked jaws in one study (195). We investigated that the tooth width and length increased significantly in 2mM LiCl treatment group (Figure 4.2, 4.3, 4.4 & 4.5). We also observed that the tooth length difference between the control and LiCl-treated samples increased with the age (Figure 4.7). Whereas the tooth width difference increased until 25dpf and it decreased at 30 dpf to the same tooth width in the control (Figure 4.7). This interesting result revealed that LiCl plays as an

activator by increasing the tooth length by activating the ameloblasts. This finding can be confirmed by the comparison of the cusp length. Not only the cusp length in LiCl-treated group were significantly higher than in the control (Figure 4.19, 4.20, 4.21 & 4.22), but also the proportion of the cusp size to the tooth length was significantly higher in treated samples (Figure 4.24). It can prove that the increase in tooth length is the result of increase in the cusp length of the LiCl treatment group. As the enameloid structure is considered the cusp part of the tooth, boosted enamel secretion of the ameloblasts is the result of the activator. However, numerous studies have been shown that Wnt signaling controls dentin thickness (244), and Wnt10b specifically regulates odontoblast differentiation and expression of noncollagenous dentin proteins (245, 246).

Another finding of this study was a noticeable decrease in cusp length (Figure 4.19, 4.20, 4.21 & 4.22), tooth width and length of WC59 treatment group (Figure 4.2, 4.3, 4.4 & 4.5). By comparing cusp length, tooth length and width between WC59 and EtOH treatment groups, we revealed that the inhibitory role of WC59 is stronger than the EtOH. Many studies have shown the effects of WC59 in zebrafish. In detail, effects of Wnt signaling inhibition on mesenchyme and epithelium development of the zebrafish swim bladder were observed in one study (247). By inhibiting the Wnt signaling pathway, it was proved that Wnt signaling plays stage-specific roles during neural crest induction in zebrafish (248). Stewart et al showed that canonical Wnt directly affects preosteoblasts by rapid changes in preosteoblast subtypes and their proliferation with short-term 100nM WC59 (249). In our study, the difference in tooth length and width between samples treated with WC59 and the control over time indicates that WC59's inhibitory effect on tooth development became more pronounced with more successive tooth replacement cycles (Figure 4.9). We showed this strong inhibitory role of WC59 in the later stages of zebrafish lifetime by observing noticeable hypodontia at 25 and 30 dpf (Figure 4.12). This study revealed that the cusp length to tooth length proportion was significantly less than the control at all the time points. This finding can prove that the WC59 suppresses the ameloblast secretion which can affect the length of the enameloid and in turn affect the tooth length (Figure 4.26)

In this study we tried to examine the interaction of EtOH and Wnt signaling pathway by using the combination treatment of EtOH with LiCl and EtOH with WC59. We analyzed that tooth length and width of EtOH and LiCl-treated samples were noticeably less than the control at all the time points (Figure 4.2, 4.3, 4.4 & 4.5) and tooth length and width difference between the treatment and control groups tended to increase from 15 dpf until 30 dpf (Figure 4.8). This interesting result can

reveal that EtOH has a strong inhibitory effect which can also neutralize the effects of LiCl. These metrics were even more decreased in EtOH and WC59 combined treatment group since they both have an inhibitory effect (Figure 4.2, 4.3, 4.4, 4.5 & 4.10). This can show that EtOH and WC59 cause much more tooth defects than the sum of their individual effects on tooth development which can prove their synergistic effect. In our study, we examined that the cusp length and the cusp length to tooth length proportion of both combined treatment groups were significantly less than the control and EtOH individual treatment group (Figure 4.19, 4.20, 4.21, 4.22 & 4.27). As mentioned before these results can illustrate that this inhibitory effect is through affecting the ameloblast secretion which is more suppressed in combination treatment groups. We showed that the tooth mineraliztion in EtOH and LiCl combined treatment was disrupted more than the LiCl and EtOH individual treatment as well as the control (Figure 4.1 M, N, O & P). However, the hypomineralization was noticeably severe in EtOH and WC59 combined-treated samples (Figure 4.1 U, V, W & X). This can prove that although the inhibitory role of combined treatments is stronger in suppressing the enameloid development, both enameloid and dentine are affected by the interaction of EtOH and Wnt signaling pathway. We also noticed that the tooth number and cusp shape was affected in later tooth replacement cycles in EtOH and LiCl combination treatment (Figure 4.12 & 4.16) while all the samples of combined EtOH and WC59 treatment showed a severe hypodontia and distorted cusp shape at all the time points (Figure 4.12 & 4.18). Numerous studies revealed the interaction of EtOH and Wnt signaling pathway. Vangipuram et al showed that expression levels of Wnt3a and Wnt5a were significantly suppressed in differentiating neural stem cells with exposure to both 20 and 100 mM concentrations of EtOH (250). They also mentioned that EtOH increased Tyr phosphorylation of GSK3b, which promotes degradation of β-catenin, a key downstream Wnt signaling pathway protein (250). Another study also showed that chronic high-dose ethanol exposures inhibit Wnt signaling, which likely contributes to the impairments in liver regeneration (251). One study on chicks showed that EtOH can destabilize nuclear β-catenin within 2 hours of ethanol exposure and significantly reduces its transcriptional activity which can cause neural crest apoptosis and craniofacial malformations (252).

Although genetic approaches have informed the multiple mechanisms by which EtOH disrupts craniofacial morphogenesis, there are few studies on how gene-EtOH interaction can affect tooth development. We identified that ethanol affects tooth development through interaction with Wnt signaling pathway by using a combination treatment of EtOH with LiCl and EtOH with WC59. However, specific molecular analysis is needed for investigating the mechanism responsible for EtOH-Wnt signaling interaction and its effects on the development of dentition.

5.3 Chemical-dependent differential expression of Wnt10a and Wnt10b

Different Wnt signaling pathways are expressed in different stages of development. The Wnt10a and Wnt10b is a ligand in the canonical Wnt pathway (β-catenin dependent) that have been identified as major regulators for tooth development (173, 194). Wnt10a is expressed in the dental epithelium and mesenchyme at the bud stage and cap stage (173). Wnt10b initially only expressed itself in the incisor epithelium, but as tooth development advanced, it started to do so in the molar primordia as well (194). In our study, we exposed 48 hpf zebrafish larvae to different treatments; The Wnt10a and Wnt10b expression was determined in the hatching stage of 48 hpf (Figure 4.28 B & C). Wnt10a is expressed in the craniofacial region at crucial stages of tooth formation, according to functional studies done on zebrafish embryos (243, 248, 253). Wnt10a expression disruptions were shown to hinder normal tooth development and stop tooth development at 5 dpf (234). Wnt10a expression was also strongly connected with the levels of mRNA expression of other tooth development genes; expression of msx1, dlx2b, eda, and axin2 was decreased with Wnt10a knockdown and raised upon wnt10a overexpression (254, 255). The mouse dental epithelium was found to co-express Wnt10a and Wnt10b during the earliest stages of tooth development (194). Unfortunately, there is no studies on Wnt10b expression in zebrafish. In addition, we discovered the reduction of Wnt10a and Wnt10b expression in the developing craniofacial region and around the pharyngeal cavity upon 1% EtOH treatment (Figure 4.28 D & E), 10nM WC59 (Figure 4.28 H & I), 1% EtOH combined with 2mM LiCl (Figure 4.28 J & K) and combined treatment of 1% EtOH and 10nM WC59 (Figure 4.28 L & M) using the digoxigenin-labeled antisense RNA probes. However, the Wnt10a and Wnt10b expression increased in the 2mM LiCl treated sample (Figure 4.28 F & G). As previously mentioned, ethanol acts as a suppressor for neural crest cell migration and it increases cell apoptosis as well as reduce the enamel and dentine formation (36, 80, 83). This might have resulted in the reduced expression of Wnt 10a and 10b in the developing craniofacial region and the lower pharyngeal jaw.

The development of the tooth is not only directly regulated by Wnt signaling pathway, but by the regulatory gene network. In Gli2/Gli3 double-mutant mice, tooth development is halted at the beginning and before the creation of the dental placodes, demonstrating a need for Shh signalling (256). In Msx1/Msx2 double mutants, a similar phenotype revealed that BMP signalling is involved in tooth initiation (257). Conditional deletion of Fgf8 in the oral epithelium caused tooth development to stop during the initiation stage, indicating the importance of FGF signalling in the process (258), and overexpression of the Wnt inhibitor Dkk1 in the ectoderm revealed the

necessity of Wnt signalling prior to placode formation (259). Changes in wnt10a expression also affected the expression of other genes involved in tooth formation, including msx1, dlx2b, eda, and axin2 (254, 255). The expression of msx1, dlx2b, eda, and axin2 significantly decreased when wnt10a was knocked down, indicating that imbalances in wnt10a expression may directly or indirectly cause tooth development to be stopped or impaired in zebrafish. However, msx1, dlx2b, eda, and axin2 expression increased in response to wnt10a overexpression (253). It is therefore essential to research how Wnt10a and Wnt10b and the gene network operate on exposure to EtOH, LiCl and WC59. This will have a clearer explanation of the fact that we can compare our data with human tooth defects in humans.

This study highlighted the effect of ethanol, activation, and inhibition of Wnt signaling pathway on tooth development, and the combined effect of chemicals on zebrafish tooth development. This is the first study to show that combining the effects of ethanol and a Wnt activator and inhibitor can increase the severity of tooth malformation. This research will contribute to a better understanding of the complex etiopathogenesis of tooth anomalies by introducing ethanol-Wnt pathway interaction.

CHAPTER 6: CONCLUSION

Conclusion

While many studies have investigated craniofacial malformations of FASD, very little attention has been given to how prenatal alcohol exposure can affect tooth development. Collectively, results from my thesis demonstrated that embryonic alcohol exposure caused abnormal tooth formation, suggesting the possible teratogenic effects of alcohol on tooth development. These changes can be due to alcohol-induced changes, alcohol and gene interactions or it can be due to the activation or inhibition of the complex metabolic mechanisms within cells. Among the cell signaling pathways responsible for tooth development, the Wnt signaling pathway has been observed in the dental epithelium and mesenchyme of early and late stages of the development of the dentition. My study also demonstrated that the Wnt-alcohol interaction caused adverse effects on tooth development.

Zebrafish tooth width, length, and shape was affected by alcohol, Wnt agonist (LiCl) and Wnt antagonist (WC59). Tooth width and length were reduced in alcohol and WC59 treatment groups while these metrics were increased in LiCl treated samples. The tooth shape was distorted in all mentioned treatments. Severe tooth defects observed upon the combined treatment of alcohol with LiCl and alcohol with WC59 resulted from the interaction of ethanol with Wnt signaling pathway. The combined treatments resulted in reduced tooth length, width and number and defects in tooth shape of zebrafish dentition. In my study, it was proved that alcohol affect the tooth size through suppressing the enameloid formation. Furthermore, it was shown that the suppressing or activating the Wnt signaling pathway has more impact on the ameloblasts secretion.

Alcohol interactions have reduced the expression of Wnt10a and Wnt10b, the two most important ligands of Wnt signaling pathway in tooth development, in craniofacial region and pharyngeal cavity. This indicates that the interaction of Wnt10a and Wnt10b gene with alcohol in zebrafish can influence tooth formation.

This study highlights the effect of alcohol and alcohol-gene interaction on tooth development. This can shed light on the mechanism of alcohol teratogenicity which can cause tooth anomalies.

CHAPTER 7: APPENDIX

Appendix 1

Acid-free Double-stain (bone and cartilage-for embryos)

1. Fix embryos in 4% PFA in 0.01M PBS (2 hours room temperature with agitation, or overnight at -4°C) – store in 0.01 M PBS.
2. Put samples directly into 50% ethanol for 10 minutes at room temperature with agitation.
3. Remove ethanol and add staining solution – agitate overnight at room temperature.
4. Rinse in distilled water (add water to tube with specimen and invert twice maximum).
5. Remove water and add bleach solution to tubes for 20 minutes at room temperature, with lids open (no agitation).
6. If fish are aged more than 20 dpf add a step here: remove bleach and wash specimens in a 1% KOH solution for 1 hour at room temperature with agitation. The blue stain will stick to the outside of larger samples, covering the bone. This step does not completely solve the problem, but it helps. The remaining blue stuck on the specimens can be scarped off gently with forceps.
7. If fish are aged less than 20 dpf : remove the bleach and add 20% glycerol solution made in 1% KOH to tubes and agitate at room temperature for 30 minutes.
8. Replace 20% glycerol solution with a 40% glycerol solution made in 1% KOH and agitate at room temperature for 2 hours.
9. Store in 100% glycerol.

Solutions:

Staining solution

1 ml of staining solution = 980 µl of Part A + 20 µl of Part B

Part A

100 ml solution:

- 5 ml 0.4% Alcian Blue in 70% ethanol
- 70 ml of 95% ethanol
- 25 ml of 20 mM MgCl2
- (Final concentration: 0.02% Alcian Blue, 20 mM MgCl2, and 70% ethanol)

Part B

10 ml solution:

- 0.5% Alizarin Red in distilled water

Bleaching solution

Mix equal volumes of 3% H2O2 and 2% KOH for a solution that is overall 1.5% H2O2 and 1% KOH.

Appendix 2

DIG High Prime DNA Labeling and Detection protocol

1. Make sure that hybridization oven is on and preheated to 100 ˚C

2. Cut out the nitrocellulose membrane big enough to fit in the Petri dish. Cut a wedge out of one corner in order to indicate the top left corner.

3. Apply a 1 µl of your labeled diluted probe from the prepared dilution series (10^{-2}, 10^{-3}, 10^{-4}, and 10^{-5}) and labeled control probe to the nitrocellulose membrane.

4. Fix the nucleic acid by baking for 30 minutes at 120˚C in a sterile glass petri dish.

5. Transfer membrane into the plastic dish (sterile) with 10 ml of Maleic acid buffer (approx. ½ the depth of the dish, enough to cover the membrane). Incubate (20˚C) with shaking (40 RPM) for 2 min.

- Maleic acid buffer recipe

Maleic acid buffer	100 ml
Maleic acid (0.1 M)	1.1607 g
NaCl (0.15 M)	0.8766 g
10X TBST in DepC H_2O	100 ml
PH set to 7.5 with solid NaOH	

6. Incubate (20˚C) for 20 minutes in Blocking solution with shaking 40 RPM.

- Blocking solution recipe

Blocking Solution	100 ml
Sheep Serum (2%)	2 g
Milk Powder	3 g
10X TBST in DepC H_2O	100 ml

7. Prepare Anti-Digoxigenin Antibody solution.

- Antibody solution recipe

Antibody solution	1001µl
Anti-Digoxigenin-AP, Fab fragments	1 µl
10X TBST in DepC H_2O	10 ml

8. Wash for 5 minutes with 10X TBST in DepC H_2O. Incubate (20˚C) with shaking (40 RPM)
9. Incubate (20˚C) with 10 ml of Anti-Digoxigenin Antibody solution for 30 minutes with shaking (40 RPM).
10. Wash with Washing buffer. Incubate (20˚C) with shaking (40 RPM). Carry this out twice for 15 minutes each, the second time with fresh Washing buffer, save the Antibody solution.

- Washing buffer recipe

Washing buffer	100 ml
Maleic acid (0.1 M)	1.1607 g
NaCl (0.15 M)	0.8766 g
Tween 20 (0.3%)	0.3 ml
DepC H_2O	Top up to 100ml
PH set to 7.5	

11. Equilibrate for 5 minutes in the Detection buffer. Incubate (20˚C) with shaking (40 RPM)

- Detection buffer recipe

Detection buffer	100 ml
Tris-HCl (0.1 M)	10 ml from 1M stock solution
NaCl (0.1 M)	0.5844 g
DepC H_2O	Top up to 100ml
PH set to 7.5	

12. Incubated at room temperature in a dark place (due to light sensitivity) in 10 ml of NBT/BCIP staining solution. No shaking. Check approximately every 2 minutes for any color change.

Appendix 3

Whole-Mount in situ Hybridization Protocol

Important considerations before starting:

- ✓ All solutions should be made with DepC H_2O unless otherwise stated in protocol.
- ✓ Gloves should be worn at all times to reduce contamination.
- ✓ Countertop work surface should be RNAase zapped to reduce contamination before use.
- ✓ All plastic containers/tubes should be DNAase/RNAase free.
- ✓ Autoclaved pipette tips and Gilson Pipettes are to be used.

Prep Day (Collection of embryos and fish) (Approx. 2 hours + Overnights)

- Collect Embryos
  - □ Dechorinate 48 hpf embryos. For older embryos – anesthetize in .1% MS222.
  - □ Fix in 4% PFA (RNAase free) for 2 hours at room temperature or overnight at 4^{o}C.

- Dehydrate in series

□ 25% MeOH in PBS	30 min at RT	1x
□ 50% MeOH in PBS	30 min at RT	1x
□ 75% MeOH in PBS	30 min at RT	1x
□ 100% MeOH	At Least Overnight	Store in -20^{o}C

- Notes
  - □ MS222 is a powder that should be made into 0.01% and 0.1% solutions fresh for each day.

Day 1: Bleach Day (Approx. 1.5 hours, longer if older fish)

- Rehydrate embryos

□ 75% MeOH in PBS	5 min at RT	1x
□ 50% MeOH in PBS	5 min at RT	1x
□ 25% MeOH in PBS	5 min at RT	1x

- Wash
  - ☐ PBST 5 min at RT 1x

- Bleach
  - ☐ Bleach according to times below, or until the embryo is a creamy white. Ensure eyes do not become bulgy.
  - ☐ General timeline for fish

Age	Approx. Bleach Time
48 hpf	25 min

  - ☐ Bleach Recipe – Make Fresh on the day

Total Amount	5 ml	Total Amount	20 ml
KOH (.5%)	0.025 g	KOH (.5%)	.1050G
H_2O_2 (3% of 30%)	150 ul	H_2O_2 (3% of 30%)	600 ul
DepC H_2O	To 5 ml	DepC H_2O	To 20 ml

- Wash
  - ☐ PBS 5 min at RT 1x

- Note: Embryos can be very sticky in PBS/MeOH solutions

- Dehydrate in series
  - ☐ 25% MeOH in PBS 5 min at RT 1x
  - ☐ 50% MeOH in PBS 5 min at RT 1x
  - ☐ 75% MeOH in PBS 5 min at RT 1x
  - ☐ Transfer into new 1.5 ml eppendorff tube
  - ☐ 100% MeOH Store in -20°C Overnight

- ✓ Embryos can now be stored in 100% MeOH at -20^{o} C for several weeks or at minimum of 2 hours before continuing on

Day 2: Pro-K and Treatment Day (Approximately 5 hours, longer if older fish)

- Rehydrate embryos in 1.5 ml eppendorf tubes
  - □ 75% MeOH in PBS 5 min at RT 1x
  - □ 50% MeOH in PBS 5 min at RT 1x
  - □ 25% MeOH in PBS 5 min at RT 1x

- Wash
  - □ PBST 5 min at RT 4x

- Permeabilize: With Proteinase K (10 ug/ml in DepC)
  - □ If using a 10 mg/ml stock, dilute by adding 1 ul of stock solution to 1000 ul of DepC H_2O

    Note: Pro-K in lower part of -20^{o}C

Age	Approx. Pro-K Time
48 hpf	23 min

- Wash
  - □ PBST 5 min at RT 2x

- Fix (In fume hood)

□ 4% PFA (DepC Treated) 20 min at RT 1x

- Wash
  - □ PBST 5 min at RT 2x

- Treat (In fume hood) – Make fresh on the day
  - □ Acetic Anhydride 30 min at RT 1x

Acetic Anhydride Recipe	6 ml Batch
DepC Water	4.5 ml
Triethanolamamine (upstairs lab cabinet)	79.9 ul
pH to 7.0	
DepC Water	To 6 ml
Acidic anhydride (under fume hood)	15 ul

- Wash
  - □ PBST 10min at RT 2x

- Prehybridize
  - □ Hyb (-) 2 hours at 70^{o}C/35 rpm

✓ **<u>Stop Point:</u>** Embryos can be stored in Hyb (-) for several weeks, or you can continue to the next step.

Continuing on or starting a new run

Note: If embryo's have been processed into Hyb (-) and stored, this is a good place to start a new in situ run. It allows you to effectively process many fish, and then run different genes on fewer numbers.

Day (1/3): Hyb (+) – Adding the probe (Approx. 2 hours)

- Pre Hyb (-)
  - □ Hyb (-) 2 hours at 70°C/35rpm

  Note: We re-do this stage to ensure the embryos are at the same permeability /solubility as previous

- Adding Hyb (+)

  □ Add 1 ml of Hyb (+) to each sample

Hyb (+) Recipe	Per tube (1 ml)	For 4 ml
Hyb (-)	890 ul	3560 ul
Yeast tRNA (5 mg/ml)	100 ul of 50 mg/ml stock	400 ul
Heparin (50 ug/ml)	10 ul of 5 mg/ml stock	40 ul
pH to 6.0 with Citric Acid	9.2 ul of 1 M citric acid	36.8 ul

Note: Multiply each reagent by the number of samples you have.

- Adding probe
  - □ Add 2-3 ul of probe (depending on strength) to each of the sample tubes.

  - □ Notes
    - Probe should not be left out of the freezer long. Putting them on ice is recommended.

- Ensure probe is mixed – flick with finger and centrifuge liquid back down for 2-3 seconds.

- Incubate overnight at 70°C/35rpm

Day (2/4): Washes and Antibody (Approx. 7 hours, with 3-4 hour break in middle)

- Washes
  - □ 75% Hyb (-) + 25% 2xSSC 15 min at 70°C/35 rpm 1x
  - □ 50% Hyb (-) + 50% 2xSSC 15 min at 70°C/35 rpm 1x
  - □ 25% Hyb (-) + 75% 2xSSC 15 min at 70°C/35 rpm 1x

    Note: These solutions should be premade and stored in the -20°C freezer

  - □ Change to fresh eppendorf tubes – Hyb (-) is very slippery and the tube caps tend not to stay in place at this point. The tubes will also likely have white precipitate throughout.

    Note: Going into this next stage – Embryos can become very sticky! Check pipette tip after each changeover!

  - □ 2xSSC 10 min at 70°C/35rpm 2x
  - □ 0.2xSSC 30 min at 70°C/35rpm 3x

  - □ Start sheep serum inactivation 30 min at 60°C
    (amount based on Blocking Buffer Recipe)

  - □ 75% 0.2xSSC + 25% PBST 10 min at Room temp/60 rpm 1x
  - □ 50% 0.2xSSC + 50% PBST 10 min at Room temp/60 rpm 1x
  - □ 25% 0.2xSSC + 75% PBST 10 min at Room temp/60 rpm 1x
  - □ 100% PBST 10 min at Room temp/60 rpm 1x

- Incubate in blocking buffer for 3-4 hours
  - □ Add 1 ml of Blocking buffer to each tube

Make Fresh on the day

Blocking Buffer recipe	1 ml/Sample	For 4 ml
1 x PBST	980 ul	3920 ul
2% Heat inactivated Sheep serum	20 ul	80 ul
Bovine serum albumin (2 mg/ml)	0.002 g	0.008 g

Note: Save at least 10 ul of blocking buffer. It is required in making the antibody recipe.

- Adding antibody

Antibody Recipe	
Blocking Buffer (saved from before)	9 ul
Anti-Digoxigenin-AP, Fab fragments	1 ul
Optional – Fish powder	A few pieces

□Allow antibody to sit in blocking buffer for at least 10 minutes before adding the antibody solution to the samples. This allows pre absorption to occur, and reduces background.

□Add 1 ul of above antibody recipe to each sample tube already containing the 1 ml of blocking buffer from 4-5 hours prior.

- Incubate overnight at 4^{o}C while shaking
  - □ Note: The incubator in the lower lab works well for this. Ensure the incubator is properly set and on early in the day, as it takes time to cool down.

Day (3/5): Antibody and Color Reaction (Approx. 4 hours then overnight)

- Remove samples from incubator and discard antibody solution

- Washes
  - □ PBST 5 min at RT

  - □ PBST 15 min at RT on same "Mandel" Shaker 12x

- Place embryos in sterile glass vials – Ensure proper labeling

- Incubate TRIS Staining Buffer
  - □ Add 1 ml of TRIS Staining Buffer to each sample 5 min at room temp 3x

  - □ Make Fresh on the day

Reagent	Stock	Final	20 ml Batch	10 ml Batch
TRIS pH 9.0	1 M	100 mM	2 ml	1 ml
$MgCl_2$	1 M	50 mM	1 ml	0.5 ml
NaCl	5 M	100 mM	400 ul	200 ul
Tween	10%	0.1%	20 ul	10 ul
Levamisole		2 mM	0.019 g	0.0095 g
DepC H_2O			To 20 ml	To 10 ml

Note: When determining batch size, allow for three changeover's per tube as well as enough for mixing NBT/BCIP staining solution

- Add Color Reaction Solution

- ☐ **Very Important**! – Ensure staining solution remaining in dark. It is a light sensitive reagent.

- Remove TRIS staining buffer and Add Color Reaction Solution
  - ☐ Approximately 1.2 ml per sample
  - ☐ Place samples in incubator at 4^{o}C overnight or at 37^{o}C until expression shows.
    - Best results have been attained at 4^{o}C overnight

Day (4/6): Stopping Color Reaction (Approx. 2 hours)

- Wash
  - ☐ PBST 5 min at Room Temperature 6x

- Fix (in fume hood)
  - ☐ 4% PFA 20 mins at room temperature 1x

- Dehydrate (for NBT/BCIP Color reactions only!) – Skip to below for Fast Red
  - ☐ 25% MeOH in PBS 10 min at RT 1x
  - ☐ 50% MeOH in PBS 10 min at RT 1x
  - ☐ 75% MeOH in PBS 10 min at RT 1x
  - ✓ 100% MeOH Store in 4^{o}C in sample box

Note: Photos should be taken while sample is in 25% or 50% MeOH.

Reagent Recipes

Hyb (-)

Reagent	% in final solution	50 ml Batch	250 ml Batch (ideal)
Deionized Formamide 100%	50	25 ml	125 ml
SSC 20x	5x	12.5 ml	62.5 ml
Tween 10% (stock solution)	0.1	50 ul	250 ul
DepC Water		Top to 50 ml	Top to 250 ml

Note: Make in fume hood. Ensure contents are well mixed. Aliquot into 50 ml flacon tube and store in -20^{o}C.

PBS

Reagent for 500 ml Batch	
NaCl	4.0 g
KCl	0.1 g
Na_2PO_4	0.693 g
KH_2PO_4	0.1 g
Top to 500 ml with DepC H_2O	
pH to 7	

To make PBST add 50 ul of Tween-10 to 50 ml of PBS

DepC H_2O

- ✓ Per 1 L of water add 100 ul of DepC (found in upstairs fridge).
- ✓ Carry out in fume hood.
- ✓ Shake for 30 minutes vigorously.
- ✓ Autoclave

CHAPTER 8: REFERENCES

References

1. Fernandes Y, Lovely CB. Zebrafish models of fetal alcohol spectrum disorders. genesis. 2021;59(11):e23460.

2. Silva P, Azimian Zavareh P, Atukorallaya D. Teleost Fish as Model Animals to Understand Alcohol Teratology. Fetal Alcohol Spectrum Disorder: Springer; 2022. p. 31-48.

3. Liu S, Narumi R, Ikeda N, Morita O, Tasaki J. Chemical-induced craniofacial anomalies caused by disruption of neural crest cell development in a zebrafish model. Developmental Dynamics. 2020;249(7):794-815.

4. Raterman S, Metz J, Wagener FA, Von den Hoff JW. Corrigendum: Zebrafish Models of Craniofacial Malformations: Interactions of Environmental Factors. Frontiers in Cell and Developmental Biology. 2021;9:650948.

5. Czarnobaj J, Bagnall KM, Bamforth JS, Milos NC. The different effects on cranial and trunk neural crest cell behaviour following exposure to a low concentration of alcohol in vitro. Archives of oral biology. 2014;59(5):500-12.

6. Lovely C, Rampersad M, Fernandes Y, Eberhart J. Gene–environment interactions in development and disease. Wiley Interdisciplinary Reviews: Developmental Biology. 2017;6(1):e247.

7. Corsello G, Giuffrè M. Congenital malformations. The Journal of Maternal-Fetal & Neonatal Medicine. 2012;25(sup1):25-9.

8. Webber DM, MacLeod SL, Bamshad MJ, Shaw GM, Finnell RH, Shete SS, et al. Developments in our understanding of the genetic basis of birth defects. Birth Defects Research Part A: Clinical and Molecular Teratology. 2015;103(8):680-91.

9. Durham E, Howie R, Cray J. Gene/environment interactions in craniosynostosis: A brief review. Orthodontics & craniofacial research. 2017;20:8-11.

10. Harris BS, Bishop KC, Kemeny HR, Walker JS, Rhee E, Kuller JA. Risk factors for birth defects. Obstetrical & gynecological survey. 2017;72(2):123-35.

11. Khokha MK, Mitchell LE, Wallingford JB. White paper on the study of birth defects. Birth Defects Research. 2017;109(2):180-5.

12. Christianson A, Howson CP, Modell B. March of Dimes: global report on birth defects, the hidden toll of dying and disabled children. March of Dimes: global report on birth defects, the hidden toll of dying and disabled children. 2005.

13. Mathews T, MacDorman MF, Thoma ME. Infant mortality statistics from the 2013 period linked birth/infant death data set. 2015.
14. Dangardt F, Chikritzhs T. Is foetal alcohol syndrome in children as old as alcohol consumption? : Wiley Online Library; 2020. p. 1926-7.
15. Ornoy A, Ergaz Z. Alcohol abuse in pregnant women: effects on the fetus and newborn, mode of action and maternal treatment. International journal of environmental research and public health. 2010;7(2):364-79.
16. Gupta KK, Gupta VK, Shirasaka T. An update on fetal alcohol syndrome—pathogenesis, risks, and treatment. Alcoholism: Clinical and Experimental Research. 2016;40(8):1594-602.
17. Lemoine D. Les enfants de parents alcoholiques Anomalies, observees de 127 cas. Quest Medical. 1968;25:477-82.
18. Smith D. Ulleland CN, Streissguth AP. Patterns of malformation in offspring of chronic alcoholic mothers I m1cet. 1973;1:1267-71.
19. Da Silva K, Wood D. The oral health status and treatment needs of children with fetal alcohol spectrum disorder. Clinical Oral Investigations. 2021;25(6):3497-503.
20. Denny L, Coles SM, Blitz R. Fetal alcohol syndrome and fetal alcohol spectrum disorders. American family physician. 2017;96(8):515-22.
21. Popova S, Lange S, Shield K, Burd L, Rehm J. Prevalence of fetal alcohol spectrum disorder among special subpopulations: a systematic review and meta-analysis. Addiction. 2019;114(7):1150-72.
22. Popova S, Lange S, Probst C, Gmel G, Rehm J. Estimation of national, regional, and global prevalence of alcohol use during pregnancy and fetal alcohol syndrome: a systematic review and meta-analysis. The Lancet Global Health. 2017;5(3):e290-e9.
23. Wilhoit LF, Scott DA, Simecka BA. Fetal alcohol spectrum disorders: characteristics, complications, and treatment. Community Mental Health Journal. 2017;53(6):711-8.
24. Wozniak JR, Riley EP, Charness ME. Clinical presentation, diagnosis, and management of fetal alcohol spectrum disorder. The Lancet Neurology. 2019;18(8):760-70.
25. Riley EP, Infante MA, Warren KR. Fetal alcohol spectrum disorders: an overview. Neuropsychology review. 2011;21(2):73-80.
26. Fainsod A, Hicks G. Special issue on fetal alcohol spectrum disorder. Biochemistry and Cell Biology. 2018;96(2):v-vi.

27. Chasnoff IJ, Wells AM, King L. Misdiagnosis and missed diagnoses in foster and adopted children with prenatal alcohol exposure. Pediatrics. 2015;135(2):264-70.
28. McLennan JD. Misattributions and potential consequences: The case of child mental health problems and fetal alcohol spectrum disorders. The Canadian Journal of Psychiatry. 2015;60(12):587-90.
29. May PA, Chambers CD, Kalberg WO, Zellner J, Feldman H, Buckley D, et al. Prevalence of fetal alcohol spectrum disorders in 4 US communities. Jama. 2018;319(5):474-82.
30. Chudley AE, Conry J, Cook JL, Loock C, Rosales T, LeBlanc N. Fetal alcohol spectrum disorder: Canadian guidelines for diagnosis. Cmaj. 2005;172(5 suppl):S1-S21.
31. Popova S, Lange S, Shield K, Mihic A, Chudley AE, Mukherjee RA, et al. Comorbidity of fetal alcohol spectrum disorder: a systematic review and meta-analysis. The Lancet. 2016;387(10022):978-87.
32. Burd L. FASD and ADHD: Are they related and How? Bmc Psychiatry. 2016;16(1):1-3.
33. Moore EM, Riley EP. What happens when children with fetal alcohol spectrum disorders become adults? Current developmental disorders reports. 2015;2(3):219-27.
34. Del Campo M, Jones KL. A review of the physical features of the fetal alcohol spectrum disorders. European journal of medical genetics. 2017;60(1):55-64.
35. Dixon MJ, Marazita ML, Beaty TH, Murray JC. Cleft lip and palate: understanding genetic and environmental influences. Nature Reviews Genetics. 2011;12(3):167-78.
36. Blanck-Lubarsch M, Dirksen D, Feldmann R, Sauerland C, Hohoff A. Tooth malformations, DMFT index, speech impairment and oral habits in patients with fetal alcohol syndrome. International Journal of Environmental Research and Public Health. 2019;16(22):4401.
37. Boschen KE, Gong H, Murdaugh LB, Parnell SE. Knockdown of Mns1 increases susceptibility to craniofacial defects following gastrulation-stage alcohol exposure in mice. Alcoholism: Clinical and Experimental Research. 2018;42(11):2136-43.
38. Dubey A, Saint-Jeannet J-P. Modeling human craniofacial disorders in Xenopus. Current pathobiology reports. 2017;5(1):79-92.
39. Gritli-Linde A. The etiopathogenesis of cleft lip and cleft palate: usefulness and caveats of mouse models. Current topics in developmental biology. 2008;84:37-138.
40. Marrs JA, Clendenon SG, Ratcliffe DR, Fielding SM, Liu Q, Bosron WF. Zebrafish fetal alcohol syndrome model: effects of ethanol are rescued by retinoic acid supplement. Alcohol.

2010;44(7-8):707-15.
41. McCarthy N, Wetherill L, Lovely CB, Swartz ME, Foroud TM, Eberhart JK. Pdgfra protects against ethanol-induced craniofacial defects in a zebrafish model of FASD. Development. 2013;140(15):3254-65.
42. Atukorala ADS, Ratnayake RK. Cellular and molecular mechanisms in the development of a cleft lip and/or cleft palate; insights from zebrafish (Danio rerio). The Anatomical Record. 2021;304(8):1650-60.
43. Sulik KK, Johnston MC. Sequence of developmental alterations following acute ethanol exposure in mice: craniofacial features of the fetal alcohol syndrome. American Journal of Anatomy. 1983;166(3):257-69.
44. Sant'Anna L, Tosello D. Fetal alcohol syndrome and developing craniofacial and dental structures–a review. Orthodontics & craniofacial research. 2006;9(4):172-85.
45. Zhang P, Wang G, Lin Z, Wu Y, Zhang J, Liu M, et al. Alcohol exposure induces chick craniofacial bone defects by negatively affecting cranial neural crest development. Toxicology Letters. 2017;281:53-64.
46. Hoyme HE, Kalberg WO, Elliott AJ, Blankenship J, Buckley D, Marais A-S, et al. Updated clinical guidelines for diagnosing fetal alcohol spectrum disorders. Pediatrics. 2016;138(2).
47. Blanck-Lubarsch M, Flieger S, Feldmann R, Kirschneck C, Sauerland C, Hohoff A. Malocclusion can give additional hints for diagnosis of fetal alcohol spectrum disorder. Alcohol and Alcoholism. 2019;54(1):56-61.
48. Richmond S, Shaw W, O'brien K, Buchanan I, Jones R, Stephens C, et al. The development of the PAR Index (Peer Assessment Rating): reliability and validity. The European Journal of Orthodontics. 1992;14(2):125-39.
49. Naidoo S, Harris A, Swanevelder S, Lombard C. Foetal alcohol syndrome: a cephalometric analysis of patients and controls. The European Journal of Orthodontics. 2006;28(3):254-61.
50. Goodlett CR, Horn KH, Zhou FC. Alcohol teratogenesis: mechanisms of damage and strategies for intervention. Experimental biology and medicine. 2005;230(6):394-406.
51. Brien JF, Clarke DW, Richardson B, Patrick J. Disposition of ethanol in maternal blood, fetal blood, and amniotic fluid of third-trimester pregnant ewes. American journal of obstetrics and gynecology. 1985;152(5):583-90.
52. Brien JF, Loomis CW, Tranmer J, McGrath M. Disposition of ethanol in human maternal

venous blood and amniotic fluid. American journal of obstetrics and gynecology. 1983;146(2):181-6.

53. Idänpään-Heikkilä J, Jouppila P, Åkerblom HK, Isoaho R, Kauppila E, Koivisto M. Elimination and metabolic effects of ethanol in mother, fetus, and newborn infant. American journal of obstetrics and gynecology. 1972;112(3):387-93.

54. Heller M, Burd L. Review of ethanol dispersion, distribution, and elimination from the fetal compartment. Birth Defects Research Part A: Clinical and Molecular Teratology. 2014;100(4):277-83.

55. Reik W, Dean W, Walter J. Epigenetic reprogramming in mammalian development. Science. 2001;293(5532):1089-93.

56. Ramsay M. Genetic and epigenetic insights into fetal alcohol spectrum disorders. Genome Medicine. 2010;2(4):1-8.

57. Pal-Bhadra M, Bhadra U, Jackson DE, Mamatha L, Park P-H, Shukla SD. Distinct methylation patterns in histone H3 at Lys-4 and Lys-9 correlate with up-& down-regulation of genes by ethanol in hepatocytes. Life sciences. 2007;81(12):979-87.

58. Liu Y, Balaraman Y, Wang G, Nephew KP, Zhou FC. Alcohol exposure alters DNA methylation profiles in mouse embryos at early neurulation. Epigenetics. 2009;4(7):500-11.

59. Sathyan P, Golden HB, Miranda RC. Competing interactions between micro-RNAs determine neural progenitor survival and proliferation after ethanol exposure: evidence from an ex vivo model of the fetal cerebral cortical neuroepithelium. Journal of Neuroscience. 2007;27(32):8546-57.

60. Deltour L, Ang HL, Duester G. Ethanol inhibition of retinoic acid synthesis as a potential mechanism for fetal alcohol syndrome. The FASEB journal. 1996;10(9):1050-7.

61. Kot-Leibovich H, Fainsod A. Ethanol induces embryonic malformations by competing for retinaldehyde dehydrogenase activity during vertebrate gastrulation. Disease models & mechanisms. 2009;2(5-6):295-305.

62. Li Y-X, Yang H-T, Zdanowicz M, Sicklick JK, Qi Y, Camp TJ, et al. Fetal alcohol exposure impairs Hedgehog cholesterol modification and signaling. Laboratory investigation. 2007;87(3):231-40.

63. de la Monte SM, Wands JR. Role of central nervous system insulin resistance in fetal alcohol spectrum disorders. Journal of population therapeutics and clinical pharmacology= Journal

de la therapeutique des populations et de la pharamcologie clinique. 2010;17(3):e390.
64. Ramanathan R, Wilkemeyer MF, Mittal B, Perides G, Charness ME. Alcohol inhibits cell-cell adhesion mediated by human L1. The Journal of cell biology. 1996;133(2):381-90.
65. Minana R, Climent E, Barettino D, Segui J, Renau-Piqueras J, Guerri C. Alcohol exposure alters the expression pattern of neural cell adhesion molecules during brain development. Journal of neurochemistry. 2000;75(3):954-64.
66. Zelner I, Koren G. Pharmacokinetics of ethanol in the maternal-fetal unit. Journal of population therapeutics and clinical pharmacology. 2013;20(3).
67. Cohen-Kerem R, Koren G. Antioxidants and fetal protection against ethanol teratogenicity: I. Review of the experimental data and implications to humans. Neurotoxicology and teratology. 2003;25(1):1-9.
68. Gemma S, Vichi S, Testai E. Metabolic and genetic factors contributing to alcohol induced effects and fetal alcohol syndrome. Neuroscience & Biobehavioral Reviews. 2007;31(2):221-9.
69. Mercer K, Hennings L, Ronis M. Alcohol consumption, Wnt/β-catenin signaling, and hepatocarcinogenesis. Biological Basis of Alcohol-Induced Cancer. 2015:185-95.
70. Muralidharan P, Sarmah S, Marrs JA. Retinal Wnt signaling defect in a zebrafish fetal alcohol spectrum disorder model. PLoS One. 2018;13(8):e0201659.
71. Ronis MJ, Mercer K, Chen J-R. Effects of nutrition and alcohol consumption on bone loss. Current osteoporosis reports. 2011;9(2):53-9.
72. Fischer M, Chander P, Kang H, Mellios N, Weick JP. Transcriptomic changes due to early, chronic intermittent alcohol exposure during forebrain development implicate WNT signaling, cell-type specification, and cortical regionalization as primary determinants of fetal alcohol syndrome. Alcoholism: Clinical and Experimental Research. 2021;45(5):979-95.
73. Nanci A. Ten Cate's Oral Histology-e-book: development, structure, and function: Elsevier Health Sciences; 2017.
74. Thesleff I, Järvinen E, Suomalainen M, editors. Affecting tooth morphology and renewal by fine-tuning the signals mediating cell and tissue interactions. Tinkering: The Microevolution of Development: Novartis Foundation Symposium 284; 2006: Wiley Online Library.
75. Bonczek O. Molekulární příčiny vzniku oligodoncie: úloha genu pro PAX9 a MSX1. Diplomová práce Masarykova Univerzita, Brno. 2012:31-44.
76. Thesleff I. The genetic basis of tooth development and dental defects. American Journal of

Medical Genetics Part A. 2006;140(23):2530-5.

77. Mina M, Kollar E. The induction of odontogenesis in non-dental mesenchyme combined with early murine mandibular arch epithelium. Archives of oral biology. 1987;32(2):123-7.

78. García-Castro MnI, Marcelle C, Bronner-Fraser M. Ectodermal Wnt function as a neural crest inducer. Science. 2002;297(5582):848-51.

79. Knecht A. Bronner-Fraser M. Induction of neural crest: a multigene process Nat Rev Genet. 2002;3:453-61.

80. Smith SM, Garic A, Flentke GR, Berres ME. Neural crest development in fetal alcohol syndrome. Birth Defects Research Part C: Embryo Today: Reviews. 2014;102(3):210-20.

81. Rovasio R, Battiato N. Role of early migratory neural crest cells in developmental anomalies induced by ethanol. International Journal of Developmental Biology. 2002;39(2):421-2.

82. Wang G, Bieberich E. Prenatal alcohol exposure triggers ceramide-induced apoptosis in neural crest-derived tissues concurrent with defective cranial development. Cell death & disease. 2010;1(5):e46-e.

83. Garic A, Flentke GR, Amberger E, Hernandez M, Smith SM. CaMKII activation is a novel effector of alcohol's neurotoxicity in neural crest stem/progenitor cells. Journal of neurochemistry. 2011;118(4):646-57.

84. Davis W, Crawford L, Cooper O, Farmer G, Thomas D, Freeman B. Ethanol induces the generation of reactive free radicals by neural crest cells in vitro. Journal of Craniofacial Genetics and Developmental Biology. 1990;10(3):277-93.

85. Chen Sy, Sulik KK. Free radicals and ethanol-induced cytotoxicity in neural crest cells. Alcoholism: Clinical and Experimental Research. 1996;20(6):1071-6.

86. Sltuckey E, Blerry C. The effects of high dose sporadic (binge) alcohol intake in mice. The Journal of Pathology. 1984;142(3):175-80.

87. Bloomquist RF. Chemical manipulation of dental patterning in Malawi cichlids. 2008.

88. Bowden DM, Weathersbee P, Clarren S, Fahrenbruch C, Goodlin B, Caffery S. A periodic dosing model of fetal alcohol syndrome in the pig-tailed macaque (Macaca nemestrina). American Journal of Primatology. 1983;4(2):143-57.

89. Hernandez JC. Morphologic effects of maternal alcohol intake on skull, mandible and tooth of the offspring in mice. Japanese Journal of Oral Biology. 1990;32(4):460-9.

90. SANT'ANNA LB. EFEITOS DA INGESTÃO DO ÁLCOOL DURANTE A GESTAÇÃO NA IMUNOEXPRESSÃO DO EGF NA AMELOGÊNESE E DENTINOGÊNESE DO 1o MOLAR INFERIOR DE RATOS: Universidade Estadual de Campinas; 2004.
91. Matthiessen M, Rømert P. Changes of secretory ameloblasts in mini-pig fetuses exposed to ethanol in vivo. Journal of Dental Research. 1988;67(11):1402-4.
92. Clarren SK, Alvord EC, Jr., Sumi SM, Streissguth AP, Smith DW. Brain malformations related to prenatal exposure to ethanol. The Journal of pediatrics. 1978;92(1):64-7.
93. Streissguth AP, Landesman-Dwyer S, Martin JC, Smith DW. Teratogenic effects of alcohol in humans and laboratory animals. Science. 1980;209(4454):353-61.
94. Church MW, Eldis F, Blakley BW, Bawle EV. Hearing, language, speech, vestibular, and dentofacial disorders in fetal alcohol syndrome. Alcoholism, clinical and experimental research. 1997;21(2):227-37.
95. de Andrade RS, Pedraza RM, Martellil DRB, Quiñones JAA, Júnior HM. Dental anomalies in fetal alcohol syndrome. A systematic. J Dent Res. 2020;4:1-5.
96. Naidoo S, Norval G, Swanevelder S, Lombard C. Foetal alcohol syndrome: a dental and skeletal age analysis of patients and controls. European journal of orthodontics. 2006;28(3):247-53.
97. Almeida L, Andreu-Fernández V, Navarro-Tapia E, Aras-López R, Serra-Delgado M, Martínez L, et al. Murine models for the study of fetal alcohol spectrum disorders: an overview. Frontiers in Pediatrics. 2020;8:359.
98. Seguin D, Gerlai R. Fetal alcohol spectrum disorders: Zebrafish in the analysis of the milder and more prevalent form of the disease. Behavioural brain research. 2018;352:125-32.
99. Barkley-Levenson AM, Crabbe JC. Bridging animal and human models: Translating from (and to) animal genetics. Alcohol research: current reviews. 2012;34(3):325.
100. Larkby C, Day N. The effects of prenatal alcohol exposure. Alcohol health and research world. 1997;21(3):192.
101. Marquardt K, Brigman JL. The impact of prenatal alcohol exposure on social, cognitive and affective behavioral domains: Insights from rodent models. Alcohol. 2016;51:1-15.
102. Boehm II SL, Lundahl KR, Caldwell J, Gilliam DM. Ethanol teratogenesis in the C57BL/6J, DBA/2J, and A/J inbred mouse strains. Alcohol. 1997;14(4):389-95.
103. Sulik KK, Johnston MC, Webb MA. Fetal alcohol syndrome: embryogenesis in a mouse

model. Science. 1981;214(4523):936-8.
104. Yoneyama N, Crabbe JC, Ford MM, Murillo A, Finn DA. Voluntary ethanol consumption in 22 inbred mouse strains. Alcohol. 2008;42(3):149-60.
105. Kitson JE, Ord J, Watt PJ. Maternal Chronic Ethanol Exposure Decreases Stress Responses in Zebrafish Offspring. Biomolecules. 2022;12(8):1143.
106. Lovely CB, Fernandes Y, Eberhart JK. Fishing for fetal alcohol spectrum disorders: zebrafish as a model for ethanol teratogenesis. Zebrafish. 2016;13(5):391-8.
107. Lomanowska AM, Melo AI. Deconstructing the function of maternal stimulation in offspring development: Insights from the artificial rearing model in rats. Hormones and Behavior. 2016;77:224-36.
108. Reimers MJ, Hahn ME, Tanguay RL. Two zebrafish alcohol dehydrogenases share common ancestry with mammalian class I, II, IV, and V alcohol dehydrogenase genes but have distinct functional characteristics. Journal of Biological Chemistry. 2004;279(37):38303-12.
109. Fernandes Y, Buckley DM, Eberhart JK. Diving into the world of alcohol teratogenesis: a review of zebrafish models of fetal alcohol spectrum disorder. Biochemistry and Cell Biology. 2018;96(2):88-97.
110. Ohashi A, de Souza Schacher HR, Pizzato CS, Vianna M, de Menezes LM. Zebrafish as model for studies in dentistry. Zebrafish. 2022;11(1):46.
111. Khan FR, Alhewairini SS. Zebrafish (Danio rerio) as a model organism. Current trends in cancer management. 2018:3-18.
112. Rai AR, Joy T, Rashmi K, Rai R, Vinodini N, Jiji P. Zebrafish as an experimental model for the simulation of neurological and craniofacial disorders. Veterinary World. 2022;15(1):22.
113. Driever W, Solnica-Krezel L, Schier A, Neuhauss S, Malicki J, Stemple D, et al. A genetic screen for mutations affecting embryogenesis in zebrafish. Development. 1996;123(1):37-46.
114. Mullins MC, Hammerschmidt M, Haffter P, Nüsslein-Volhard C. Large-scale mutagenesis in the zebrafish: in search of genes controlling development in a vertebrate. Current Biology. 1994;4(3):189-202.
115. Engeszer RE, Patterson LB, Rao AA, Parichy DM. Zebrafish in the wild: a review of natural history and new notes from the field. Zebrafish. 2007;4(1):21-40.
116. Spence R. Zebrafish models in neurobehavioral research. NeuroMethods. 2011;52(3):211-22.

117. Mills D. Aquarium fish: Dk Pub; 1993.
118. Bilotta J, Saszik S, DeLorenzo AS, Hardesty HR. Establishing and maintaining a low-cost zebrafish breeding and behavioral research facility. Behavior Research Methods, Instruments, & Computers. 1999;31(1):178-84.
119. Spence R, Smith C, Ashton R. Oviposition decisions are mediated by spawning site quality in wild and domesticated zebrafish, Danio rerio. Behaviour. 2007;144(8):953-66.
120. Streisinger G, Walker C, Dower N, Knauber D, Singer F. Production of clones of homozygous diploid zebra fish (Brachydanio rerio). Nature. 1981;291(5813):293-6.
121. Kimmel CB, Law RD. Cell lineage of zebrafish blastomeres: I. Cleavage pattern and cytoplasmic bridges between cells. Developmental biology. 1985;108(1):78-85.
122. Kimmel CB, Sessions SK, Kimmel RJ. Morphogenesis and synaptogenesis of the zebrafish Mauthner neuron. Journal of Comparative Neurology. 1981;198(1):101-20.
123. Parng C. In vivo zebrafish assays for toxicity testing. Current opinion in drug discovery & development. 2005;8(1):100-6.
124. Hill AJ, Teraoka H, Heideman W, Peterson RE. Zebrafish as a model vertebrate for investigating chemical toxicity. Toxicological sciences. 2005;86(1):6-19.
125. Shen C, Zuo Z. Zebrafish (Danio rerio) as an excellent vertebrate model for the development, reproductive, cardiovascular, and neural and ocular development toxicity study of hazardous chemicals. Environmental Science and Pollution Research. 2020;27(35):43599-614.
126. Zhao S, Huang J, Ye J. A fresh look at zebrafish from the perspective of cancer research. Journal of Experimental & Clinical Cancer Research. 2015;34(1):1-9.
127. Gore AV, Monzo K, Cha YR, Pan W, Weinstein BM. Vascular development in the zebrafish. Cold Spring Harbor perspectives in medicine. 2012;2(5):a006684.
128. Kanungo J, Cuevas E, F Ali S, Paule MG. Zebrafish model in drug safety assessment. Current Pharmaceutical Design. 2014;20(34):5416-29.
129. Santoriello C, Zon LI. Hooked! Modeling human disease in zebrafish. The Journal of clinical investigation. 2012;122(7):2337-43.
130. Howe K, Clark MD, Torroja CF, Torrance J, Berthelot C, Muffato M, et al. The zebrafish reference genome sequence and its relationship to the human genome. Nature. 2013;496(7446):498-503.
131. Lewis KE, Eisen JS. From cells to circuits: development of the zebrafish spinal cord.

Progress in neurobiology. 2003;69(6):419-49.

132. Barbazuk WB, Korf I, Kadavi C, Heyen J, Tate S, Wun E, et al. The syntenic relationship of the zebrafish and human genomes. Genome research. 2000;10(9):1351-8.

133. Charles BK, William WB, Seth RK, Bonnie U, Thomas FS. Stages of embryonic development of the zebrafish. Developmental dynamics. 1995;203(3):253-310.

134. Spence R, Gerlach G, Lawrence C, Smith C. The behaviour and ecology of the zebrafish, Danio rerio. Biological reviews. 2008;83(1):13-34.

135. Carpio Y, Estrada MP. Zebrafish as a genetic model organism. Biotecnología Aplicada. 2006;23(4):265-70.

136. Lieschke GJ, Currie PD. Animal models of human disease: zebrafish swim into view. Nature Reviews Genetics. 2007;8(5):353-67.

137. Nusslein-Volhard C, Dahm R. Zebrafish: Oxford University Press; 2002.

138. Linney E, Upchurch L, Donerly S. Corrigendum to "Zebrafish as a neurotoxicological model"[Neurotoxicology and Teratology 26 (2004) 709–718]. Neurotoxicology and Teratology. 2005;1(27):175.

139. Lele Z, Krone P. The zebrafish as a model system in developmental, toxicological and transgenic research. Biotechnology advances. 1996;14(1):57-72.

140. Mork L, Crump G. Zebrafish craniofacial development: a window into early patterning. Current topics in developmental biology. 2015;115:235-69.

141. Van Otterloo E, Williams T, Artinger KB. The old and new face of craniofacial research: How animal models inform human craniofacial genetic and clinical data. Developmental biology. 2016;415(2):171-87.

142. Machado RG, Eames BF. Using zebrafish to test the genetic basis of human craniofacial diseases. Journal of Dental Research. 2017;96(11):1192-9.

143. Mariotti M, Carnovali M, Banfi G. Danio rerio: the Janus of the bone from embryo to scale. Clinical Cases in Mineral and Bone Metabolism. 2015;12(2):188.

144. Witten P, Harris M, Huysseune A, Winkler C. Small teleost fish provide new insights into human skeletal diseases. Methods in cell biology. 2017;138:321-46.

145. Duncan KM, Mukherjee K, Cornell RA, Liao EC. Zebrafish models of orofacial clefts. Developmental Dynamics. 2017;246(11):897-914.

146. Küchler EC, Silva LAd, Nelson-Filho P, Sabóia TM, Rentschler AM, Granjeiro JM, et al.

Assessing the association between hypoxia during craniofacial development and oral clefts. Journal of Applied Oral Science. 2018;26.

147. Makkar H, Verma SK, Panda PK, Jha E, Das B, Mukherjee K, et al. In vivo molecular toxicity profile of dental bioceramics in embryonic Zebrafish (Danio rerio). Chemical research in toxicology. 2018;31(9):914-23.

148. Rajendran S, Annadurai G, Rajeshkumar S. Characterization and toxicology evaluation of zirconium oxide nanoparticles on the embryonic development of zebrafish, Danio rerio. Drug and Chemical Toxicology. 2018;42(1):104-11.

149. Alifui-Segbaya F, Bowman J, White AR, Varma S, Lieschke GJ, George R. Toxicological assessment of additively manufactured methacrylates for medical devices in dentistry. Acta biomaterialia. 2018;78:64-77.

150. Zhao L, Si J, Wei Y, Li S, Jiang Y, Zhou R, et al. Toxicity of porcelain-fused-to-metal substrate to zebrafish (Danio rerio) embryos and larvae. Life sciences. 2018;203:66-71.

151. Chao C-C, Hsu P-C, Jen C-F, Chen I-H, Wang C-H, Chan H-C, et al. Zebrafish as a model host for Candida albicans infection. Infection and immunity. 2010;78(6):2512-21.

152. Xiao X, Wu Z-C, Chou K-C. A multi-label classifier for predicting the subcellular localization of gram-negative bacterial proteins with both single and multiple sites. PloS one. 2011;6(6):e20592.

153. Lu J-J, Lo H-J, Wu Y-M, Chang J-Y, Chen Y-Z, Wang S-H. DST659 genotype of Candida albicans showing positive association between biofilm formation and dominance in Taiwan. Medical Mycology. 2018;56(8):972-8.

154. Swidergall M, Khalaji M, Solis NV, Moyes DL, Drummond RA, Hube B, et al. Candidalysin is required for neutrophil recruitment and virulence during systemic Candida albicans infection. The Journal of infectious diseases. 2019;220(9):1477-88.

155. CH㈱ LSLYL. Generation and characterization of single chain variable fragment against Alphaenolase of Candida albicans. Int J Mol Sci㈱ 2020㈱21.2903.

156. Hajishengallis G, Darveau RP, Curtis MA. The keystone-pathogen hypothesis. Nature Reviews Microbiology. 2012;10(10):717-25.

157. Castillo DM, Sánchez-Beltrán MC, Castellanos JE, Sanz I, Mayorga-Fayad I, Sanz M, et al. Detection of specific periodontal microorganisms from bacteraemia samples after periodontal therapy using molecular-based diagnostics. Journal of clinical periodontology. 2011;38(5):418-27.

158. Reyes L, Herrera D, Kozarov E, Roldan S, Progulske-Fox A. Periodontal bacterial invasion and infection: contribution to atherosclerotic pathology. Journal of clinical periodontology. 2013;40:S30-S50.

159. Williams R, Barnett A, Claffey N, Davis M, Gadsby R, Kellett M, et al. The potential impact of periodontal disease on general health: a consensus view. Current medical research and opinion. 2008;24(6):1635-43.

160. Menke AL, Spitsbergen JM, Wolterbeek AP, Woutersen RA. Normal anatomy and histology of the adult zebrafish. Toxicologic pathology. 2011;39(5):759-75.

161. Crucke J, Huysseune A. Blocking VEGF signaling delays development of replacement teeth in zebrafish. Journal of Dental Research. 2015;94(1):157-65.

162. Huysseune A, Sire J-Y. Development and fine structure of pharyngeal replacement teeth in juvenile zebrafish (Danio rerio)(Teleostei, Cyprinidae). Cell and tissue research. 2000;302(2):205-19.

163. Wautier K, Huysseune A. A quantitative analysis of pharyngeal tooth shape in the zebrafish (Danio rerio, Teleostei, Cyprinidae). Archives of Oral Biology. 2001;46(1):67-75.

164. Huysseune A, Sire J-Y. The role of epithelial remodelling in tooth eruption in larval zebrafish. Cell and tissue research. 2004;315(1):85-95.

165. Huysseune A, Thesleff I. Continuous tooth replacement: the possible involvement of epithelial stem cells. Bioessays. 2004;26(6):665-71.

166. Azimian Zavareh P, Silva P, Gimhani N, Atukorallaya D. Effect of Embryonic Alcohol Exposure on Craniofacial and Skin Melanocyte Development: Insights from Zebrafish (Danio rerio). Toxics. 2022;10(9):544.

167. Zhang Y, Zhang Y, Zheng X, Xu R, He H, Duan X. Grading and quantification of dental fluorosis in zebrafish larva. Archives of Oral Biology. 2016;70:16-23.

168. Van der heyden C, Huysseune A. Dynamics of tooth formation and replacement in the zebrafish (Danio rerio)(Teleostei, Cyprinidae). Developmental dynamics: an official publication of the American Association of Anatomists. 2000;219(4):486-96.

169. Pinheiro-da-Silva J, Luchiari AC. Embryonic ethanol exposure on zebrafish early development. Brain and Behavior. 2021;11(6):e02062.

170. Manikandan P, Sarmah S, Marrs JA. Ethanol Effects on Early Developmental Stages Studied Using the Zebrafish. Biomedicines. 2022;10(10):2555.

171. Muralidharan P, Sarmah S, Marrs JA. Zebrafish retinal defects induced by ethanol exposure are rescued by retinoic acid and folic acid supplement. Alcohol. 2015;49(2):149-63.
172. Arenzana F, Carvan III MJ, Aijon J, Sanchez-Gonzalez R, Arevalo R, Porteros A. Teratogenic effects of ethanol exposure on zebrafish visual system development. Neurotoxicology and teratology. 2006;28(3):342-8.
173. Tamura M, Nemoto E. Role of the Wnt signaling molecules in the tooth. Japanese Dental Science Review. 2016;52(4):75-83.
174. Nüsslein-Volhard C, Wieschaus E. Mutations affecting segment number and polarity in Drosophila. Nature. 1980;287(5785):795-801.
175. Rijsewijk F, Schuermann M, Wagenaar E, Parren P, Weigel D, Nusse R. The Drosophila homology of the mouse mammary oncogene int-1 is identical to the segment polarity gene wingless. Cell. 1987;50(4):649-57.
176. Nusse R, Brown A, Papkoff J, Scambler P, Shackleford G, McMahon A, et al. A new nomenclature for int-1 and related genes: The Wnt gene family. Cell. 1991;64(2):231.
177. Sarkar L, Sharpe PT. Expression of Wnt signalling pathway genes during tooth development. Mechanisms of Development. 1999;85(1):197-200.
178. Wang B, Li H, Liu Y, Lin X, Lin Y, Wang Y, et al. Expression patterns of WNT/β-CATENIN signaling molecules during human tooth development. Journal of molecular histology. 2014;45(5):487-96.
179. Kantaputra P, Sripathomsawat W. WNT10A and isolated hypodontia. American Journal of Medical Genetics Part A. 2011;155(5):1119-22.
180. van den Boogaard M-J, Créton M, Bronkhorst Y, van der Hout A, Hennekam E, Lindhout D, et al. Mutations in WNT10A are present in more than half of isolated hypodontia cases. Journal of medical genetics. 2012;49(5):327-31.
181. Adaimy L, Chouery E, Mégarbané H, Mroueh S, Delague V, Nicolas E, et al. Mutation in WNT10A Is Associated with an Autosomal Recessive Ectodermal Dysplasia: The Odonto-onycho-dermal Dysplasia. The American Journal of Human Genetics. 2007;81(4):821-8.
182. Cluzeau C, Hadj-Rabia S, Jambou M, Mansour S, Guigue P, Masmoudi S, et al. Only four genes (EDA1, EDAR, EDARADD, and WNT10A) account for 90% of hypohidrotic/anhidrotic ectodermal dysplasia cases. Human mutation. 2011;32(1):70-2.
183. Bohring A, Stamm T, Spaich C, Haase C, Spree K, Hehr U, et al. WNT10A Mutations Are

a Frequent Cause of a Broad Spectrum of Ectodermal Dysplasias with Sex-Biased Manifestation Pattern in Heterozygotes. The American Journal of Human Genetics. 2009;85(1):97-105.
184. Nagy N, Wedgeworth E, Hamada T, White JM, Hashimoto T, McGrath JA. Schöpf-Schulz-Passarge syndrome resulting from a homozygous nonsense mutation in WNT10A. Journal of Dermatological Science. 2010;58(3):220-2.
185. Castori M, Castiglia D, Brancati F, Foglio M, Heath S, Floriddia G, et al. Two families confirm Schöpf-Schulz-Passarge syndrome as a discrete entity within the WNT10A phenotypic spectrum. Clinical genetics. 2011;79(1):92-5.
186. Kantaputra P, Kaewgahya M, Jotikasthira D, Kantaputra W. Tricho-odonto-onycho-dermal dysplasia and WNT10A mutations. American Journal of Medical Genetics Part A. 2014;164(4):1041-8.
187. Vink CP, Ockeloen CW, Ten Kate S, Koolen DA, Ploos van Amstel JK, Kuijpers-Jagtman A-M, et al. Variability in dentofacial phenotypes in four families with WNT10A mutations. European Journal of Human Genetics. 2014;22(9):1063-70.
188. Plaisancié J, Bailleul-Forestier I, Gaston V, Vaysse F, Lacombe D, Holder-Espinasse M, et al. Mutations in WNT10A are frequently involved in oligodontia associated with minor signs of ectodermal dysplasia. American Journal of Medical Genetics Part A. 2013;161(4):671-8.
189. Yu M, Liu Y, Liu H, Wong SW, He H, Zhang X, et al. Distinct impacts of bi-allelic WNT10A mutations on the permanent and primary dentitions in odonto-onycho-dermal dysplasia. American Journal of Medical Genetics Part A. 2019;179(1):57-64.
190. Yang J, Wang SK, Choi M, Reid BM, Hu Y, Lee YL, et al. Taurodontism, variations in tooth number, and misshapened crowns in Wnt10a null mice and human kindreds. Molecular genetics & genomic medicine. 2015;3(1):40-58.
191. Xu M, Horrell J, Snitow M, Cui J, Gochnauer H, Syrett CM, et al. WNT10A mutation causes ectodermal dysplasia by impairing progenitor cell proliferation and KLF4-mediated differentiation. Nature communications. 2017;8(1):1-21.
192. Yu M, Liu Y, Wang Y, Wong S, Wu J, Liu H, et al. Epithelial Wnt10a is essential for tooth root furcation morphogenesis. Journal of dental research. 2020;99(3):311-9.
193. Yu P, Yang W, Han D, Wang X, Guo S, Li J, et al. Mutations in WNT10B are identified in individuals with oligodontia. The American Journal of Human Genetics. 2016;99(1):195-201.
194. Magruder S, Carter E, Williams MA, English J, Akyalcin S, Letra A. Further evidence for

the role of WNT 10A, WNT 10B and GREM 2 as candidate genes for isolated tooth agenesis. Orthodontics & Craniofacial Research. 2018;21(4):258-63.

195. Parsons KJ, Trent Taylor A, Powder KE, Albertson RC. Wnt signalling underlies the evolution of new phenotypes and craniofacial variability in Lake Malawi cichlids. Nature communications. 2014;5(1):1-11.

196. Walker M, Kimmel C. A two-color acid-free cartilage and bone stain for zebrafish larvae. Biotechnic & Histochemistry. 2007;82(1):23-8.

197. Aliesfehani T. Modified double skeletal staining protocols with Alizarinred and Alcian blue in laboratory animals. Annals of Military & Health Sciences Research• Vol. 2015;13(2).

198. Thisse B, Thisse C. In situ hybridization on whole-mount zebrafish embryos and young larvae. In situ hybridization protocols: Springer; 2014. p. 53-67.

199. Williams JF, Smith VC, Abuse CoS, Levy S, Ammerman SD, Gonzalez PK, et al. Fetal alcohol spectrum disorders. Pediatrics. 2015;136(5):e1395-e406.

200. Mattson SN, Bernes GA, Doyle LR. Fetal alcohol spectrum disorders: a review of the neurobehavioral deficits associated with prenatal alcohol exposure. Alcoholism: Clinical and Experimental Research. 2019;43(6):1046-62.

201. Tsang TW, Lucas BR, Carmichael Olson H, Pinto RZ, Elliott EJ. Prenatal alcohol exposure, FASD, and child behavior: a meta-analysis. Pediatrics. 2016;137(3).

202. Gareri J, Brien J, Reynolds J, Koren G. Potential role of the placenta in fetal alcohol spectrum disorder. Pediatric Drugs. 2009;11(1):26-9.

203. Kimmel CB, Ballard WW, Kimmel SR, Ullmann B, Schilling TF. Stages of embryonic development of the zebrafish. Developmental dynamics. 1995;203(3):253-310.

204. Loucks E, Carvan III MJ. Strain-dependent effects of developmental ethanol exposure in zebrafish. Neurotoxicology and teratology. 2004;26(6):745-55.

205. Tamura M, Nemoto E, Sato MM, Nakashima A, Shimauchi H. Role of the Wnt signaling pathway in bone and tooth. Frontiers in Bioscience-Elite. 2010;2(4):1405-13.

206. Mukherjee R. FASD: The current situation in the UK. Advances in Dual Diagnosis. 2019.

207. Landgraf MN, Albers L, Rahmsdorf B, Vill K, Gerstl L, Lippert M, et al. Fetal alcohol spectrum disorders (FASD)–What we know and what we should know–The knowledge of German health professionals and parents. european journal of paediatric neurology. 2018;22(3):507-15.

208. Astley SJ, Clarren SK. Diagnosing the full spectrum of fetal alcohol-exposed individuals:

introducing the 4-digit diagnostic code. Alcohol and alcoholism. 2000;35(4):400-10.
209. Greenbaum R, Koren G. Fetal alcohol spectrum disorder–New diagnostic initiatives. Paediatrics & Child Health. 2002;7(3):139-41.
210. Streissguth AP, Bookstein FL, Barr HM, Sampson PD, O'malley K, Young JK. Risk factors for adverse life outcomes in fetal alcohol syndrome and fetal alcohol effects. Journal of Developmental & Behavioral Pediatrics. 2004;25(4):228-38.
211. Hu K, Da Silva K. Access to oral health care for children with fetal alcohol spectrum disorder: a cross-sectional study. BMC Oral Health. 2022;22(1):1-8.
212. Church MW, Eldis F, Blakley BW, Bawle EV. Hearing, language, speech, vestibular, and dentofacial disorders in fetal alcohol syndrome. Alcoholism: Clinical and Experimental Research. 1997;21(2):227-37.
213. Naidoo S, Chikte U, Laubscher R, Lombard C. Fetal alcohol syndrome: anthropometric and oral health status. J Contemp Dent Pract. 2005;6(4):101-15.
214. Pećina-Hrncević A, Buljan L. [Fetal alcohol syndrome--case report]. Acta stomatologica Croatica. 1991;25(4):253-8.
215. Jackson IT, Hussain K. Craniofacial and oral manifestations of fetal alcohol syndrome. Plastic and reconstructive surgery. 1990;85(4):505-12.
216. Webb S, Hochberg MS, Sher MR. Fetal alcohol syndrome: report of case. Journal of the American Dental Association (1939). 1988;116(2):196-8.
217. Autti-Rämö I, Fagerlund A, Ervalahti N, Loimu L, Korkman M, Hoyme HE. Fetal alcohol spectrum disorders in Finland: clinical delineation of 77 older children and adolescents. American journal of medical genetics Part A. 2006;140(2):137-43.
218. Patterson C. Osteichthyes: teleostei. The fossil record. 1993;2:621-56.
219. Huysseune A, Van der heyden C, Sire JY. Early development of the zebrafish (Danio rerio) pharyngeal dentition (Teleostei, Cyprinidae). Anatomy and Embryology. 1998;198(4):289-305.
220. Sire JY, Davit-Beal T, Delgado S, Van Der Heyden C, Huysseune A. First-generation teeth in nonmammalian lineages: evidence for a conserved ancestral character? Microscopy research and technique. 2002;59(5):408-34.
221. Wiweger MI, Zhao Z, van Merkesteyn RJ, Roehl HH, Hogendoorn PC. HSPG-deficient zebrafish uncovers dental aspect of multiple osteochondromas. PLoS One. 2012;7(1):e29734.
222. Jackman WR, Draper BW, Stock DW. Fgf signaling is required for zebrafish tooth

development. Developmental Biology. 2004;274(1):139-57.
223. Huysseune A, Sire J-Y. Early development of the zebrafish (Danio rerio) pharyngeal dentition (Teleostei, Cyprinidae). Anatomy and embryology. 1998;198(4):289-305.
224. Kieser JA. Fluctuating odontometric asymmetry and maternal alcohol consumption. Annals of Human Biology. 1992;19(5):513-20.
225. Al-Ani AH, Antoun JS, Thomson WM, Merriman TR, Farella M. Hypodontia: an update on its etiology, classification, and clinical management. BioMed Research International. 2017;2017.
226. Whitehurst T. Foetal alcohol spectrum disorders: the 21st century intellectual disability. Cognitive Impairments: causes, diagnosis and treatment. 2010.
227. Murawski NJ, Moore EM, Thomas JD, Riley EP. Advances in diagnosis and treatment of fetal alcohol spectrum disorders: from animal models to human studies. Alcohol research: current reviews. 2015;37(1):97.
228. Bartlett J, Dwyer S, Beniash E, Skobe Z, Payne-Ferreira T. Fluorosis: a new model and new insights. Journal of dental research. 2005;84(9):832-6.
229. Karaman GE, Ünal İ, Beler M, Üstündağ FD, Cansız D, Üstündağ ÜV, et al. Toothpastes for children and their detergent contents affect molecular mechanisms of odontogenesis in zebrafish embryos. Drug and chemical toxicology. 2022:1-11.
230. Liu F, Chu EY, Watt B, Zhang Y, Gallant NM, Andl T, et al. Wnt/β-catenin signaling directs multiple stages of tooth morphogenesis. Developmental biology. 2008;313(1):210-24.
231. Sarkar L, Sharpe PT. Expression of Wnt signalling pathway genes during tooth development. Mechanisms of development. 1999;85(1-2):197-200.
232. Järvinen E, Salazar-Ciudad I, Birchmeier W, Taketo MM, Jernvall J, Thesleff I. Continuous tooth generation in mouse is induced by activated epithelial Wnt/β-catenin signaling. Proceedings of the National Academy of Sciences. 2006;103(49):18627-32.
233. Liu F, Millar S. Wnt/β-catenin signaling in oral tissue development and disease. Journal of dental research. 2010;89(4):318-30.
234. Yuan Q, Zhao M, Tandon B, Maili L, Liu X, Zhang A, et al. Role of WNT 10A in failure of tooth development in humans and zebrafish. Molecular genetics & genomic medicine. 2017;5(6):730-41.
235. Ruiz-Heiland G, Lenz S, Bock N, Ruf S. Prevalence of WNT10A gene mutations in non-

syndromic oligodontia. Clinical Oral Investigations. 2019;23(7):3103-13.
236. Song S, Zhao R, He H, Zhang J, Feng H, Lin L. WNT10A variants are associated with non-syndromic tooth agenesis in the general population. Human genetics. 2014;133(1):117-24.
237. Handrigan GR, Richman JM. A network of Wnt, hedgehog and BMP signaling pathways regulates tooth replacement in snakes. Developmental biology. 2010;348(1):130-41.
238. Yuan G, Yang G, Zheng Y, Zhu X, Chen Z, Zhang Z, et al. The non-canonical BMP and Wnt/β-catenin signaling pathways orchestrate early tooth development. Development. 2015;142(1):128-39.
239. Lin M, Li L, Liu C, Liu H, He F, Yan F, et al. Wnt5a regulates growth, patterning, and odontoblast differentiation of developing mouse tooth. Developmental Dynamics. 2011;240(2):432-40.
240. Wang X-P, O'Connell DJ, Lund JJ, Saadi I, Kuraguchi M, Turbe-Doan A, et al. Apc inhibition of Wnt signaling regulates supernumerary tooth formation during embryogenesis and throughout adulthood. 2009.
241. Sarkar L, Sharpe P. Inhibition of Wnt signaling by exogenous Mfrzbl protein affects molar tooth size. Journal of dental research. 2000;79(4):920-5.
242. Fraser GJ, Bloomquist RF, Streelman JT. Common developmental pathways link tooth shape to regeneration. Developmental biology. 2013;377(2):399-414.
243. Huysseune A, Soenens M, Elderweirdt F. Wnt signaling during tooth replacement in zebrafish (Danio rerio): pitfalls and perspectives. Frontiers in physiology. 2014;5:386.
244. Lim WH, Liu B, Cheng D, Hunter DJ, Zhong Z, Ramos DM, et al. Wnt signaling regulates pulp volume and dentin thickness. Journal of Bone and Mineral Research. 2014;29(4):892-901.
245. Yamashiro T, Zheng L, Shitaku Y, Saito M, Tsubakimoto T, Takada K, et al. Wnt10a regulates dentin sialophosphoprotein mRNA expression and possibly links odontoblast differentiation and tooth morphogenesis. Differentiation. 2007;75(5):452-62.
246. Vogel P, Read R, Hansen G, Powell D, Kantaputra P, Zambrowicz B, et al. Dentin dysplasia in Notum knockout mice. Veterinary pathology. 2016;53(4):853-62.
247. Yin A, Korzh S, Winata CL, Korzh V, Gong Z. Wnt signaling is required for early development of zebrafish swimbladder. PloS one. 2011;6(3):e18431.
248. Lewis JL, Bonner J, Modrell M, Ragland JW, Moon RT, Dorsky RI, et al. Reiterated Wnt signaling during zebrafish neural crest development. 2004.

249. Stewart S, Gomez Alan W, Armstrong Benjamin E, Henner A, Stankunas K. Sequential and Opposing Activities of Wnt and BMP Coordinate Zebrafish Bone Regeneration. Cell Reports. 2014;6(3):482-98.

250. Vangipuram SD, Lyman WD. Ethanol affects differentiation-related pathways and suppresses Wnt signaling protein expression in human neural stem cells. Alcoholism: Clinical and Experimental Research. 2012;36(5):788-97.

251. Xu CQ, de la Monte SM, Tong M, Huang CK, Kim M. Chronic Ethanol-Induced Impairment of Wnt/β-Catenin Signaling is Attenuated by PPAR-δ Agonist. Alcoholism: Clinical and Experimental Research. 2015;39(6):969-79.

252. Smith SM, Garic A, Berres ME, Flentke GR. Genomic factors that shape craniofacial outcome and neural crest vulnerability in FASD. Frontiers in genetics. 2014;5:224.

253. Lekven AC, Thorpe CJ, Waxman JS, Moon RT. Zebrafish wnt8 encodes two wnt8 proteins on a bicistronic transcript and is required for mesoderm and neurectoderm patterning. Developmental cell. 2001;1(1):103-14.

254. Borday-Birraux V, Van der Heyden C, Debiais-Thibaud M, Verreijdt L, Stock D, Huysseune A, et al. Expression of Dlx genes during the development of the zebrafish pharyngeal dentition: evolutionary implications. Evolution & development. 2006;8(2):130-41.

255. Zeng X, Huang H, Tamai K, Zhang X, Harada Y, Yokota C, et al. Initiation of Wnt signaling: control of Wnt coreceptor Lrp6 phosphorylation/activation via frizzled, dishevelled and axin functions. 2008.

256. Hardcastle Z, Mo R, Hui C, Sharpe PT. The Shh signalling pathway in tooth development: defects in Gli2 and Gli3 mutants. Development. 1998;125(15):2803-11.

257. Satokata I, Ma L, Ohshima H, Bei M, Woo I, Nishizawa K, et al. Msx2 deficiency in mice causes pleiotropic defects in bone growth and ectodermal organ formation. Nature genetics. 2000;24(4):391-5.

258. Trumpp A, Depew MJ, Rubenstein JL, Bishop JM, Martin GR. Cre-mediated gene inactivation demonstrates that FGF8 is required for cell survival and patterning of the first branchial arch. Genes & development. 1999;13(23):3136-48.

259. Andl T, Reddy ST, Gaddapara T, Millar SE. WNT signals are required for the initiation of hair follicle development. Developmental cell. 2002;2(5):643-53.